Characterization of a Putative Flavonoid 3', 5'-Hydroxylase (PtF3'5'H1) in *Populus*

by

Hao Tang
B.Sc., Nanjing Agricultural University, 2012

A Thesis Submitted in Partial Fulfillment
of the Requirements for the Degree of

Master of Science

in the Department of Biology

Supervisory Committee

Characterization of a Putative Flavonoid 3', 5'-Hydroxylase (PtF3'5'H1) in *Populus*

by

Hao Tang
B.Sc., Nanjing Agricultural University, 2012

Supervisory Committee

Dr. C. Peter Constabel, Department of Biology
Supervisor

Dr. Jürgen Ehlting, Department of Biology
Departmental Member

Dr. Alisdair Boraston, Department of Biochemistry and Microbiology
Outside Member

Abstract

Supervisory Committee
Dr. C. Peter Constabel, Department of Biology
Supervisor
Dr. Jürgen Ehlting, Department of Biology
Departmental Member
Dr. Alisdair Boraston, Department of Biochemistry and Microbiology
Outside Member

Proanthocyanidins (PAs), also known as condensed tannins (CTs), are oligomers or polymers of flavan-3-ols. They have a very important role in plant-environment interactions, such as defense against herbivory and pathogens. They may also be important for light stress tolerance. In poplar, PAs can make up as much as 30% of the leaf dry weight. The synthesis of PAs in poplar was demonstrated to be inducible by both abiotic and biotic stresses. The B-ring hydroxylation pattern of flavan-3-ols directly affects the structure of PAs, and many studies have shown that B-ring hydroxylation of PAs is associated with their biological functions, including effects on leaf litter decomposition rate and anti-herbivore activity. Anthocyanins are very important colour pigments in plants, and share the intermediate leucoanthocyanidin with PAs. The role of anthocyanins in plant pollination, light stress tolerance, and seed dispersal has been well studied. A change in B-ring hydroxylation pattern can modify the colour of anthocyanins dramatically and also change their biological function. Flavonoid 3'-hydroxylase and flavonoid 3', 5'-hydroxylase (F3'H and F3'5'H) are the two enzymes involved in determining the B-ring hydroxylation pattern of both PAs and anthocyanins. The objective of this study is to characterize the possible role of flavonoid 3', 5'-hydroxylase in PA and anthocyanin biosynthesis in poplar. A candidate F3'5'H was identified in the

Populus trichocarpa genome database based on previous expression profile experiments, and called PtF3’5’H1. The predicted protein shares high sequence similarity with previously characterized F3’5’H proteins from other plants. To test the function of PtF3’5’H1 directly, transgenic hybrid poplar plants overexpressing PtF3’5’H1 were generated. Preliminary LC-MS analysis showed that the hydroxylation pattern of the PA in the transgenic poplars was not significantly modified. Likewise, overexpression of PtF3’5’H1 in poplar did not change the overall amount of PAs. These results suggest that overexpression of PtF3’5’H1 in poplar is not sufficient to modify the B-ring hydroxylation pattern of PA, and that additional factors may be required. By contrast, the transgenic PtF3’5’H1 overexpressing poplar did show an alteration in anthocyanin profile. In leaves of transgenic poplars, several putative delphinidin derivatives were observed at greater levels than in the wild type, indicating that PtF3’5’H1 participates in the anthocyanin production in poplar. However, transiently introducing PtF3’5’H1 into *Nicotiana benthamiana* had no effect on the anthocyanin profile in this plant. I conclude that PtF3’5’H1 is very likely to be involved in the anthocyanin synthesis in poplar, while the function of PtF3’5’H1 in poplar PA synthesis has yet to be demonstrated.

Table of Contents

.

List of Tables

List of Figures

List of Abbreviations

Agro-infiltration	*Agrobacterium* infiltration
AHA10	Autoinhibited H(+)-ATPase isoform 10
ANR	Anthocyanidin reductase
ANS	Anthocyanidin synthase
AtGL3	*Arabidopsis thaliana* trichome development locus GLABRA3
AtPAP1	*Arabidopsis thaliana* production of anthocyanin pigment 1
BAN	BANYULS protein
bHLH	Basic helix–loop-helix proteins
BSA	Bovine serum albumin
CHI	Chalcone isomerase
CHS	Chalcone synthase
CTs	Condensed tannins
CVD	Cardiovascular disease
DFR	Dihydroflavonol reductase
DW	Dry weight
eGFP	Enhanced green fluorescent protein
EDTA	Ethylenediaminetetraacetic acid
EF1β	Elongation factor 1-beta
EST	Expressed sequence tag
F3H	Flavanone 3-hydroxylase
F3’H	Flavonoid 3’-hydroxylase
F3’5’H	Flavonoid 3’, 5’-hydroxylase
HPLC	High-performance liquid chromatography
INRA	The French National Institute for Agricultural Research
LAR	Leucoanthocyanidin reductase
LB	Luria-Bertani broth
LC-MS	Liquid chromatography–mass spectrometry
MATE	Multi-drug and toxic compound extrusion protein
MOPS	3-(N-morpholino) propanesulfonic acid
MYB	Myeloblastosis transcription factors
NAD^+	Nicotinamide adenine dinucleotide
$NADP^+$	Nicotinamide adenine dinucleotide phosphate
NCBI	National Center for Biotechnology Information
P450	Cytochrome P450 protein superfamily
PAR	Photosynthetically active radiation
PAs	Proanthocyanidins
PC	Procyanidin
PD	Prodelphinidin
PtF3’5’H1	*Populus trichocarpa* flavonoid 3’, 5’-hydroxylase 1
PtF3’5’H2	*Populus trichocarpa* flavonoid 3’, 5’-hydroxylase 2
ROS	Reactive oxygen species
RT-PCR	Reverse transcription polymerase chain reaction
RT-qPCR	Real-time reverse transcription polymerase chain reaction
SPMs	Secondary plant metabolites

T-DNA	Transfer DNA
TT2	Transparent testa2
TT8/ AtbHLH042	Transparent testa8
TT12	Transparent testa12
UFGT	UDP-glucose:flavonoid-3-O-glucosyltransferase
UV	Ultraviolet
WPM	Woody plant medium

Acknowledgments

I would like to first thank my supervisor, Dr. C. Peter Constabel, for providing me this great opportunity to work on my own project. I appreciate his support and guidance throughout my research. I would also like to thank my committee members Drs. Jürgen Ehlting and Alisdair Boraston for their valuable advice and guidance. Thank you to Dr. Kazuko Yoshida for help with vector construction and for teaching me numerous new lab skills. Thank you to Cuong H. Le, Russell Chedgy and Dr. Vincent Walker for assistance in HPLC analysis. Thank you to David Ma and Tieling Zhang for helping me and providing much advice. Thank you to Gerry Holmes for help in my writing. Thank you to Brad Binges for technical support at the greenhouse. I would also like to thank all the members in the Constabel and Ehlting labs for their generous help throughout my research.

1. Chapter One: Introduction

1.1 Flavonoids introduction

1.1.1 Secondary plant metabolites

Secondary plant metabolites (SPMs) are defined as small organic compounds that do not directly contribute to basic plant metabolisms, such as photosynthesis or respiration, but have other adaptive roles in plants (Theis and Lerdau, 2003). SPMs are often nutritionally valueless, toxic, or have anti-nutritional properties (Acamovic and Brooker, 2005). However, they have been described in many reports to be important for the interaction of the plant and its environment (Pichersky et al., 2006; Chen et al., 2009). In higher plants, SPMs can be divided into nitrogen-containing molecules (alkaloids) and compounds not containing nitrogen (terpenoids, polyketides, and phenolics) (Patra et al., 2013).

1.1.2 Flavonoid structure and diversity

Flavonoids are one group of the most abundant SPMs in plants. They are derived from the phenylpropanoid pathway which produces many plant-specific secondary metabolites including lignin, coumarins, and stilbenoids (Winkel-Shirley, 2002). In general, flavonoids have a fifteen-carbon skeleton that consists of two phenyl rings connected by a three-carbon bridge (C6-C3-C6) (Iwashina, 2000). Flavonoids often exist as glycosides in vacuoles after conjugation with sugars (Aoki et al., 2000). In higher plants, there are seven major groups of flavonoids, including chalcones, flavones, flavanones, flavonols, dihydroflavonols, anthocyanidins, and proanthocyanidins (or PAs) (Winkel-Shirley, 2001) (Figure 1-1).

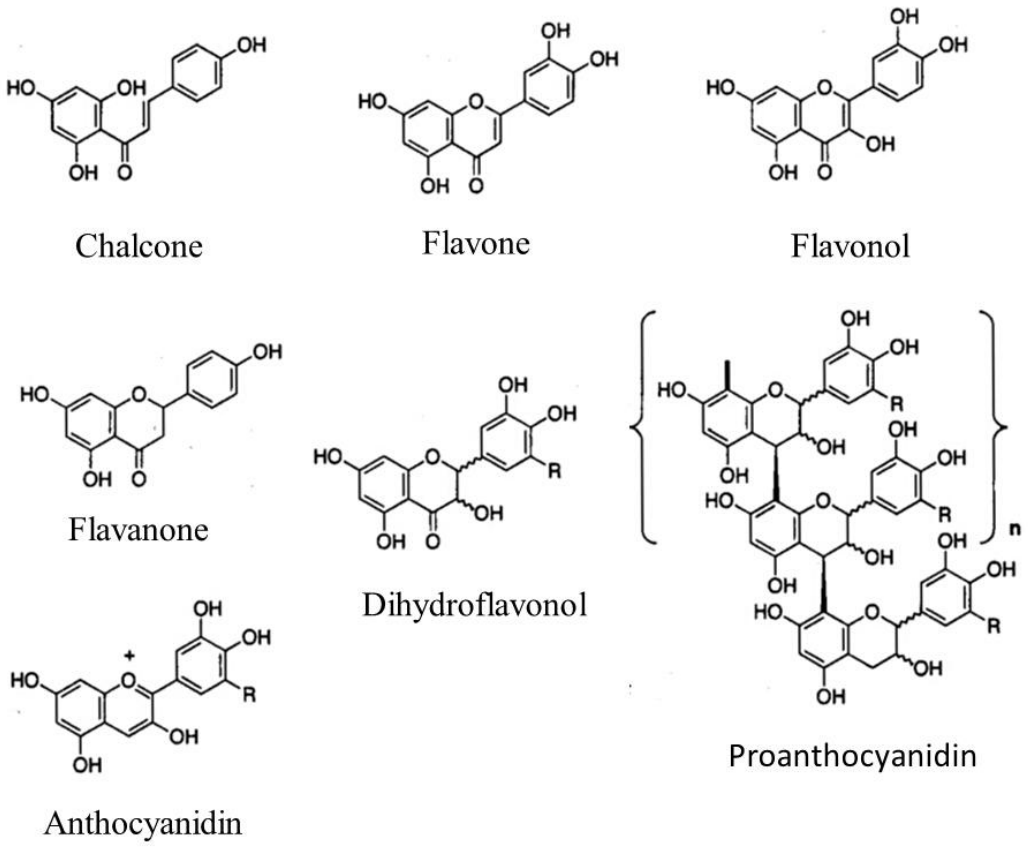

Figure 1-1. Common structures of seven major groups of flavonoids.

Flavonoids exist in all vascular and non-vascular plants, including mosses and ferns (Winkel-Shirley, 2002). However, some specific flavonoids may only be present in certain species (Winkel-Shirley, 2001). For instance, isoflavonoids are found mostly in legumes, while 3-deoxyanthocyanins are only found in a few species such as sorghum (*Sorghum bicolor*), maize (*Zea mays*), and gloxinia (*Sinningia cardinalis*) (Winkel-Shirley, 2001). As a closely related compound to flavonoids, stilbenes are only synthesized by a few species like grape (*Vitis vinifera*), peanut (*Arachis hypogaea*) and pine (*Pinus sylvestris*) (Winkel-Shirley, 2001). Therefore, the distribution of flavonoids is determined by the evolutionary history of that species.

1.1.3 The function of flavonoids

Since plants are immobile and cannot avoid environmental stresses by escaping like animals do, there has always been selective pressure for plants to gain protective mechanisms against adverse environmental conditions. Flavonoids can have very diverse functions in plants. Many studies revealed their roles in plants' interaction with environmental stress, herbivores, and pathogens (Mol et al., 1998; Winkel-Shirley, 2002; Peer and Murphy, 2007). One important role of flavonoids in plants is to function as sunscreens to protect plants from excess UV light. In *Arabidposis*, chalcone synthase (CHS) mutant plants, deficient in flavonols, are more sensitive to UV stress (Li et al., 1993). Likewise, *Arabidopsis* mutants with enhanced flavonoid composition are more tolerant to UV stress (Bieza and Lois, 2001). In poplar, Warren et al. (2003) found that UV stress can induce the production of flavonol glycosides. These studies indicate that flavonoids are associated with plant resistance to UV stress. Flavonoids are also found to be associated with plant resistance against frost, drought, and tolerance to toxic metals (such as aluminium) (Pizzi and Cameron, 1986; Barceló and Poschenrieder, 2002; Tattini et al., 2004; Moore et al., 2005)

In addition to abiotic stress, plants interact with microbes (including pathogens) and herbivores. Plants also develop symbiotic relationships with microbes so that both can benefit from each other. In legumes, plant roots can exude flavonoids as signals to help N_2-fixing bacteria infect the plants and form nodules to help the plant obtain additional nitrogen (Mathesius, 2003; Cooper, 2004; Kobayashi et al., 2004). In wheat, the flavanone naringenin was reported to stimulate the colonization of roots by diazotrophic bacteria, and promote the development of lateral roots (Webster et al., 1998).

Benoit and Berry (1997) found that flavonoids can affect the nodulation of red alder (*Alnus rubra*) by *Frankia* (Actinomycetales).

There are also studies on plant-pathogen interactions, which showed that flavonoids can function as defense compounds. Skadhauge et al. (1997) conducted a study on barley mutants and found that both proanthocyanidins and dihydroquercetin can be used as defense compounds against *Fusarium* species. Beckman (2000) found that anthocyanins are able to help plant fight against wilt disease. Padmavati et al. (1997) found out that the growth rate of *Pyricularia oryzae* (a fungal blast pathogen) on rice is negatively related to the content of naringenin, kaempferol, quercetin, and dihydroquercetin. Flavonoids can sometimes be induced after plants being infected by pathogen. After infection by *Cytonaema* sp., *Eucalyptus globulus* can form wound periderm with accumulation of catechin in lesion margins (Eyles et al., 2003). In addition, unripe fruits like bitter orange and apple are more resistant to fungal decay since they contain more flavonoid derivatives such as naringin, sinensetin, and nobiletin, which suggests that flavonoids have a function in post-harvest resistance against pathogens in fruits (Arcas et al., 2000; Lattanzio, 2003).

Flavonoids are also reported to play an important role in plant-herbivore interactions. In feeding tests, some insects showed high sensitivity to flavonoids such as rutin and dihydroflavonol (Haribal and Feeny, 2003; Chen et al., 2004; Thoison et al., 2004). In a genetic study with groundnut, Mallikarjuna et al. (2004) found a positive correlation between flavonols quercetin and larval mortality of the tobacco army worm *Spodoptera litura*.

The flower colour of plants is mainly controlled by flavonoids, carotenoids and betalains (Tanaka et al., 2008). Among the flavonoids, anthocyanins are the most important pigments. There are six major anthocyanidins (aglycones of anthocyanins): pelargonidin, cyanidin, peonidin, delphinidin, petunidin, and malvidin (Tanaka and Brugliera, 2013) (Figure 1-2). The colour of anthocyanins ranges from yellow to red to violet and blue (Tanaka and Brugliera, 2013). There are many factors that determine the colour of anthocyanins, including the number of hydroxyl groups on the B-ring of anthocyanidins (a greater number of hydroxyl groups will shift anthocyanin colour towards the blue), co-pigments, and metal ions (Yoshida et al., 2009).

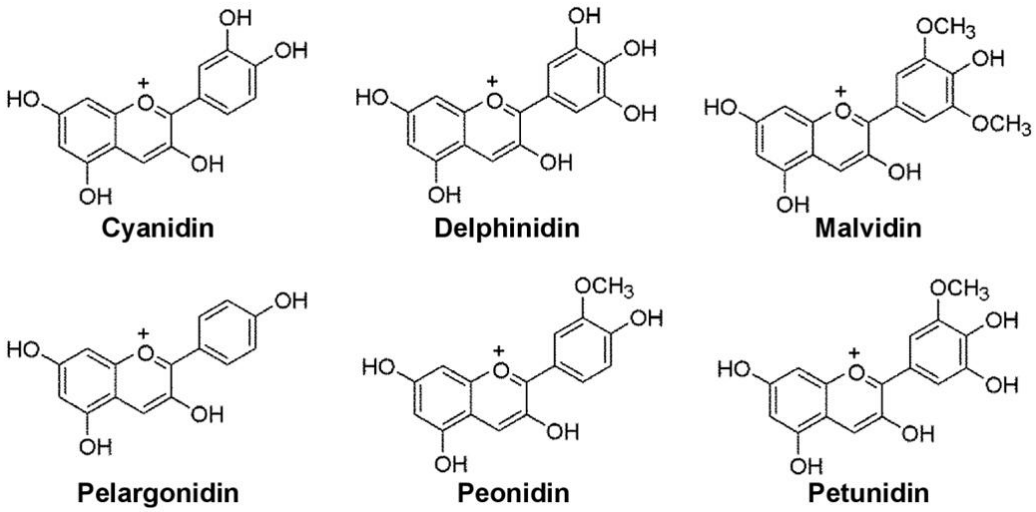

Figure 1-2. Common structures of six major classes of anthocyanidins.

Since anthocyanins are stored in the vacuole, the pH in the vacuole can also affect the colour of anthocyanins. Anthocyanins tend to be red and comparatively more stable at lower pH, while blue and less stable at neutral or higher pH (Yoshida et al., 2009). By chelating the hydroxyl groups on the B-ring of anthocyanins, ferrous and aluminium ions

can help anthocyanins yield blue colour (Yoshida et al., 2009). With these colourful pigments, plants can recruit more pollinators and seed dispersers (Tanaka and Brugliera, 2013). Anthocyanins also have a potential role in protecting plants from UV irradiation, thus functioning as sunscreens for plants. Acylated anthocyanins absorb strongly in the UV region (Giusti et al., 1999). In maize husk tissue, anthocyanins can protect DNA from UV-B irradiation damage (Stapleton and Walbot, 1994). Likewise, anthocyanin-deficient mutants of *Arabidopsis* are more sensitive to UV-B (Li et al., 1993).

Flavonoids also have health benefits to humans. In a survey by Samieri et al. (2014) to explore the relation between flavonoid intake in midlife and healthy aging adults, the higher consumption of flavones, flavanones, anthocyanins, and flavonols was associated with a lower incidence rate of major chronic diseases or major impairments in cognitive or physical function or mental health. McCullough et al. (2012) found that the consumption of five groups of flavonoid (anthocyanidins, flavan-3-ols, flavones, flavonols, and proanthocyanidins) is associated with lower cardiovascular disease (CVD) mortality individually. Quercetin, a flavonol which is ubiquitous in vegetables, fruit, tea and wine, is considered to have strong reactive oxygen species (ROS) scavenging and anti-inflammatory properties (Orsolić et al., 2004; Cushnie and Lamb, 2005).

1.2 Proanthocyanidins

1.2.1 Structure and diversity of proanthocyanidins

Proanthocyanidins (PAs), also known as condensed tannins (CTs), are polymers of flavan-3-ols and therefore one class of flavonoids. The common structures of three major classes of PAs are shown below (Figure 1-3). PAs are one of the major flavonoid

compounds found in higher plants (Xie and Dixon, 2005). Flavan-3-ols, the building blocks of PAs, have the typical C6-C3-C6 flavonoid skeletons. Six major classes of flavan-3-ols are epicatechin, catechin, epialfzelechin, alfzelechin, epigallocatechin, and gallocatechin (Figure 1-3). Depending on different numbers of hydroxyl groups on the B-ring, PAs can be defined as propelargonidins (4'-hydroxyl), procyanidins (3', 4'-hydroxyl) and prodelphinidins (3', 4', 5'-hydroxyl) (He et al., 2008). PAs are wide-spread through the plant kingdom (Xie and Dixon, 2005). They can be the prominent flavonoid compounds in seed coats, leaves, fruits, and flowers of many woody plants (Xie and Dixon, 2005). PAs are common in the human diet as they can be found in cereal grains, tea, red wine, cocoa, and cider (Santos-Buelga and Scalbert, 2000).

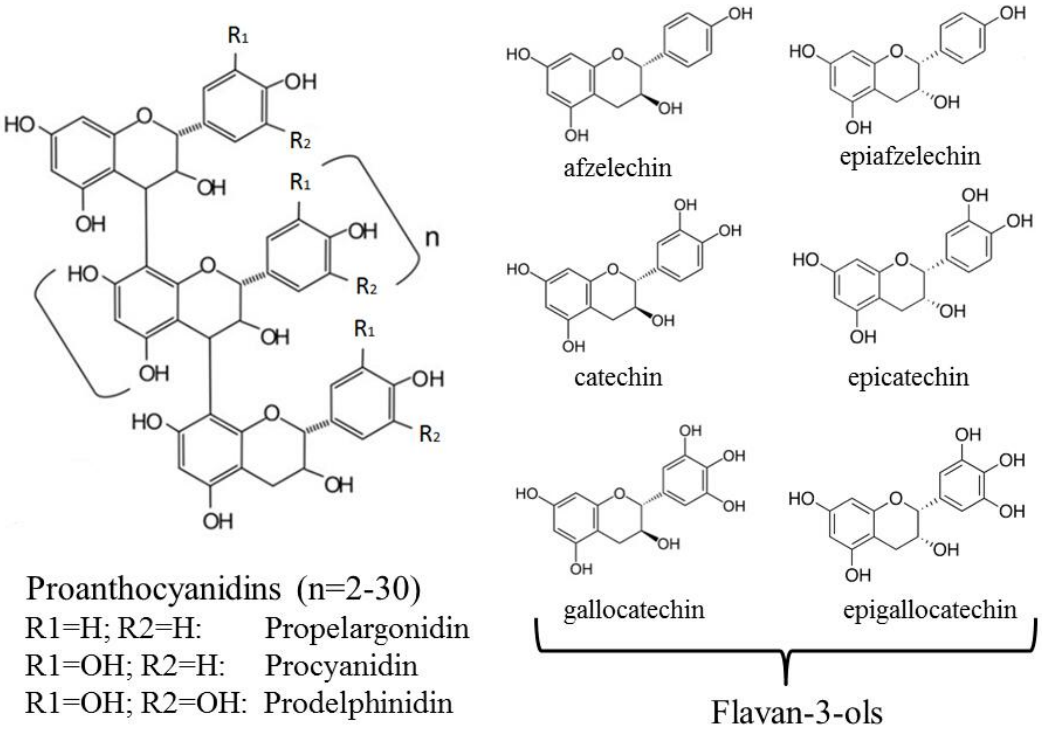

Figure 1-3. Common structures of three major classes of proanthocyanidins and six classes of flavan-3-ols.

1.2.2 The biological function of PAs

PAs have been studied by researchers since the 1960s and they are believed to play an important role in plant-herbivore, plant-microbial interactions and possibly in UV stress tolerance (Feeny, 1970; McArt et al., 2009; Mellway et al., 2009). In food plants, PAs can affect their taste by contributing bitterness and astringency (Santos-Buelga and Scalbert, 2000). PAs antioxidant and anti-inflammatory properties give them a potential role in preventing human diseases, including cancers (Yokozawa et al., 2012). PAs also have benefits when they present at moderate concentration in forage, as they can protect ruminant animals from pasture bloat and enhance the nutrition of the forage (Pang et al., 2007; Zhao and Dixon, 2009).

The anti-herbivore activity of PAs has been investigated in many experimental systems. In a study done by Peters and Constabel (2002), feeding by forest tent caterpillar (*Malacosoma disstria*) and satin moth (*Leucoma salicis*) larvae strongly induced DFR expression in trembling aspen (*Populus tremuloides*), and led to significant accumulation of PAs. The pupal mass and survival rate of *Rheumaptera hastata* caterpillars was significantly reduced when feeding with PA coated (3% dry weight) birch leaves (Bryant et al., 1993). These facts suggest that PAs could be involved in plant herbivore interaction. However, Lindroth and Hwang (1996) found that the leaf consumption rate of gypsy moth larvae is not correlated with PA concentration but with aspen phenolic glycosides. Another study found that neither growth nor reproductive rates of gypsy moth are related to PAs (Osier et al., 2000). One possible theory to explain the function of PAs is that PAs can form complexes with digestive enzymes or their substrates in insect guts so as to affect digestion (Hagerman et al., 1998). In mammalian digestive systems, PAs

can bind with proteins and thus decrease digestion (Shimada, 2006; McArt et al., 2009). By contrast, few studies were able to show any anti-nutritive evidence of PAs on insect herbivores (Bernays et al., 1981). This may be a result of chemical conditions in guts, such as pH (Martin et al., 1985). Therefore, there is a potential for PAs to function in plant defense against herbivores, but only when gut conditions are suitable. The interaction between PAs and herbivore was reviewed by Barbehenn and Constabel (2011), who concluded that tannins can decrease protein digestion in vertebrate herbivores rather than insect herbivores.

PAs may also help protect against microbial and pathogen stress in plants. In poplar, overexpression of PtLAR3 (LAR, leucoanthocyanidin reductase) led to PA accumulation and increased plant resistance to the fungal pathogen *Marssonina brunnea* f.sp. *multigermtubi* (Yuan et al., 2012). Miranda et al. (2007) found that in hybrid poplar (*P. trichocarpa* × *P. deltoides*), leaf rust (*Melampsora medusae*) infection can trigger the transcriptional response of genes encoding enzymes required for PA synthesis. Scalbert (1991) proposed a series of hypotheses behind PAs anti-microbial activity. In his explanation, PAs may bind iron and cause iron depletion in plants, which becomes a limitation for bacterial growth (Scalbert, 1991). Also PAs are proposed to inhibit the enzyme activity of microbes and decrease the amount of useful substrates (Scalbert, 1991). A role in perturbing the electron transport system on the membrane of microbes is another explanation for PAs anti-microbial activity (Scalbert, 1991).

1.2.3 The importance of B-ring hydroxylation pattern to PA activity

The biological properties of PAs can be influenced by the ratio of prodelphinidin and procyanidin subunits, degree of polymerization, interflavan bond position, chain

length, and configuration of the polymers (Zucker et al., 1983; Ayres et al., 1997; Behrens et al., 2003). Ayres et al. (1997) found that PAs with higher ratio of prodelphinidins and average molecular mass appear to have comparatively stronger anti-herbivore activity. In a study conducted by Kraus et al. (2003), PAs comprised of more PC than PD units are more reactive in both the Folin and butanol-HCl assays. Helsper et al. (1993) revealed that procyanidins B2 and C1 from *Vicia faba* (which have fewer 2, 3-*cis* units) have stronger trypsin inhibitor activity. Scioneaux et al. (2011) looked into the PAs composition in two *Populus* species and two hybrids (Fremont (*P. fremontii*), narrowleaf cottonwood (*P. angustifolia*), their F1 hybrids and backcrosses to narrowleaf cottonwood), and found that the prodelphinidin subunit ratio and PA chain length inversely correlate with the rate of leaf decomposition. In all the four "cross types" of *Populus*, the backcross to narrowleaf with the longest chain length and highest percentage of prodelphinidin subunit, shows the slowest decomposition rate (Scioneaux et al., 2011). Nierop et al. (2006) noted that prodelphinidins decreased N mineralization rates more than procyanidins did in Corsican pine litter. In other literature, correlation of PA structure and biochemical properties have been discussed, including interaction with protein, chelation of metals and antioxidant activity (Sarni-Manchado et al., 1998; Weber et al., 2006). Sarni-Manchado et al. (1998) found that PAs with a higher degree of polymerization have a greater capacity to precipitate salivary proteins than lower molecular weight polymers. Similarly, a recent research has demonstrated that PAs ability to precipitate bovine serum albumin (BSA) is associated with its size (Harbertson et al., 2014). The efficiency increased with the degree of polymerization increased from

trimers to octamers (monomers and dimers did not precipitate BSA) (Harbertson et al., 2014).

1.3 Proanthocyanidin synthesis

As one of the end products of the flavonoid pathway, PAs share the same upstream pathway with anthocyanins. Many genes involved in PAs synthesis in plants have been characterized (Nesi et al., 2001; Tanner et al., 2003; Baudry et al., 2004; Bogs et al., 2005; Pang et al., 2007; He et al., 2008; Mellway et al., 2009; Yuan et al., 2012; Liu et al., 2013). By investigating mutants in *Arabidopsis*, maize, barley and other species, the pathway of PAs in plants has been mostly revealed. However, the final step, which is the polymerization and transportation of PAs, still requires further exploration (Jende-Strid, 1993; Abrahams et al., 2002; Cone, 2007).

The general flavonoid pathway in plants which leads to the biosynthesis of PAs is shown in Figure 1-4. The first step is the condensation of three malonyl-CoA with one *p*-coumaroyl-CoA to produce a naringenin chalcone (Kreuzaler and Hahlbrock, 1972). This reaction is catalyzed by chalcone synthase (CHS). CHS has been cloned and characterized in many plants, including *Populus trichocarpa*, *Vitis vinifera*, *Glycine max*, *Ginkgo biloba* and many other species (Sparvoli et al., 1994; Akada and Dube, 1995; Pang et al., 2007; Sun et al., 2011). Isomerization of the naringenin chalcone can happen spontaneously. However, chalcone isomerase (CHI) can accelerate this reaction dramatically (Cain et al., 1997). Via the action of CHS and CHI, the basic chalcone skeleton (C6-C3-C6) aromatic rings are formed. In *Arabidopsis*, CHI is localized on endoplasmic reticulum and tonoplast of the epidermal cells (Saslowsky and Winkel-

Shirley, 2001). Characterization of CHI has been performed in many plants (Sparvoli et al., 1994; Nishihara et al., 2005). A recent study found that in *Solanum lycopersicum*, CHI can affect the production of terpenoids in glandular trichomes via an unknown mechanism (Kang et al., 2014).

Two enzymes of the cytochrome P450 family, flavonoid 3'-hydroxylase and flavonoid 3', 5'-hydroxylase (F3'H and F3'5'H), can carry out hydroxylation on the B-ring of naringenin to form eriodictyol and pentahydroxyflavanone, respectively (Figure 1-4) (Marles et al., 2003). Naringenin, eriodictyol and pentahydroxyflavanone have one, two, and three hydroxyls on their B-ring, respectively. All of these can be hydroxylated on the C-ring to form dihydroflavonols (dihydrokaempferol, dihydroquercetin and dihydromyricetin, respectively) by flavanone 3-β-hydroxylase (F3H). It has been also hypothesized that F3'H and F3'5'H can use dihydrokaempferol as their substrate to form dihydroquercetin and dihydromyricetin, respectively (Figure 1-4). Via these enzymes, the B-ring hydroxylation patterns of flavonone, dihydroflavonol and their downstream products, anthocyanidin and PA are determined (Holton et al., 1993; Werck-Reichhart and Feyereisen, 2000; Schuler and Werck-Reichhart, 2003; Tanaka and Brugliera, 2013). The important role of F3'5'H in anthocyanin and PA synthesis will be discussed later.

The dihydroflavonols (dihydrokaempferol, dihydroquercetin and dihydromyricetin) are further converted into leucoanthocyanidins (leucopelargonidin, leucocyanidin and leucodelphinidin, respectively) by dihydroflavonol 4-reductase (DFR). Then, the flavonoid pathway separates into two branches. First, anthocyanidin synthase (ANS) can oxidize leucoanthocyanidins into anthocyanidins (pelargonidin, cyanidin, and

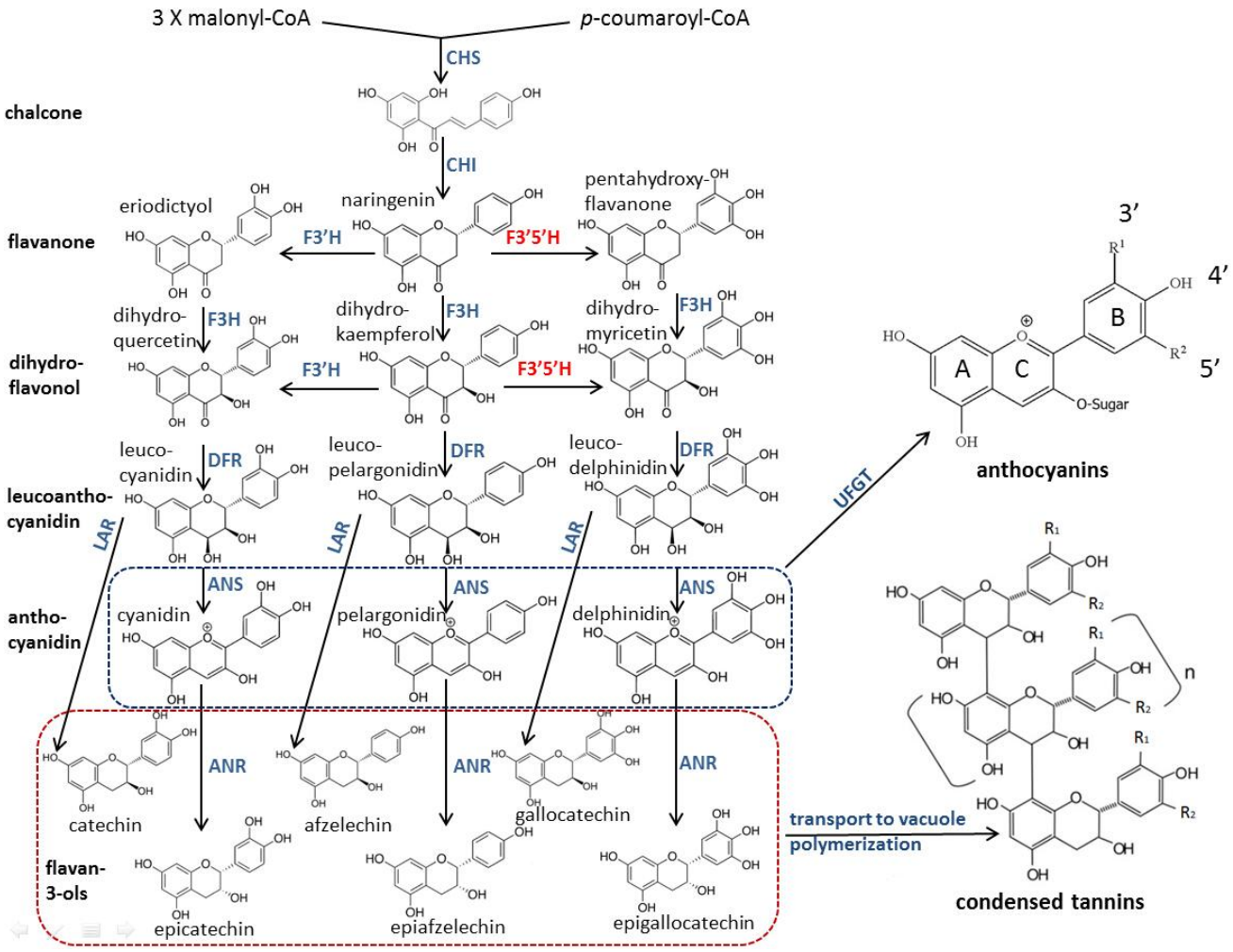

Figure 1-4. General flavonoid pathway in plants leads to the biosynthesis of PAs. Enzyme abbreviations: CHS, chalcone synthase; CHI, chalcone isomerase; F3'H, flavonoid 3'-hydroxylase; F3'5'H, flavonoid 3', 5'-hydroxylase; F3H, flavanone 3-hydroxylase; DFR, dihydroflavonol reductase; ANS, anthocyanidin synthase; LAR, lecuoanthocyanidin reductase; ANR, anthocyanidin reductase; UFGT, flavonoid 3-O-glucosyltransferase.

delphinidin, respectively) (Saito et al., 1999). ANS is a key enzyme in anthocyanidin and proanthocyanidin synthesis, and has been cloned and characterized in many species such as *Brassica juncea*, *Vitis vinifera* and *Theobroma cacao* (Lin-Wang et al., 2010; Yan et al., 2011; Liu et al., 2013). Again, there are two options to catalyze anthocyanidins to the next products. Anthocyanidin can be converted into (2R,3R)-flavan-3-ols [(-)-

epiafzelechin, (-)-epicatechin and (-)-epigallocatechin, respectively] and ultimately PAs by the action of anthocyanidin reductase (ANR) (Xie et al., 2003; Xie et al., 2004). Alternatively, anthocyanidins are conjugated to a sugar (glucoside, galactoside, arabinoside) by a glycosyltransferase (for example, UDP-glucose: flavonoid 3-O-glucosyltransferase) to produce anthocyanin (Ford et al., 1998).

In another branch of the pathway, leucoanthocyanidins will be converted into (2R,3S)-flavan-3-ols [(+)-afzelechin, (+)-catechin and (+)-gallocatechin, respectively] by leucoanthocyanidin reductase (LAR) (Tanner et al., 2003). Some species have two homologous LAR genes such as *Vitis vinifera* and *Gossypium arboretum*, LAR genes in *Populus trichocarpa* are encoded by at least three highly related genes. By contrast, in runner bean (*Phaseolus coccineus*), loblolly pine (*Pinus taeda*), and caloosa grape (*Vitis shuttleworthii*), there is only one copy of the LAR gene (Bogs et al., 2006; Yuan et al., 2012; Wang et al., 2013). Since there is no LAR gene in *Arabidopsis thaliana*, all PAs in *Arabidopsis* are derived from (2R,3R)-flavan-3-ols (Dixon, 2005).

The last step of PAs synthesis is the polymerization of PAs from monomers that are produced via the ANR or LAR pathways described above. (2R, 3R)-flavan-3-ols, (2R, 3S)-flavan-3-ols and (2R,3S,4S)-flavan-3,4-diols are all potential precursors that can be incorporated into PAs directly. However, the enzymes and mechanisms behind this reaction still remain unknown, including the polymerization and transportation of PAs (Marles et al., 2003; Tanner et al., 2003; Dixon, 2005; Xie and Dixon, 2005). Recently, two toxic compound extrusion (MATE) transporters have been characterized from *Arabidopsis* and *Medicago truncatula*, and both of them are able to transport epicatechin 3'-*O*-glucoside, precursor of PA (Marinova et al., 2007; Zhao and Dixon, 2009).

1.4 Regulation of proanthocyanidin biosynthesis

PA synthesis in plants is controlled by a series of regulatory genes at the transcriptional level. They can be divided into three distinct families, basic helix–loop-helix proteins (bHLH), MYB transcriptional factors, and WD40-like protein (Lepiniec et al., 2006). In *Arabidopsis*, PA biosynthesis is shown to be regulated by a complex of the MYB (AtTT2), bHLH (AtbHLH042), and WD40-like proteins (Baudry et al., 2004; Gonzalez et al., 2008). The MYB factor (TT2) is responsible for recognizing target genes, and activating the late PA biosynthetic genes, including DFR, BAN, TT12, and AHA10 (ATPase) (Nesi et al., 2001; Sharma and Dixon, 2005). In poplar, a TT2-like R2R3 MYB protein MYB134 was discovered, which can trigger the production of PA (Mellway et al., 2009). Overexpression of MYB134 in transgenic poplar causes activation of specific PA pathway genes and leads to significant increase of PA concentration. In addition, PtMYB115, an R2R3 MYB protein in poplar was also found to be able to promote the synthesis of PAs (Franklin, 2013). In strawberry (*Fragaria ananassa*), FaMYB9/FaMYB11, FabHLH3, and FaTTG1 are the respective functional homologs of AtTT2, AtTT8 and AtTTG1 (Schaart et al., 2013).

In some plants, PA synthesis can be modulated by environmental factors. For example, wounding, pathogen, and light stress can regulate the biosynthesis of PAs in poplar by triggering the expression of PtMYB134 (Mellway et al., 2009). In tea leaves (*Camellia sinensis*), infection by blister blight resulted in a shift of the proanthocyanidin stereochemistry from 2,3-trans (catechin and gallocatechin) towards 2,3-cis (epicatechin and epigallocatechin) (Nimal Punyasiri et al., 2004). In European silver birch (*Betula*

pendula), increased carbon dioxide and ozone can lead to accumulation of PAs in their leaves (Peltonen et al., 2005).

1.5 Poplar as an experimental system for PA metabolism and regulation

Poplar is wide-spread in North America (Brunner et al., 2004). It is a keystone species in several ecosystems, and the first tree to be genetically transformed (Fillatti et al., 1987). Poplar is easy to propagate in tissue culture. *Agrobacterium*-mediated plant transformation in poplar has been proven to be efficient and stable. Another advantages of using poplar as a model system to study plant metabolism is that it has a sequenced genome (*Populus trichocarpa*, subspecies of *Populus balsamifera*) (Tuskan et al., 2006). Comprehensive *in silico* expression data is available through tools such as the Poplar Expression browser from the Bio-Analytic Resource for Plant Biology (Wilkins et al., 2009). In addition, poplar has an active, interesting inducible defense response system which involves the production of PAs (Major and Constabel, 2006; Constabel and Lindroth, 2010).

Populus is an attractive plant for PA studies. In poplar, phenolic glycosides and PAs together comprise more than 30% of leaf dry weight (Lindroth and Hwang, 1996). In *Populus*, the composition of PAs is strongly controlled by genetics and developmental zone (Rehill et al., 2006). In research using two *Populus* species and two hybrids (Fremont (*Populus fremontii*), narrowleaf cottonwood (*P. angustifolia*), their F1 hybrids and backcrosses to narrowleaf cottonwood), concentration of PAs is found to be associated with species and developmental zones (Rehill et al., 2006). Backcross hybrid has the highest PA concentration (16.7% DW) among the four species and hybrids, F1

(2.3% DW) and Fremont (0.4% DW) have the lowest PA concentration, while narrowleaf cottonwood has an intermediate concentration (10.5% DW) (Rehill et al., 2006). Developmental zones can also affect PA concentration. The juvenile zone is often intermediate compared to the mature zone and juvenile ramets (Rehill et al., 2006). In *P. tremula* × *P. tremuloides* (clone INRA 353-38), PA is found to be most abundant in root tissues, some in stems and very little in leaves (Franklin, 2013). In quaking aspen (*Populus tremuloides*), light availability is also found to be a very important factor affecting PA concentrations. Remarkable differences of PA concentration among genotypes and nutrient treatment is found under high light conditions, while little difference is found under low light conditions (Osier and Lindroth, 2006). Lindroth et al. (2001) found elevated CO_2 can increase the concentration of PA in quaking aspen (*Populus tremuloides*). In a study done by Mellway et al. (2009), both wounding, pathogen infection and UV-B can affect the expression of PtMYB134 so as to regulate the production of PA in poplar. Much quantitative research of PAs in poplar has been carried out, while little is known about the qualitative variation of PAs among different species and tissues. In the study mentioned above by Scioneaux et al. (2011), four different *Populus* species and hybrids showed a different PA profile. PAs in narrowleaf poplar (*P. angustifolia*) and back-cross to narrowleaf contain 40%-50% prodelphinidin subunits and have a comparatively long chain length. While Fremont poplar (*P. fremontii*) has a low portion of prodelphinidin (20%) and the chain length is short. These results are consistent with the low expression of F3’5’H in Fremont (Rehill et al., 2006). In F1 hybrids, PA is mainly comprised of procyanidin and the chain length is longer than that of Fremont poplar but shorter than that of narrowleaf poplar. No strong effect of season

or developmental zone is found on qualitative characteristics of PAs (Scioneaux et al., 2011).

1.6 Flavonoid 3', 5'-hydroxylase and its role in anthocyanin synthesis

Flavonoid 3', 5'-hydroxylase belongs to the cytochrome P450 protein family. The P450s are a large class of heme-containing mixed-function oxidases catalyzing NADPH- or NADH-dependent oxygenation reactions on a broad range of substrates (Graham and Peterson, 1999; Werck-Reichhart and Feyereisen, 2000; Schuler and Werck-Reichhart, 2003). P450s are found in all organisms, in prokaryotes as well as in eukaryotes, with the highest proliferation in plants (Nelson et al., 2004). In *Arabidopsis*, P450 coding sequences represent around 1% of the gene complement. Most plant P450s are bound to the endoplasmatic reticulum (Hasemann et al., 1995; Rupasinghe et al., 2003). P450s are classified with respect to their amino acid sequence identity (Nebert and Nelson, 1991). P450s that share more than 40% identity are classified as a family and members of a family share more than 55% identity form a subfamily. Groups of P450 genes with a clear monophyletic origin are designated as a clan. The F3'H and F3'5'H are grouped into the subfamilies CYP75B and CYP75A. Together they form the CYP75 family and are part of the CYP71 clan.

Two flavonoid 3', 5'-hydroxylase genes (F3'5'H) are present in the *Populus* genome, but RT-PCR amplification from a wide range of genotypes and tissues yields no product for F3'5'H2, suggesting that the activity of F3'5'H in poplar is executed by a single expressed gene (Tsai et al., 2006; Dr. Vincent Walker, unpublished work). Both F3'H and F3'5'H genes were first isolated from petunia (Holton et al., 1993; Brugliera et

al., 1999). Their homologs are subsequently isolated from other plants such as gentian (Tanaka et al., 1996), grape (Bogs et al., 2006), *Arabidopsis* (Schoenbohm et al., 2000), tomato (Olsen et al., 2010), and apple (Han et al., 2010).

The activity of F3’5’H was first demonstrated in the microsomal fraction of *Verbena hybrid* flowers, followed by the flowers of *Callistephus chinensis*, *Lathyrus odoratus*, and *Petunia hybrid* (Forkmann and Heller, 1999). The biochemical function of F3’5’H is usually verified by the recombinant protein assay or/and colour changes in plants (Tanaka, 2006). F3’H and F3’5’H can catalyze the B-ring hydroxylation of flavanones, dihydroflavonols, flavonols, and flavones. Both flavanones and dihydroflavonols are precursors of anthocyanins (Tanaka, 2006). F3’H is responsible for introducing hydroxyl group at the 3’- position of B-ring, while F3’5’H is responsible for introducing hydroxyl groups at both the 3’- and 5’- position of B-ring (Figure 1-4). Thus, F3’H and F3’5’H together control the B-ring hydroxylation pattern of anthocyanins.

The normal function of F3’5’H in plants usually requires a cytochrome P450 reductase to transfer electrons from NADPH to F3’5’H. In petunia, a cytochrome b5 is found to specifically transfer electrons to F3’5’H, which helps the production of delphinidin (Vetten et al., 1999). The activities of F3’H and F3’5’H in *Gerbera hybrida* (gerbera) and African daisy have been shown to be associated with their C-terminal region sequences. The B-ring hydroxylation pattern of flavonoid changed when one or two amino acid residues in the C-terminal region of *Gerbera hybrida* (gerbera) and African daisy F3’H and F3’5’H were substituted (Seitz et al., 2007).

Characterization of F3’5’H in many plants has shown its role in anthocyanin synthesis. In grapevine, transcription levels of VvF3’H and VvF3’5’H are consistent with

the accumulation levels of the respective hydroxylated anthocyanin and PAs (Bogs et al., 2006). F3’5’H is desired for the genetic transformation of species like rose or carnation, which do not naturally possess F3’5’H activity and therefore cannot produce blue colours based on delphinidin derivatives (Tanaka et al., 1998; Forkmann and Martens, 2001; Fukui et al., 2003; Tanaka et al., 2005). The ectopic expression of VvF3’H and VvF3’5’H in petunia changed the anthocyanin composition and altered the flower colour (Bogs et al., 2006). Expression of viola F3’5’H in transgenic rose led to accumulation of delphinidin and generated a blue colour flower petals (Katsumoto et al., 2007). Qi et al. (2013) successfully produced petunia with blue flowers by expressing *Phalaenopsis* F3’5’H and *Hyacinthus orientalis* DFR in it.

However, F3’5’H from one species does not always function as expected in another species. Since chrysanthemum lack blue flowers, He et al. (2013) tried to rebuild the delphinidin pathway by down-regulating CmF3’H (RNAi) and overexpressing the *Senecio cruentus* F3’5’H gene in chrysanthemum. In those plants, the amount of cyanidin was increased significantly, but not delphinidin. This indicates that introducing novel blue color might require manipulation of additional factors in the flavonoid pathway. Possible factors restricting the application of F3’5’H in anthocyanin synthesis could be the substrate specificity of DFR, which catalyzes the next step of reaction in the flavonoid pathway (Figure 1-4). DFRs in some species have distinct preferences for substrates and their degree of hydroxylation. For example, DFRs in petunia and *Saussurea medusa* cannot use dihydrokaempferol as their substrate (Gerats et al., 1982; Johnson et al., 1999; Yuan et al., 2012). This directly leads to different ratios of pelargonidin with cyanidin and delphinidin downstream. By analyzing the sequences of

DFRs from different species, Johnson et al. (2001) identified a region that determines the substrate specificity of DFRs. By changing a single amino acid in this region, they successfully generated a DFR, which can use dihydrokaempferol as its preferred substrate rather than dihydroquercetin (Johnson et al., 2001).

1.7 Predicted roles of F3’5’H in PA synthesis

Due to the prevelance of prodelphinidin unit in many PA polymers, F3’5’H is predicted to participate in PAs synthesis. Using flavanone and dihydroflavonol as substrates, F3’5’H can change the B-ring hydroxylation pattern of the PA precursors. This is predicted to lead to the production of prodelphinidin, which has three hydroxyls on its B-ring. Correlation of F3’5’H expression level and PAs composition confirms this idea. In grape (*Vitis vinifera*), temporal and tissue-specific expression of VvF3’5’H1 is in correspondence with the accumulation of the prodelphinidin units. All of the PA subunits in the seeds comprise only 3’, 4’-hydroxylated units (catechin and epicatechin), whereas more than 50% subunits of PA in the berry skins contain the 3’, 4’, 5’-hydroxylated epigallocatechin. This correlates with the generally low expression of VvF3’5’H1 in seeds and its relatively high expression in skin (Downey et al., 2003; Bogs et al., 2006). By contrast, in flower, stem, and tendril, the expression level of F3’H is higher than F3’5’H, and a comparatively higher amount of quercetin than myricetin as well as a higher amount of procyanidin than prodelphinidin are found (Jeong et al., 2006). These results suggest that the expression pattern of VvF3’5’H1 is consistent with its involvement in hydroxylation of both anthocyanins, flavonols, and PAs in grape berries, and suggest its functions in PA synthesis in grape (Bogs et al., 2006). In *Populus*, a

correlation between prodelphinidin-type subunits of PAs and the expression of flavonoid 3', 5'-hydroxylase is found in F1 hybrids of narrowleaf and Fremont, which indicates the composition of proanthocyanidins in *Populus* reflects the levels of flavonoid 3', 5'-hydroxylase (Tsai et al., 2006; Scioneaux et al., 2011). However, in a study done by Robbins et al. (2005), introducing F3'5'H from *Eustoma grandiflorum* into *Lotus* root cultures increased the amount of PAs, but did not alter the degree of polymer hydroxylation. This suggests that there are other mechanisms controlling the hydroxylation pattern of PA in *Lotus*.

Despite a few studies on the relationship between F3'5'H and PA B-ring hydroxylation pattern, it is still unknown if overexpressing the endogenous F3'5'H in a given species can change the PA hydroxylation pattern. Since proanthocyanidins share the same upstream precursors as anthocyanidins, I predicted that F3'5'H is a critical enzyme in the PAs synthesis in *Populus*. Stronger expression of F3'5'H in poplar may lead to more 3', 4', 5'-hydroxylated units in PAs, which could change the bioactivity of PAs. With that, such transgenic poplar could gain some novel characteristics in terms of stress resistance.

1.8 Objectives

The overall objective of this thesis research is to determine the role of PtF3'5'H1 in PA and anthocyanin synthesis in poplar. The specific questions to be addressed are: 1) Can the degree of hydroxylation of PA be affected by PtF3'5'H1 overexpression? 2) Could PtF3'5'H1 overexpression affect PA concentration? 3) Is PtF3'5'H1 involved in anthocyanin biosynthesis in poplar? Since poplar hairy root is fast-growing and abundant

in phenolics, it was chosen as a first tool to conduct PA synthesis research. Overexpression of PtF3’5’H1 in transgenic hairy root culture of 717 (*P. tremula* × *P.alba*) plants was conducted to investigate the function of PtF3’5’H1 in PA synthesis. To test the role of PtF3’5’H1 in both anthocyanins and proanthocyanidins synthesis in poplar directly, PtF3’5’H1 overexpressing hybrid aspen plants were generated. In addition, agrobacterium-infiltration of AtPAP1 (*Arabidopsis* production of anthocyanin pigment 1, MYB transcription factor), At GL3 (*Arabidopsis* bHLH transcription factor), and PtF3’5’H1 in *Nicotiana benthamiana* leaf was carried out as a separate functional assay to test the role of PtF3’5’H 1 in anthocyanin synthesis.

2. Chapter Two: Methods

2.1 Phylogenetic analysis

Nucleotide sequences were downloaded from NCBI nucleotide and EST databases (www.ncbi.nlm.nih.gov/) using PtF3’5’H1 as bait. Alignment was done using Clustal Omega software (http://www.clustal.org/omega/) (Sievers et al., 2011). A phylogenetic tree was constructed based on the approximate maximum likelihood method using FastTree (http://microbesonline.org/fasttree/) (Price et al., 2009). Bootstraps (1,000 replicates) were calculated by using Seqboot, values have been labeled on the branches. Fig Tree (version 1.4.0) was used to present and edit the tree (http://tree.bio.ed.ac.uk/software/figtree/).

2.2 Generation of transgenic plants overexpressing PtF3’5’H1

2.2.1 Vector construction and Agrobacterium transformation

P. tremula × *P. tremuloides* clone INRA 353-38 cultures were available in the Constabel lab. Plants were micropropagated *in vitro* using McCown’s woody plant medium (Caisson, North Logan, Utah, United States) (For composition, see Table A-1). cDNA of *Populus trichocarpa* was made in the lab by using young leaves of *Populus trichocarpa* grown in the Bev Glover greenhouse at the University of Victoria. The sequence of PtF3’5’H1 was amplified from cDNA of *Populus trichocarpa* using a primer set of PtF3’5’H1 attB1 (5’-AAAAAGCAGGCTATGGCCTTAAACATGGTCCT-3’) and PtF3’5’H1 attB2 (5’-AGAAAGCTGGGTTTAAGCAAGATATGCGTTAGGT-3’). An entry clone was generated by performing a BP recombination reaction between an *att*B-flanked DNA fragment and an *att*P-containing donor vector (pDONR™ 221).

Subsequently, an expression clone was generated by performing an LR recombination reaction between an *att*L-containing entry clone and an *att*R-containing destination vector (pMDC32, obtained from Dr. Kazuko Yoshida). A map of pMDC32:PtF3’5’H1 vector is shown in Figure 2-1 (SnapGene Viewer version 2.6.2). The sequence of pMDC32:PtF3’5’H1 vector was sent to Operon (Huntsville, Alabama, United States) for sequencing and confirmed the insertion of full coding sequence.

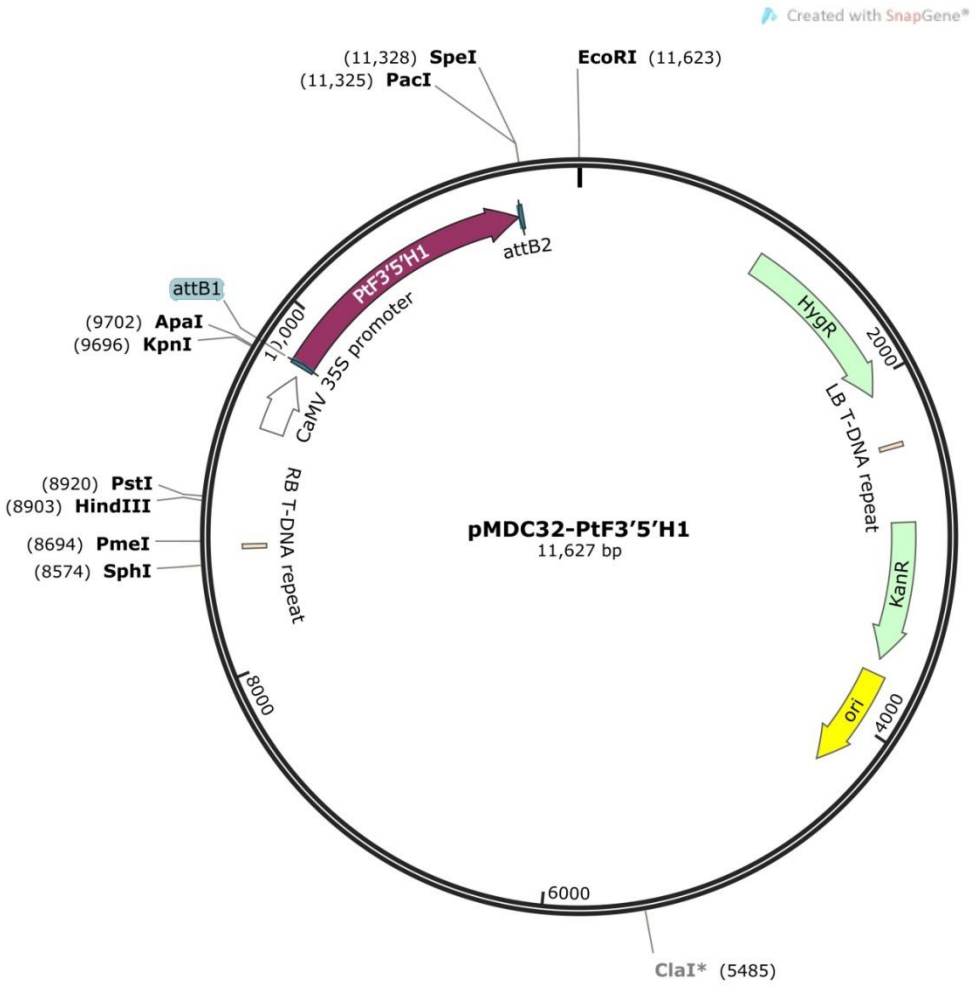

Figure 2-1. A map view of pMDC32:PtF3’5’H1 plant expression vector.

The pMDC32:PtF3’5’H1 plasmid was transferred into *Agrobacterium tumefaciens* strain GV3101 (MP90) by electroporation. pMDC32:PtF3’5’H1 plasmid (2

µL) and GV3101 (MP90) competent cells (40 µL) were pipetted into an electroporation cuvette (90 µL Signature™ Disposable Electroporation Cuvette, VWR, Randor, Pennsylvania, United States) and mixed well by pipetting. The cuvette was then electroporated at 1300 V using an Eppendorf Electroporator 2510 (Eppendorf, Hamburg, Germany). Subsequently, 1 mL of LB liquid medium (For composition, see Table A-1) was added, and the cuvette was incubated (MaxQ™ 4000 Benchtop Orbital Shakers, Thermo Fisher Scientific, Waltham, Massachusetts, United States) at 28℃ for 2 hours. The culture (100 µL) was then spread on LB solid medium with antibiotics (For composition, see Table A-1). Colonies that appeared on the plates were checked for positive transformation by colony PCR (Mastercycler Gradient, Eppendorf, Hamburg, Germany).

To prepare for plant transformation, positive colonies were chosen. *Agrobacterium tumefaciens* cells carrying pMDC32:PtF3’5’H1 were grown overnight in LB liquid medium with antibiotics (For composition, see Table A-1) at 28℃, 225 rpm. *Agrobacterium* cells carrying empty pMDC32 vector were used as control. Cells were centrifuged at 3,500 rpm for 35 min and re-suspended in induction medium (For composition, see Table A-1) to an OD_{600} of 0.5. The *Agrobacterium* suspension was placed back in the shaking incubator (28℃) for an additional 30 to 60 min until the suspension reached an OD_{600} of approximately 0.6. Leaves were excised from *P. tremula* × *P. tremuloides* clone INRA 353-38 *in vitro* plantlets (2 to 4 months old) and wounded with multiple fine cuts with a sterile scalpel across the leaf and vein. The leaves were then immediately placed into the *Agrobacterium* suspension and shaken at 130 rpm for 1 hour at 28℃. The leaves were blotted dry on sterile filter paper, plated abaxial (bottom)

side down on callus induction medium 1 (For composition, see Table A-1) and incubated in the dark for two days (22°C). The leaves were subsequently transferred to callus induction medium 2 (For composition, see Table A-1) and incubated for three weeks in darkness. The explants were then transferred to shoot induction medium (For composition, see Table A-1) and grown under light conditions in growth chambers. When shoots reached 0.5 to 1 cm in height, plants were excised and placed onto root induction medium (For composition, see Table A-1) in magenta boxes (Caisson, North Logan, Utah, United States). Positive transformants after rooting were confirmed by semi-quantitative PCR using primer set F3'5'H1AF (5'-AGCCGGATTTTCTGGACGTT-3') and F3'5'H1AR (5'-CGCCGATTTCGACCAATGAC-3').

2.2.2 Plant growth conditions in greenhouse and harvest

Positive transformants were micropropagated on McCown's woody plant medium (For composition, see Table A-1). The plants were grown in the Bev Glover greenhouse (UVic) for about 3 months before being harvested. Plantlets were acclimated in Sunshine Mix #4 (Sungro, Seba beach, AB, Canada) in a mist chamber for 4 weeks before being moved into the greenhouse and grown in Sunshine Mix #4 with fertilizer (5.65 g/L soil ACER® 21-7-14 (Plant Products Co. Ltd, Brampton, ON, Canada), 0.77 g/L soil Micromax Micronutrients (Scotts-Sierra, Marysville, Ohio, United States), 3.01 g/L soil dolomite lime (IMASCO, Surrey, BC, Canada), and 0.29 g/L soil superphosphate 0-20-0 (Green Valley, Surrey, BC, Canada)). Plants were randomly placed in the greenhouse and rotated every week, supplemental light was provided to give a day length of 16 hour light and the temperature was maintained between 18°C and 28°C. Plants were maintained in the greenhouse for 12 weeks, and reached an average height of 72.4 cm.

Prior to harvest, plants were moved outside of the greenhouse (Victoria, BC, Canada, May 22 – May 29, 2014) to be exposed to natural sunlight for one week (average UV-B intensity during the day was 0.125 mW/cm^2, average Photosynthetically Active Radiation (PAR) was 1252.3 μmol/s/m^2, accumulated precipitation was 8.4 mm, average high and low temperature at 18.6°C and 9.6°C with the mean temperature at 14.1°C). When harvested, the plants had reached an average height of 84.6 cm.

Leaves of various ages (LPI (leaf plastochron index) 1-6, 10-12, and 13-15), periderm, and roots were harvested. One leaf of LPI 10 had been harvested prior to the plants being moved outside. Mid-veins of the leaves were removed before freezing samples in liquid nitrogen. Samples were stored at -80 ℃ until analyzed.

2.3 Generation of transgenic poplar hairy roots overexpressing PtF3'5'H1

Populus tremula × *Populus alba* clone INRA 717-1-B4 cultures were available in the Constabel lab. Plants were micropropagated *in vitro* using McCown's woody plant medium (For composition, see Table A-1). pMDC32 modified with eGFP (enhanced green fluorescence protein) driven by the rolD promoter for the hairy root expression vector was obtained from David Ma. The pMDC32 (eGFP):PtF3'5'H1 plasmid was made as described above and moved into *Agrobacterium rhizogenes* strain ARqual by electroporation (same conditions as above) (Figure 2-2).

Agrobacterium rhizogenes cells carrying pMDC32 (eGFP):PtF3'5'H1 were grown overnight in MG/L medium (For composition, see Table A-1) at 28 ℃, 225 rpm. *Agrobacterium* cells carrying empty pMDC32 (eGFP) vectors were used as a control. Cells were centrifuged at 3,500 rpm for 20 min and re-suspended in induction broth (For

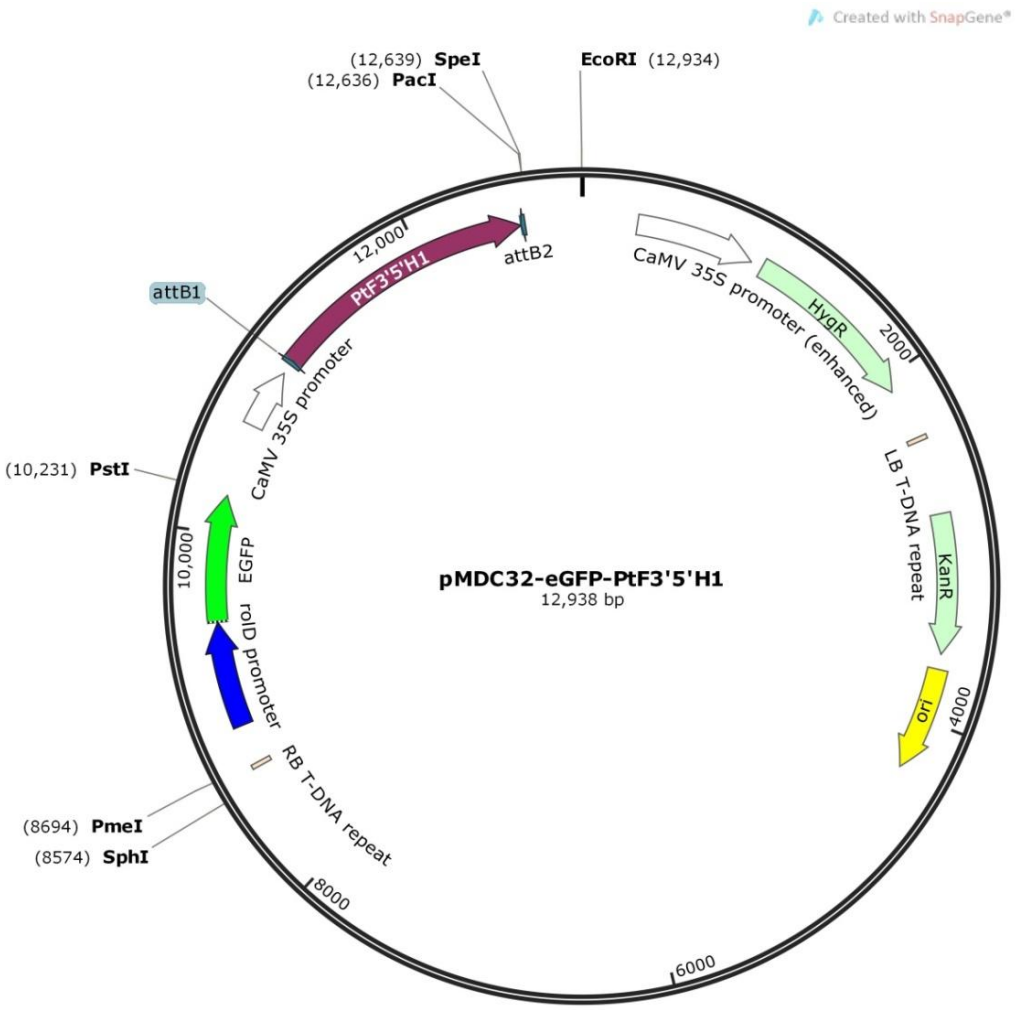

Figure 2-2. A map view of pMDC32 (eGFP):PtF3'5'H1 plant expression vector.

composition, see Table A-1) to an OD_{600} of 0.6-0.8. Leaves were excised from *Populus tremula* × *Populus alba in vitro* plants (2 to 4 months old) and wounded with multiple fine cuts with a sterile scalpel across the leaf and mid-vein. The leaves were then immediately placed into the *Agrobacterium* suspension and incubated at 100 rpm for 90 min at 28 ℃. The leaves were then blotted dry on sterile filter paper and plated abaxial (bottom) side down on co-cultivation medium (For composition, see Table A-1) and

incubated in the dark for 2 days (22 ℃). Explants were subsequently transferred to antibiotic medium (For composition, see Table A-1) to kill *Agrobacterium*, and maintained in the dark. The leaves were transferred to fresh medium every week. After the appearance of roots, explants were moved to selection medium (For composition, see Table A-1) to select for positive transformants. Roots were maintained by transferring to fresh selection medium every week. Positive transformants were screened by GFP detection under UV light using an Olympus SZX7 Zoom Stereomicroscope.

2.4 Transient transformation of *Nicotiana benthamiana* by *Agrobacterium* infiltration

A. tumefaciens GV3101 (pMP90) with pMDC32 and pMDC32:PtF3’5’H1 were described earlier. In addition, *A. tumefaciens* GV3101 (pMP90) with pMDC32:AtPAP1 and pMDC32:AtGL3 were provided by Dr. Kazuko Yoshida in Dr. Peter Constabel’s lab. All the transformed *A. tumefaciens* strain GV3101 was kept at -80 ℃ as glycerol stocks for long term storage.

To prepare for infiltration, *Agrobacterium* stocks were streaked out on solid LB medium with antibiotics (For composition, see Table A-1). The plates were incubated in darkness for 2 days. After incubation, separated colonies were picked and inoculated in 50 mL conical tubes containing 10 mL of LB liquid medium with antibiotics (For composition, see Table A-1). The inoculated cultures were then incubated at 28 ℃ overnight (225 rpm). The *Agrobacterium* in each falcon tube was centrifuged and re-suspended in 10 mM $MgCl_2$ until an absorbance reading of 0.6-0.8 at 600 nm. Three combinations of the *Agrobacterium* culture were made in 15 mL conical tubes for transformation: pMDC32 vector only (negative control), equal volumes of

pMDC32:AtPAP1 and pMDC32:AtGL3 (positive control), equal volumes of pMDC32:PtF3’5’H1, pMDC32:AtPAP1, and pMDC32:AtGL3.

N. benthamiana was grown from seed and maintained in the Bev Glover greenhouse at the University of Victoria. Plants in growth chamber received a 16 hours of light per day, from 6 am to 10 pm, with photosynthetically active radiation (PAR) intensity at 110 μmol/s/m^2. Temperature in the growth chamber was controlled around 22 ℃. Plants were watered three times a week. After growing for about 5 weeks, *N. benthamiana* plants reached a height of about 12 cm and were ready for agroinfiltration. Three days prior to agroinfiltration, water was withheld to increase the transformation efficiency. Leaves with a length of 3 cm are considered ideal for infiltration. No more than two leaves were infiltrated on each plant. *Agrobacterium* with different construct was carefully injected into the back side of the leaves using a blunt 1 mL syringe. The infiltrated plants were grown in the growth chamber for one week with normal water supply to give time for the transgene to be expressed and metabolites to accumulate.

One week after infiltration, leaves were excised from the plants. Three leaf discs with a radius of 7 mm were punched from the infiltrated leaf (avoiding the initial injection spot) using a cork borer. Nine discs (about 0.3 g each) of infiltrated *N. benthamiana* leaves were then extracted in 6 mL of 100% methanol with 1% HCl in 15 mL conical tubes. The tubes were kept in darkness and rotated on the Belly Dancer shaker (Stovall Life Science Incorporated, Greensboro, North Carolina, United States) for 2 hours to extract anthocyanins. Subsequently, extract containing mainly anthocyanin and chlorophyll was placed into borosilicate disposable glass culture tubes and concentrated

under vacuum overnight using the Savant SpeedVac SC 110A Concentrator. The extract was analyzed by HPLC as described below (Section 2.9).

2.5 Extraction of plant tissue for analysis of total phenolics

Approximately 20 mg of freeze-dried plant tissues was placed in a cryotube (Thermo Fisher Scientific, Waltham, Massachusetts, United States) with 1.5 mL of 100% HPLC grade methanol (Sigma-Aldrich, St. Louis, Missouri, United States). Samples were homogenized in cryotubes using a PRECELLYS® 24 homogenizer (Bertin Technologies, Tarnos, France) for two cycles (each 45 seconds, 5,500 rpm). Samples were then sonicated for 10 min (75T Ultrasonic Water Bath, VWR, Radnor, Pennsylvania, United States). After sonicating, samples were centrifuged for 10 min at 15,000 rpm (Eppendorf Centrifuge 5424, Hamburg, Germany), and the supernatant was transferred into borosilicate disposable glass culture tubes (Ulti Dent Scientific, St. Laurent, QC, Canada). 100% HPLC grade methanol (1 mL) was added into the pellet, after vortexing, sonicating, and centrifuging, the supernatant was transferred into the glass culture tubes above. One additional mL of HPLC grade methanol was added to the pellet, extracted and centrifuged as above, and then added to the extract in the glass culture tubes. Extracts were used for HPLC (3 mL) and the butanol-HCl tannin assay (0.5 mL). For HPLC analysis, borosilicate disposable glass culture tubes with extracts were dried in a Savant SpeedVac SC 110A Concentrator overnight. Subsequently, the dried extracts were weighed and re-suspended in 300 µL of 100% methanol. Samples were pre-cleaned through Strata-X 33-µm solid-phase extraction columns (Phenomenex, Torrance, California, United States) to remove chlorophyll and other non-phenolic metabolites.

Before eluting samples, the Strata-X column was washed with 100% methanol followed by dH_2O. The samples were eluted in approximately 9 mL of 100% methanol and again dried overnight in the Savant SpeedVac SC 110A Concentrator. For HPLC analysis, the dried extracts were re-suspended in 100% methanol to a final concentration of 5 mg/mL.

2.6 Butanol-HCl assay for quantification of PA

Freeze-dried leaf (LPI 1-6, LPI 10-12 and LPI 13-15), root, stem periderm, and hairy root tissues were extracted in 100% methanol (see detailed extraction method in Section 2.5 phenolics extraction). The butanol-HCl assay was modified from Porter et al. (1985). Extract (0.5 mL) was added to 2 mL of butanol-HCl (95:5 v/v) and 66.75 µL of iron reagent (2% w/v $NH_4Fe(SO_4)_2$ in 2 N HCl). The reaction mix was heated in a water bath at 95 ℃ for 40 min in sealed 15 mL conical tubes and allowed to cool for 20 min. 200 µL of each reaction was loaded onto a 96 well plate (Costar™ Cell Culture Plates, Corning Incorporated, Corning, New York, United States). A Perkin Elmer Victor TM X5 multiple plate reader (Perkin Elmer, Waltham, Massachusetts, United States) was used to read the absorbance of the reaction at 550 nm. Absorbance readings of unheated replicate samples were used as controls and readings subtracted to correct for anthocyanins and other pigments in extracts.

2.7 RNA extraction and reverse transcription

RNA was extracted by following the method published by Muoki et al. (2012). Approximately 100 mg of frozen plant tissues ground to fine powder in liquid nitrogen using a mortar and pestle was used for RNA extraction. Ground frozen tissue powder was

added to 1 mL of buffer I (2% cetyltrimethylammonium bromide (CTAB) (w/v), 2% polyvinylpolypyrrolidone (PVPP) (w/v), 100 mM (hydroxymethyl) aminomethane (Tris-HCl (pH, 8.0)), 125 mM tetraethylenediamine acetic acid (EDTA (pH, 8.0)), 2 M sodium chloride, and 2% β-mercaptoethanol) and ground in mortar until obtaining a liquid mixture. The mixture was transferred into a 2 mL Eppendorf tube, which was then incubated in a water bath (Precision 280-Series Water Bath, Thermo Fisher Scientific, Waltham, Massachusetts, United States) at 65 ℃ for 15 min. During incubation, tubes were mixed twice by vortexing (Vortex-Genie 2, Bohemia, New York, United States). The mixture was then added to 1 mL of chloroform: IAA (isoamyl alcohol) (24:1 v/v) and mixed well by vortexing. After centrifuging at 13,000 rpm for 10 min at room temperature, the supernatant was pipetted into a new tube and another 1 mL of chloroform: IAA was added. The tubes were again mixed well by vortexing and then centrifuged again at 13,000 rpm for 10 min at room temperature. The supernatant was transferred to a second tube. Extraction buffer Ⅱ (1 mL) (phenol saturated with Tris buffer with a pH of 8, sodium dodecyl sulfate (SDS, 0. 1% (w/v)), sodium acetate (0.32 M (w/v)), and EDTA (0.01M, pH 8.0) was added to the tube and vortexed. Chloroform (200 μL) was added and vortexed again. Samples were centrifuged at 13,000 rpm for 10 min at 4 ℃. The supernatant was again transferred to a new tube and added with 0.6 volume ratio of isopropanol (RNAse free). The sample was left at room temperature for 10 min and then centrifuged at 13,000 rpm for 10 min at 4 ℃. The supernatant was removed, and the RNA pellet was washed with 70% ethanol (RNAse free) and dried in a sterile flow hood. When dry, the pellet was resuspended in 22 μL of diethylpyrocarbonate (DEPC) treated distilled H_2O. The quality of the RNA was assessed by denaturing gel

electrophoresis (gel composition: 0.5 g agarose in 50 mL of 1 × MOPS (0.04 M MOPS, 0.01 M sodium acetate, 1 μM EDTA)). RNA and purity concentration was measured using NanoDrop 2000 UV-Vis Spectrophotometer (Thermo Scientific, Wilmington, Delaware, United States). RNA was stored at -20 ℃ for short term usage and -80 ℃ for long term storage.

To obtain cDNA for qPCR from RNA, total RNA was treated with DNase I (Amplification Grade) (Invitrogen, Carlsbad, California, United States) to eliminate possible genomic DNA contamination. The DNase treatment reaction included 2.5 μL of DNase I, 2.5 μL of 10× DNase I Reaction Buffer, 2.5 μg of RNA, and the volume adjusted to 25 μL using DEPC treated H_2O (refer to DNase I user manual for detailed steps). SuperScript Ⅱ reverse transcriptase (Invitrogen, Carlsbad, California, United States) was used to carry out RT-PCR reactions and synthesize cDNA. RT-PCR reaction included 1 μL of oligo(dT) primers (Life Technologies, Carlsbad, California, United States), 1 μL of 10 μM dNTP mix, 4 μL 5×first-strand buffer, 2 μL 100 mM DTT (dithiothreitol), 0.5 μg of RNA and the volume was adjusted to 19.5 μL (refer to SuperScript Ⅱ reverse transcriptase user manual for detailed steps).

2.8 qPCR

Quantitative polymerase chain reaction (qPCR) was performed using the QuantiTect SYBR Green RT-PCR kit (Qiagen, Mississauga, ON, Canada). Each reaction contained 2 μL of 1:20 diluted cDNA template (5 ng) (for ANR2, 1:5 diluted cDNA template was used), 0.5 μL of 10 μM forward and reverse primers (See Table 2-1), 7.5 μL of 2×Quantitect master mix (Hot Start Taq DNA polymerase, deoxyribonucleotide

triphosphate mix, SYBR Green I dye, ROX reference dye, and PCR buffer), and 4.5 μL of water for a final reaction volume of 15 μL. For each reaction, at least two identical technical replicates were analyzed. For each sample, a no-reverse transcriptase control was also included. qPCR was performed on a Bio-Rad CFX96 Touch™ Real-Time PCR Detection System (Bio-Rad Laboratories, Hercules, California, United States). The PCR cycle conditions were: 10 min at 95 ℃ followed by 40 cycles of 95 ℃ for 30 sec, 58 to 60 ℃ for 20 sec (See Table 2-1 for annealing temperatures), 72 ℃ for 30 sec followed by one cycle of 95 ℃ for one min, 58 to 60 ℃ for 30 sec, and 95 ℃ for 30 sec. Annealing temperatures were optimized for optimal primer efficiency. Primer efficiency was estimated by calculating the slope of a 4 × dilution series of template concentration.

Table 2-1. List of primers used for qPCR analysis.

Gene name	Forward primer	Reverse primer	Amplication length (bp)	Annealing temperature (℃)
EF1β	AAGAGGACAAGAAGGCAGCA	CTAACCGCCTTCTCCAACAC	145	58
Act	CCCATTGAGCACGGTATTGT	TACGACCACTGGCATACAGG	235	56
F3'5'H1A	AGCCGGATTTTCTGGACGTT	CGCCGATTTCGACCAATGAC	220	60
ANR1	GCTACCCTGCCTCCAAGACA	CGTGCGTGATTGAGATCGAGCC	228	58
DFR1	CTTATAACTGCCCTTTCTCTGA	AGATCATGAATGGTGGCTT	173	58
DFR2	CCAAGACTTTAGCAGAGCA	TGTTAGCATCATCCGAGTTG	282	58
CHS1	TGTGTGAATACATGGCTCCGTCTCT	GGATTTTGGCTGACCCCACTCTT	119	58
ANS1	GCGAGCAAAATTCTGTCAGC	TCATAGAAGAGTTGCAGGC	224	58
LAR3	CCTCGAATGTGGCCACCCCAC	GCTATGCTTGCACCACCAACAGC	201	58

Efficiency was calculated using the slope in the following equation: primer efficiency %= $((10^{-(1/slope)})-1)100$. Poplar housekeeping gene elongation factor 1-beta (EF1β, accession number: XM_002299613) and actin (accession number: XM_002298674.2) were used to normalize the expression of target genes by the $2^{-\Delta\Delta CT}$ method (Livak and Schmittgen, 2001). The CT is the number of cycles that it takes for each reaction to reach a certain amount of fluorescence. In this method, genes (usually housekeeping gene) expressed at a

constant level between the samples were used as control to test the difference in expression level of target genes (Livak and Schmittgen, 2001).

2.9 Anthocyanin extraction

2.9.1 Anthocyanin extraction from poplar young leaves

Anthocyanins were extracted from poplar by following a combination of protocols derived from previous studies (Lea et al., 2007; Pang et al., 2007; Nemie-Feyissa et al., 2014). About 25 mg of freeze-dried poplar young leaves (LPI 1-6) were weighed and put into Eppendorf tubes containing 0.5 mL of methanol with 1% HCl. The tubes were kept in the dark when shaken on the Belly Dancer shaker (Stovall Life Science Incorporated, Greensboro, North Carolina, United States) for extraction (2 hours). The liquid was transferred to new tubes with 0.5 mL of H_2O and mixed by vortexing. One mL of chloroform was further added and the tubes were mixed by vortexing again. Tubes were then centrifuged (Microcentrifuge model 5424, Eppendorf, Hamburg, Germany) at 4,000 rpm for 5 min. The supernatant was kept at -20 ℃ until loaded onto the HPLC.

2.9.2 *Anthocyanin extraction from N. benthamiana* leaves

Similar to extracting anthocyanins from poplar leaves, anthocyanin in *N. benthamiana* leaves were extracted by following a combination of protocols derived from previous studies (Lea et al., 2007; Pang et al., 2007; Nemie-Feyissa et al., 2014). The concentrated pellet was re-suspended with 1.5 mL methanol with 1% HCl. After sonicating for 5 min, samples were then transferred to 15 mL falcon tubes. Equal amount of H_2O (1.5 mL) was added to the samples and mixed by vortexing. Subsequently, 3 mL

of chloroform was added and mixed by vortexing again. After centrifuging for 5 min, supernatant containing mainly anthocyanins was measured by a GENESYS™ 10S UV-Vis Spectrophotometer at both 530 nm (anthocyanin) and 657 nm (chlorophyll). The relative anthocyanin content was estimated as A530-A657 for the absorbance of anthocyanin and chlorophyll, respectively. After measurement, the samples were proceeded with HPLC (see below).

2.10 Analysis of phytochemicals by high-performance liquid chromatography

Analysis of phenolics was performed using a Dionex UltiMate® 3000 HPLC system with auto sampler column compartment and photodiode array detector (Dionex, Sunnyvale, California, United States) plus a Phenomenex Kinetex C18 column (150 × 4.6, 2.6 µm; 100 Å) (Torrance, California, United States). 20 µL of the extract was injected into the system for each sample. Separation was performed with an elution gradient consisting of solvent A (0.4% formic acid in dH_2O) and solvent B (0.4% formic acid in acetonitrile) over 55 min at a flow rate of 1 mL per min. The gradient consisted of 5% B for 5 min, increased to 14% B in 6 min, increased to 38% B in 29 min, increased to 100% B in 2 min, maintained at 100% B for 5 min, decreased to 5% B in 2 min, maintained at 5% B for 5 min. Analysis was performed with Chromeleon 7 software (Dionex, Sunnyvale, California, United States). The baseline was added manually for calculation of peak areas.

Analysis of anthocyanins was performed using the same HPLC system and column. 20 µL of the extract was injected onto the system for each sample. Separation was performed with an elution gradient consisting of solvent A (4% formic acid in dH_2O)

and solvent B (4% formic acid, 50% acetonitrile, 46% dH_2O) over 27.5 min at a flow rate of 1 mL per min. The gradient consisted of 15% B for 7.5 min, increased to 45% B in 12.5 min, increased to 100% B in 3 min, maintained at 100% B for 1 min, decreased to 15% B in 1 min, maintained at 15% B for 2 min. Analysis was performed with Chromeleon 7 software (Dionex, Sunnyvale, California, United States). The baseline was added manually for calculation of peak area. Compounds were putatively identified by comparing retention times and UV spectra from the literature. Compounds were quantified at 520 nm.

3. Chapter Three: Results

3.1 *In silico* analysis of poplar F3'5'H genes

A number of F3'5'H genes from diverse plant species are functionally characterized, including *Catharanthus roseus*, *Epimedium sagittatum* and *Solanum tuberosum* (Kaltenbach et al., 1999; Boase et al., 2010; Huang et al., 2012). In the poplar genome, two putative F3'5'H genes are present (POPTR_0009s07320 and POPTR_0001s28140), and share 87% sequence similarity (Tsai et al., 2006). Phylogenetic analysis showed that both predicted proteins clustered in a clade with characterized F3'5'H proteins (Figure 3-1). This clade was distinct from the F3'H group, which is responsible for the 3'-position hydroxylation of the flavonoid B-ring. Therefore, the two identified candidate genes are likely to encode the F3'5'H proteins.

Previous RT-PCR expression studies of PtF3'5'H2 from various poplar tissues had shown no or low expression, whereas PtF3'5'H1 was highly expressed in young poplar leaf, female and male catkins (Vincent Walker and C. Peter Constabel, Unpublished data). In addition, MYB115 overexpression poplars with high expression of PA pathway genes had shown a dramatic induction of PtF3'5'H1, indicating the possible role of PtF3'5'H1 in PA synthesis in poplar (Franklin, 2013). Therefore, PtF3'5'H1 was chosen for further studies.

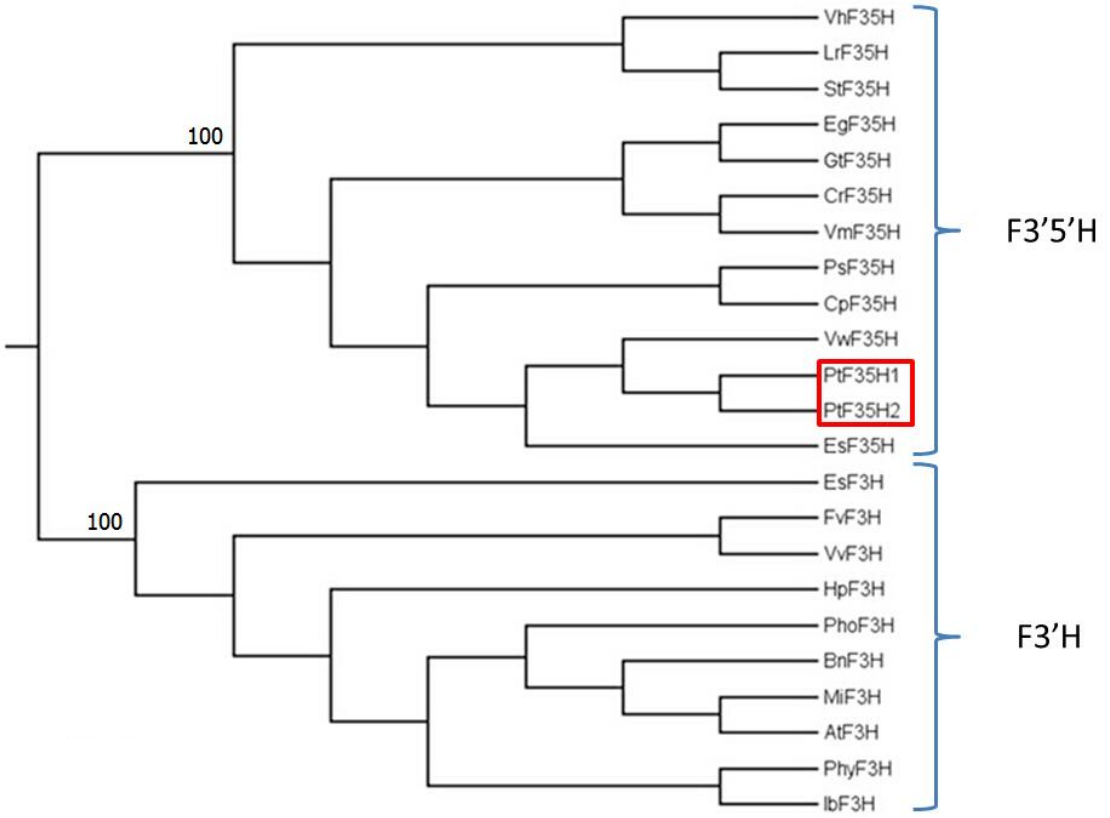

Figure 3-1. Phylogenetic tree representing functionally characterized flavonoid 3', 5'-hydroxylase and flavonoid 3'-hydroxylases.
Sequences of functionally characterized flavonoid 3'-hydroxylases and flavonoid 3', 5'-hydroxylases were obtained from NCBI nucleotide and EST databases. Alignment was done using Clustal Omega alignment software. Phylogenetic tree was constructed based on approximately maximum likelihood methods using FastTree. Bootstraps (1000 replicates) were calculated from Seqboot and values of percentage have been labeled on the branches. Accession numbers from GenBank: *Catharanthus roseus* CrF3'5'H, CAA09850.1; *Cyclamen persicum* CpF3'5'H, ACX37698.1; *Epimedium sagittatum* EsF3'5'H, ADE80942.1; *Eustoma grandiflorum* EgF3'5'H, BAD34460.1; *Gentiana triflora* GtF3'5'H, BAA12735.1; *Lycianthes rantonnei* LrF3'5'H, AAG49300.1; *Pisum sativum* PsF3'5'H, ADW66160.1; *Solanum tuberosum* StF3'5'H, AAV85470.1; *Verbena hybrid* VhF3'5'H, BAE72871.1; *Vinca major* VmF3'5'H, BAC97831.1; *Viola wittrockiana* VwF3'5'H, BAF93855.1; *Arabidopsis thaliana* AtF3'H, AAG16745.1; *Brassica napus* BnF3'H, ABC58723.1; *Epimedium sagittatum* EsF3'H, ADE80941.1; *Fragaria vesca* FvF3'H, AEE60883.1; *Hieracium pilosella* HpF3'H, ABC47161.1; *Ipomoea batatas* IbF3'H, AEH42499.1; *Matthiola incana* MiF3'H, AAG49301.1; *Pelargonium hortorum* PhoF3'H, AAG49315.1; *Petunia hybrida* PhyF3'H, AAD56282.1; *Vitis vinifera* VvF3'H, CAI54278.1. NCBI reference sequence: *Populus trichocarpa* PtF3'5'H1, XM_002313968.2; *Populus trichocarpa* PtF3'5'H2, XM_002298428.1.

3.2 Expression profiling of PtF3’5’H1 in various poplar tissues

In silico analysis using the Poplar eFP browser, a web-based expression profile tool for *P. trichocarpa*, suggested that PtF3’5’H1 was most abundant in young poplar leaves and male, female catkins (Figure 3-2, 3-3) (Wilkins et al., 2009). In contrast, very little expression was detected in mature leaves, roots or xylem (Figure 3-2, 3-3) (Wilkins et al., 2009). By contrast, PtF3’5’H2 had a comparatively high expression level in female and male catkins, while very low expression was found in all the other tissues (Figure 3-4) (Wilkins et al., 2009).

To verify the expression pattern of PtF3’5’H1 in a hybrid aspen (*P. tremula* × *P. tremuloides*), RT-qPCR was performed. The plants were grown in the Bev Glover greenhouse (UVic) with supplemental light (16 hours daylight) at 18 ℃ to 28 ℃ for approximately 3 months before harvest. The leaves of LPI 1-6 (young), 10-12 (medium), 13-15 (mature), stem periderm, and root were analyzed. Male catkins were obtained from native *Populus trichocarpa*. This analysis showed that PtF3’5’H1 was most highly expressed in young leaves and stem periderm (Figure 3-5). The lowest expression level was detected in medium and mature leaves. Male catkins and roots had a moderate expression level compared to other tissues (Figure 3-5). This data is similar to the *in silico* analysis obtained from the Poplar eFP Browser (Figure 3-2, 3-3). Thus, it can be concluded that PtF3’5’H1 is most highly expressed in young leaves and stem periderm, but is expressed at a low level in mature leaves.

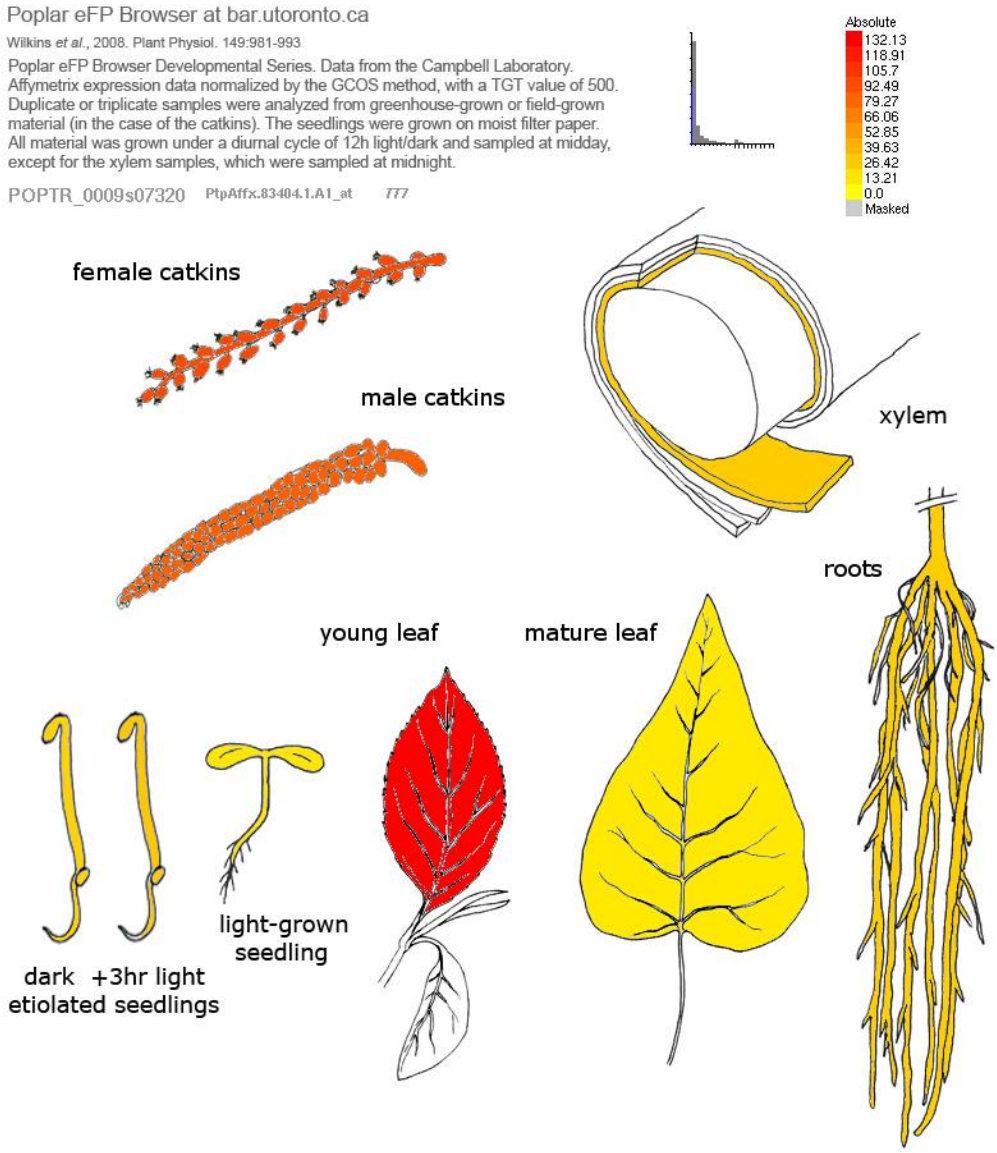

Figure 3-2. *In silico* analysis of the relative expression level of PtF3'5'H1 in various poplar tissues (picture).
The poplar eFP browser (http://bar.utoronto.ca/efppop/cgi-bin/efpWeb.cgi) was queried with ID: POPTR_0009s07320. This analysis provided an *in silico* read-out of the expression profile of *Populus trichocarpa* PtF3'5'H1. The expression file is based on Affymetrix microarray data.

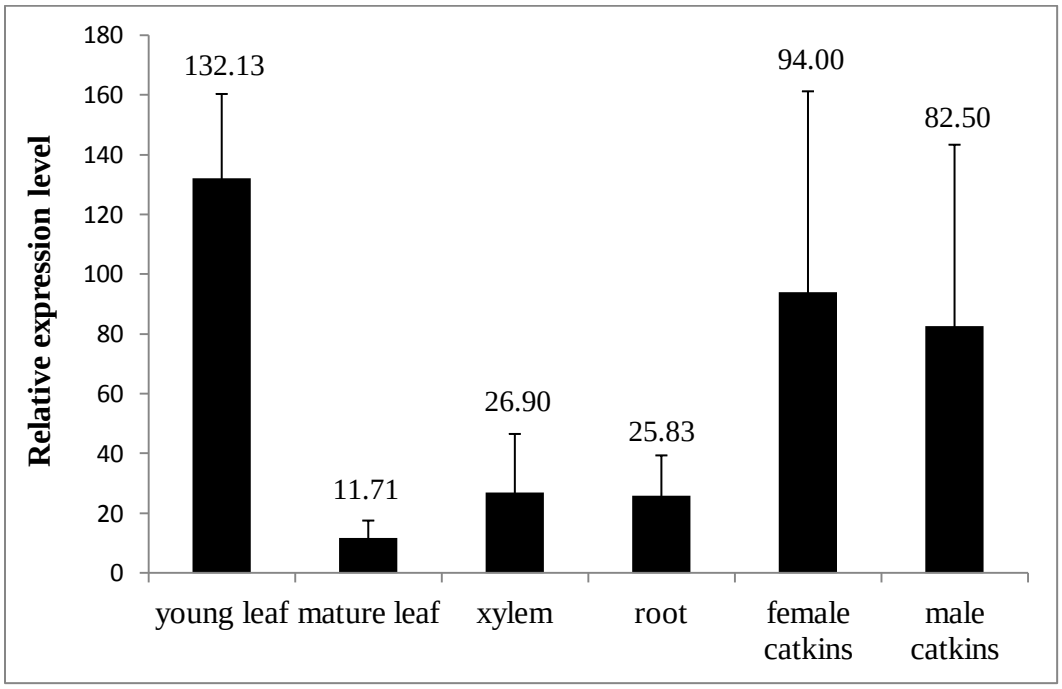

Figure 3-3. *In silico* analysis of the relative expression level of PtF3'5'H1 in various poplar tissues (graph).
The expression data from Figure 3-2 were plotted as a bar graph of the expression levels to better visualize differences. Bars represent means of expression levels, error bars represent standard error (n=3).

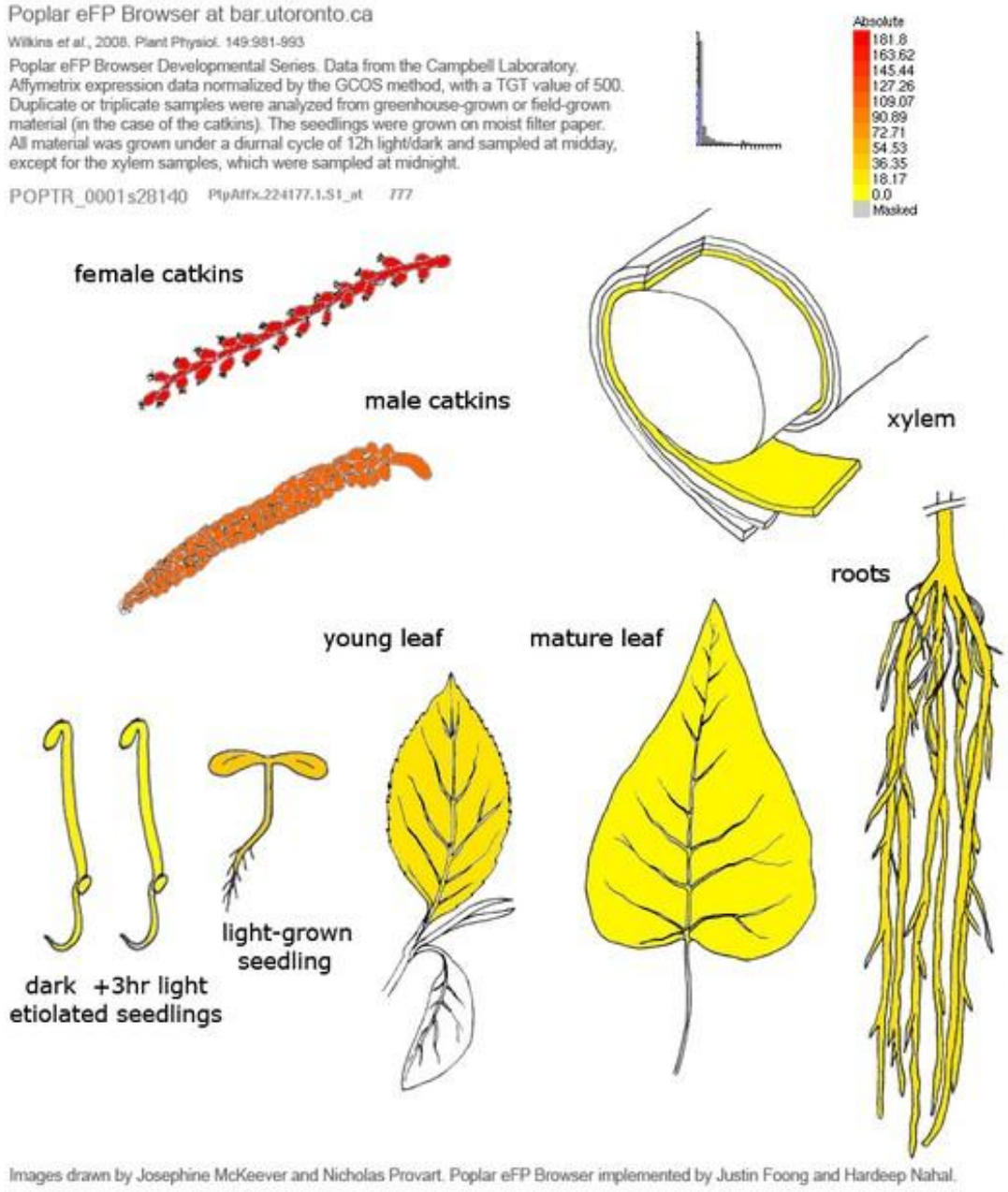

Figure 3-4. *In silico* analysis of the relative expression level of PtF3'5'H2 in various poplar tissues.
The poplar eFP browser (http://bar.utoronto.ca/efppop/cgi-bin/efpWeb.cgi) was queried with ID: POPTR_0001s28140. This analysis provided an *in silico* read out of the expression profile of *Populus balsamifera* PtF3'5'H1. The expression file is based on Affymetrix microarray data.

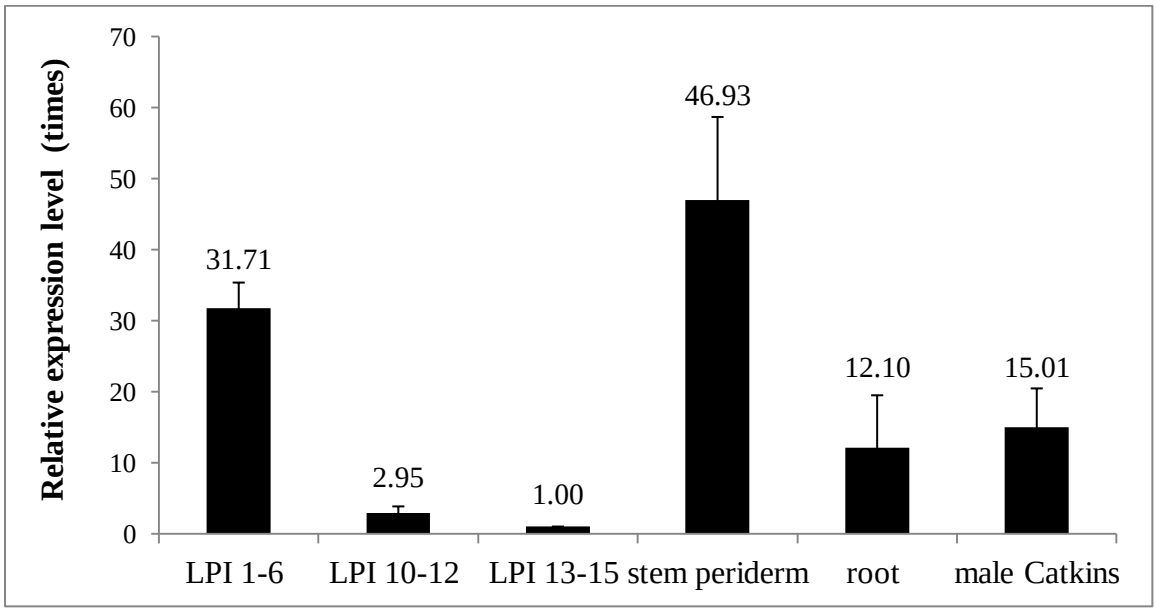

Figure 3-5. Relative expression level of PtF3'5'H1 in various poplar tissues of young *P. tremula* × *P. tremuloides* samplings.
Plant tissues were collected from *P. tremula* × *P. tremuloides* grown in the Bev Glover greenhouse (UVic, 16 hour daylight, 18 ℃ to 28 ℃). Plants received one week of natural sunlight before harvest. RT-qPCR was performed to check the expression profile of PtF3'5'H1. LPI 1-6, young leaves; LPI 10-12, medium leaves; LPI 13-15, mature leaves. Bars represent means of expression levels, error bars represent standard error (n=3).

3.3 PA profile in *P. tremula* × *P. tremuloides* (INRA clone of 353-38)

To have a better understanding of the distribution of PAs in the tissue analyzed for PtF3'5'H1 expression level by RT-qPCR, the butanol-HCl assay for PAs was performed using methanol extracts of freeze dried tissues. The highest concentration of PAs was in the root (39.84 mg/g, SE=10. 04, n=3) (Figure 3-6). In contrast, a lower concentration of PAs was detected in all leaf samples (young, medium, mature), and stem periderm (Figure 3-6). Among all leaf tissues, young leaves had the highest level of PAs, followed by medium leaves, and then mature leaves. This suggests that the concentration of PAs in poplar leaves is associated with the younger leaf developmental zone (leaf age),

paralleling the expression of PtF3’5’H1. The other tissues showed no correspondence of PAs with PtF3’5’H1, however.

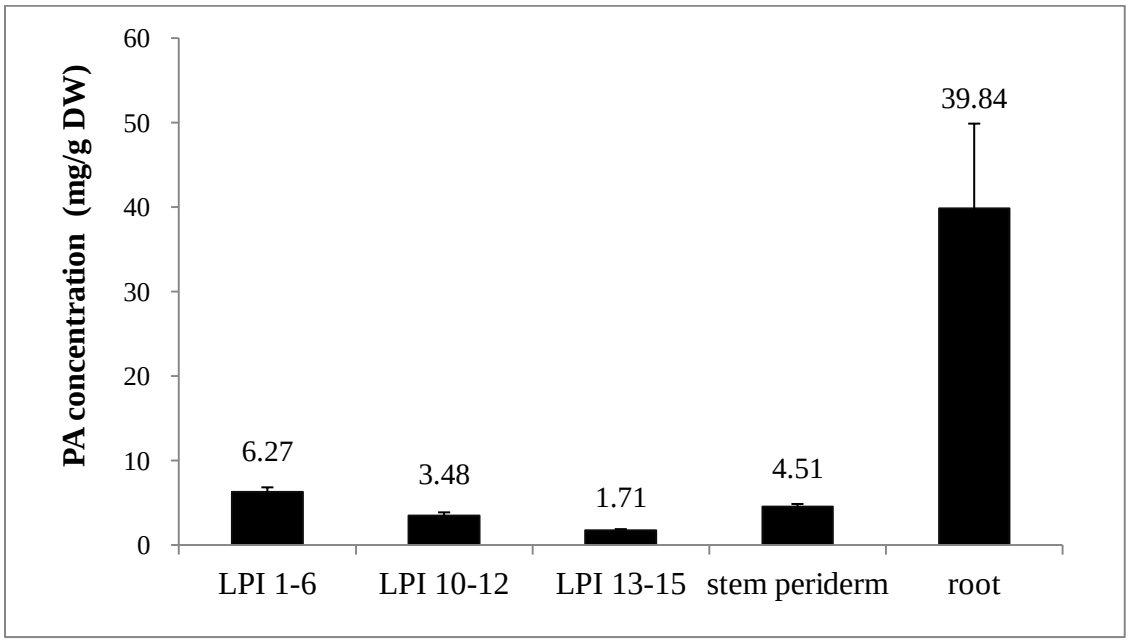

Figure 3-6. PA concentration in different *P. tremula* × *P. tremuloides* tissues. Plant tissues were collected from *P. tremula* × *P. tremuloides* grown in the Bev Glover greenhouse (UVic, 16 hour daylight, 18 ℃ to 28 ℃). Plants received one week of natural sunlight before harvest. LPI 1-6, young leaves; LPI 10-12, medium leaves; LPI 13-15, mature leaves. Tissues were freeze-dried and PAs in methanolic extracts were quantified by the butanol-HCl assay. DW stands for dry weight. Bars represent means of PA concentration, error bars represent standard error (n=3).

3.4 Generation of transgenic hairy root cultures overexpressing PtF3’5’H1

In order to test if overexpressing PtF3’5’H1 can affect the accumulation of PA in poplar, *P. tremula* × *P. alba* INRA clone 717-1-B4 was subjected to hairy root transformation. This approach allows for rapid regeneration of transgenic tissues, and this particular poplar hybrid is most susceptible to *Agrobacterium rhizogenes* infection. A vector based on pMDC32 with eGFP (enhanced green fluorescent protein) (Yang et al.,

1996) carrying the PtF3’5’H1coding sequence under the control of the double 35S promoter was constructed. A pMDC32 (eGFP) vector without PtF3’5’H1 was made as an empty vector control. Eight sets of *Agrobacterium* (*Agrobacterium rhizogenes* strain ARqual) infections were performed, with approximately 45 leaf explants for each set. In total, approximately 180 leaves were infected by *A. rhizogenes* carrying the PtF3’5’H1 overexpressing vector, and 180 leaves were infected by *A. rhizogenes* carrying the empty pMDC32 (GFP) vector.

From eight sets of infection, 50 individual roots were gained (23 from PtF3’5’H1 overexpressing vector, 27 from the empty vector), a success rate of 13.9%. Individual independently grown roots were subcultured on antibiotic-containing solid medium to generate triplicate clonal cultures. After subculture, it took 1 to 2 months for the root to reach sufficient growth for chemical analysis. Because of the eGFP marker on the plasmid, positive transformants showed a green fluorescence under a microscope with UV light. Hairy roots that were not transformed with the vector containing the transgene in pMDC32 showed no fluorescence, whereas roots that were successfully transformed showed intense fluorescence (Figure 3-7). The green fluorescence was due to eGFP expression, which indicated the presence of the T-DNA and transgene.

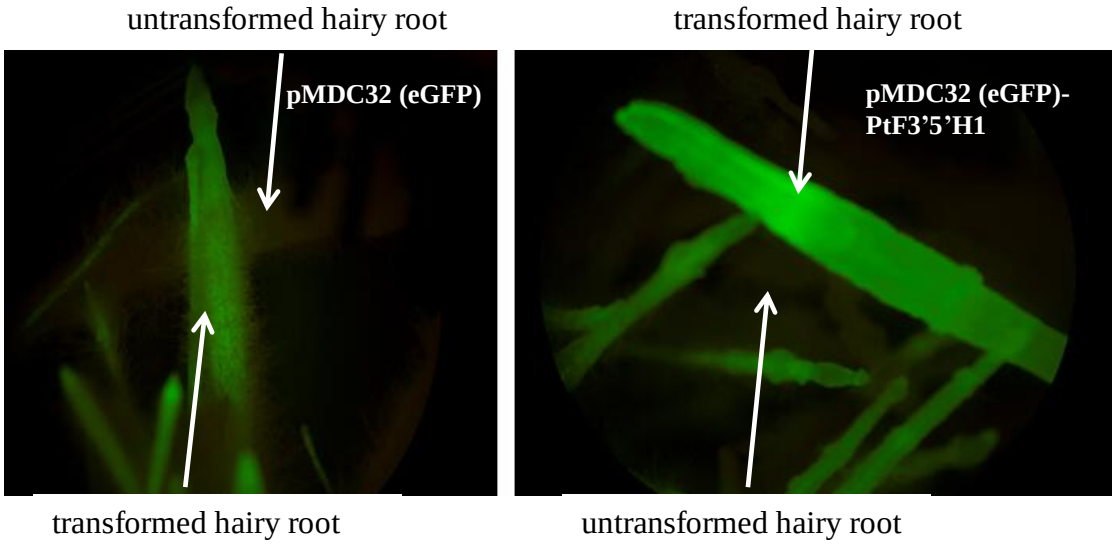

Figure 3-7. Poplar hairy roots containing pMDC32 (eGFP) and pMDC32 (eGFP)-PtF3'5'H1.
On the left, one successful transformant (pMDC32 (eGFP)) with green fluorescence is shown. Untransformed hairy roots can be seen in the back of the image with no fluorescence. On the right, a successful transformant (pMDC32 (eGFP)-PtF3'5'H1) with green fluorescence is shown.

3.5 Overexpressing PtF3'5'H1 in poplar hairy roots

PA concentrations were measured by the butanol-HCl (tannin) assay to test if overexpression of PtF3'5'H1 in poplar hairy roots had any effect on overall PA accumulation. PA concentrations showed substantial variability between each line. However, none of the PtF3'5'H1 overexpressing transgenic hairy root lines showed any significant increase in PA levels, compared to empty vector control hairy roots (Figure 3-8, 3-9). The average PA levels across all the transgenic and control hairy roots were 36.19 mg/g and 30.87 mg/g, respectively, but they were not statistically different (t-test, $p > 0.05$).

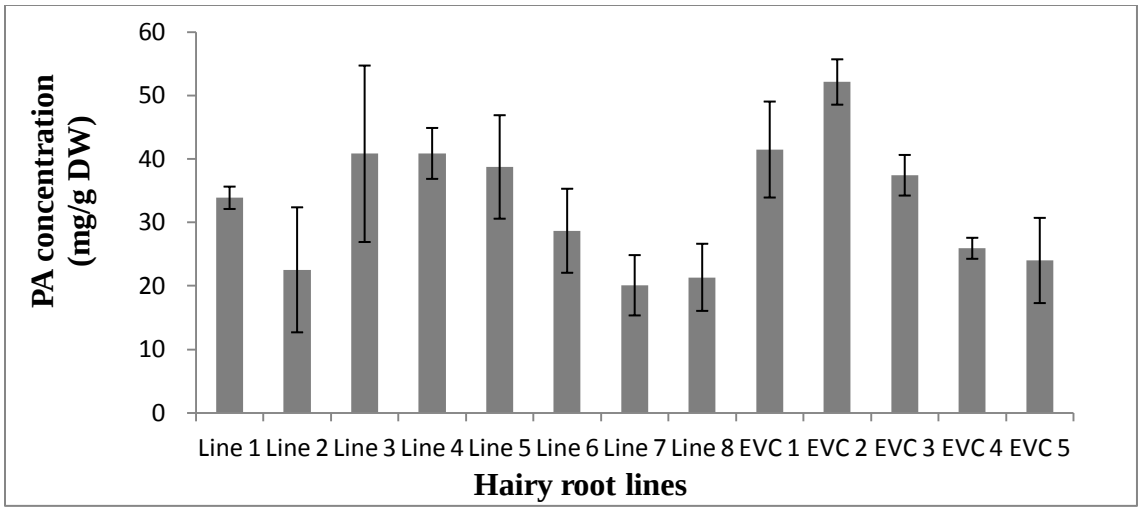

Figure 3-8. PA concentration in empty vector control and PtF3'5'H1 overexpressing poplar hairy roots.
Eight independent PtF3'5'H1 overexpressing hairy root lines and five empty vector control lines were extracted and measured for PAs by the butanol-HCl assay. Each line includes the means of three replicates of an independent hairy root clone. Error bars indicate standard error (n=3). EVC indicates empty vector control lines. DW stands for dry weight.

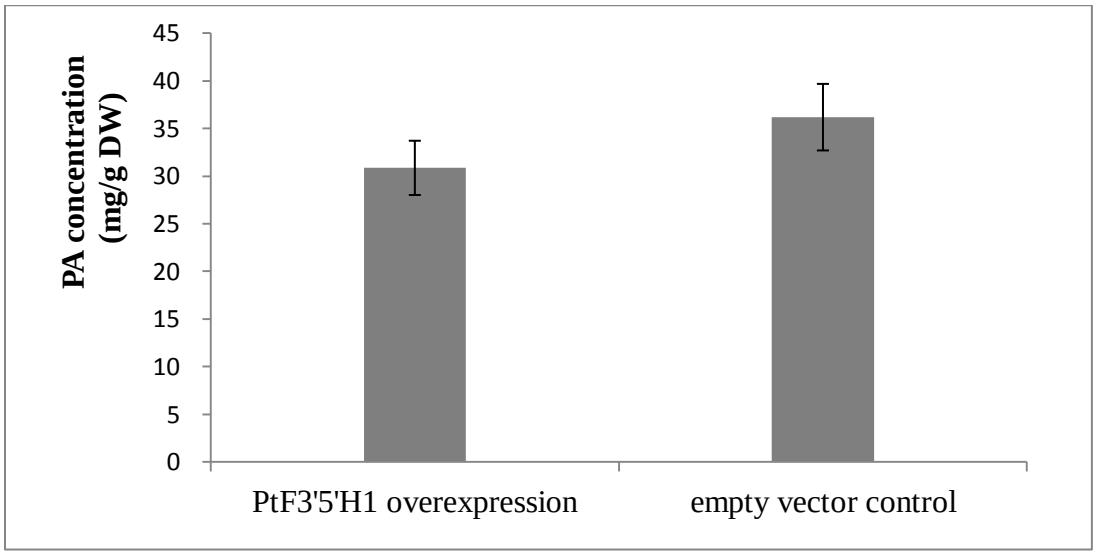

Figure 3-9. PA concentration in empty vector control and PtF3'5'H1 overexpressing poplar hairy roots.
PA concentration of 24 PtF3'5'H1 overexpressing hairy roots and 15 empty vector control hairy roots in Figure 3-7 were averaged (8 transgenic lines and 5 control lines, each has 3 biological replicates). Bars represent means of PA concentration and error bars indicate standard error. A pairwise t-test was done to test for a significant difference of PA concentration between PtF3'5'H1 overexpressing and empty vector control hairy roots, which showed no significant difference ($p > 0.05$). DW stands for dry weight.

3.6 Generation of transgenic poplar plants overexpressing PtF3’5’H1

P. tremula × *P. tremuloides* INRA clone 353-38 was used for poplar whole plant transformation because of its abundant tannin content and susceptibility to *Agrobacterium tumefaciens* infection. A pMDC32 vector carrying the gene encoding PtF3’5’H1 under the control of the single 35S promoter was constructed (Figure 2-1). Six sets of infections were performed with *Agrobacterium* (*Agrobacterium tumefaciens* strain GV3101 (MP90)) carrying the vector using 45 leaves for each set. In total, approximately 270 leaves were infected.

After infection, explants were transferred to callus induction medium to select for positive transformants. Thirty-five calli that successfully developed on callus induction medium were then transferred to shoot induction medium, approximately 4-5 weeks after infection. Twelve shoots were excised and transferred to root induction medium, of which nine survived, produced roots, and grew into plantlets. Since each of them originated from separate calli, nine independent transformation lines were gained. Positive transformants were confirmed by semi-quantitative PCR by using PtF3’5’H1A forward and reverse primers to detect the expression PtF3’5’H1 (See Table 2-1 and Figure A-1).

Individual transgenic lines were then micropropagated on WPM medium to generate multiple replicate plantlets for each independent transgenic line ($n \geq 5$). For each line, after semi-quantitative PCR, the five independent transgenic lines with the highest PtF3’5’H1 expression levels were acclimated in the mist chamber and grown in the greenhouse. To ensure sufficient plant material for the biochemical and molecular analysis, at least five plants for each line (including 353 wild-type plants) were

transferred to the greenhouse and grown for 3 months. Prior to harvest, plants were moved outside the greenhouse to receive sunlight treatment (see methods for details) for 7 days in order to induce higher levels of anthocyanins and PAs.

Expression of PtF3’5’H1 was measured in all transgenic and wild-type lines by RT-qPCR. Expression levels of PtF3’5’H1 in transgenic poplar were much higher than in wild-type controls (Figure 3-10). These results confirmed that the plants were successfully transformed and expressing the transgene at high levels.

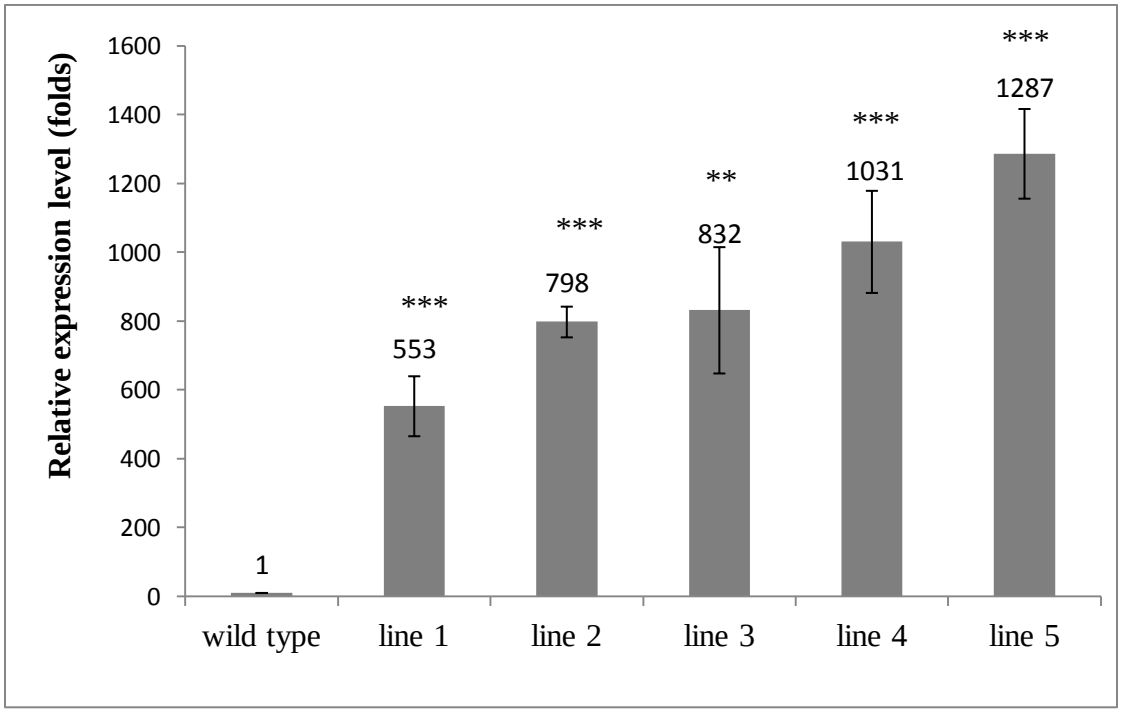

Figure 3-10. Relative expression level of PtF3'5'H1 in 353 wild-type and PtF3’5’H1 overexpressing poplar.
RNA was extracted from medium leaves (LPI 10-12) of wild-type and transgenic 353 poplar (*P. tremula* × *P. tremuloides*). Plants received one week of natural sunlight before harvest.The expression is normalized against the geometric mean of elongation factor 1-β (EF1β) and actin, two housekeeping genes. Bars represent means of expression levels and error bars indicate standard error ($n \geq 5$ plants). A pairwise t-test was done to test for a significant difference between wild-type and each of the transgenic lines. Asterisks indicate the results from t-test of the means ($p \leq 0.01$, **; $p \leq 0.001$, ***)

3.7 Overexpressing PtF3’5’H1 in transgenic poplar did not alter the overall amount of PAs

To test if PtF3’5’H1 overexpression has any influence on PA concentration, the butanol-HCl assay was performed to measure total PA content (Porter et al., 1985). A variety of tissues were analyzed, including young leaves (LPI 1-6), medium leaves (LPI 10-12), mature leaves (LPI 13-15), stem periderm, and root. PA levels in young leaves of lines 1 and 5 showed no significant difference compared to wild-type (t-test, $p > 0.05$), but in lines 2 and 3 showed a slight reduction (t-test, $p \leq 0.05$), and in line 4 a very significant reduction of PA levels was observed (t-test, $p \leq 0.01$) (Figure 3-11).

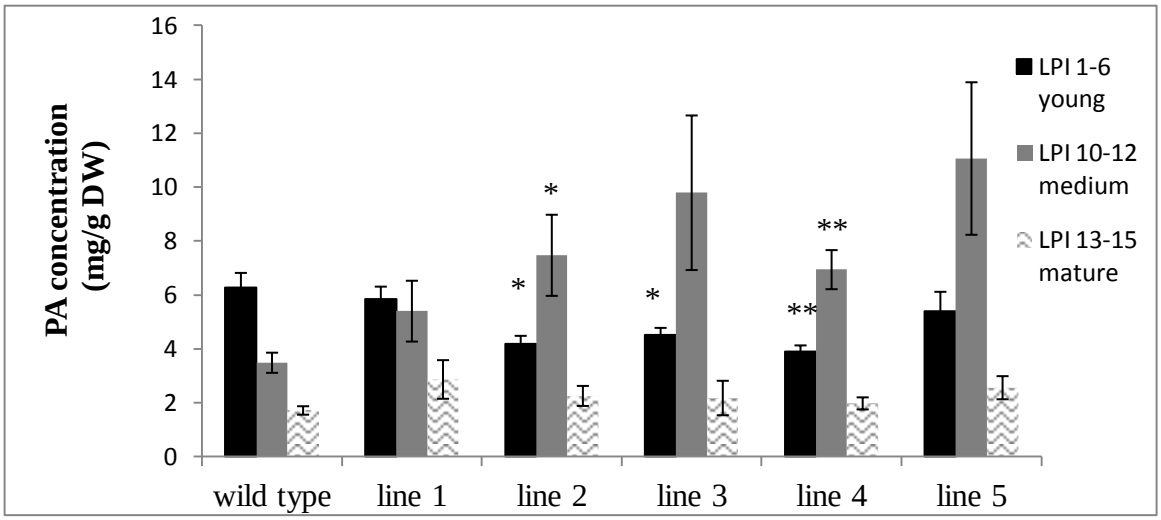

Figure 3-11. PA concentration in young, medium and mature leaves of 353 wild-type and PtF3’5’H1 overexpressing poplar.
Plant tissues were collected from *P. tremula* × *P. tremuloides* grown in the Bev Glover greenhouse (16 hour daylight, 18 ℃ to 28 ℃). Plants received one week of natural sunlight before harvest. LPI 1-6, young leaves; LPI 10-12, medium leaves; LPI 13-15, mature leaves. Different tissues were indicated with different colours. Bars represent means of PA concentration and error bars indicate standard error ($n \geq 5$). A pairwise t-test was done to test for a significant difference between wild-type and each of the transgenic lines. Asterisks indicate the results from t-test of the means ($p \leq 0.05$, *; $p \leq 0.01$, **). DW stands for dry weight.

In medium leaves, lines 1, 3 and 5 showed no significant difference to wild-type (t-test, $p > 0.05$), line 2 showed a significant enhancement (t-test, $p \leq 0.05$), line 4 showed a very significant induction of PA levels compared to wild-type (t-test, $p \leq 0.01$) (Figure 3-11). In mature leaves, none of the transgenic lines showed any difference compared to wild-type (t-test, $p > 0.05$) (Figure 3-11).

In roots, the transgenic lines also showed no significant difference with wild-type (t-test, $p > 0.05$) (Figure 3-12). In stem periderm, line 1 showed enhanced PA levels compared to wild-type (t-test, $p \leq 0.01$), while all the other lines showed no significant difference with wild-type (t-test, $p > 0.05$) (Figure 3-12).

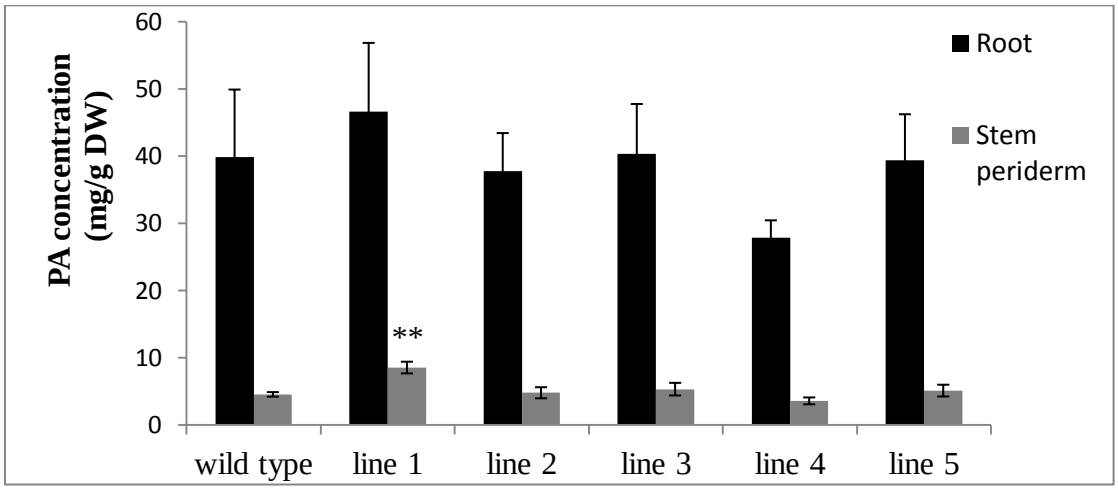

Figure 3-12. Root and stem periderm PA concentration in 353 wild-type and PtF3'5'H1 overexpressing poplar.
Plant tissues were collected from *P. tremula* × *P. tremuloides* grown in the Bev Glover greenhouse (UVic, 16 hour daylight, 18 ℃ to 28 ℃). Plants received one week of natural sunlight before harvest. Different tissues were indicated with different colours. Bars represent means of PA concentration and error bars indicate standard error ($n \geq 5$). A pairwise t-test was done to test for a significant difference between wild-type and each of the transgenic lines. Asterisks indicate the results from t-test of the means ($p \leq 0.01$, **). DW stands for dry weight.

In summary, I conclude that overexpression of PtF3'5'H1 in poplar does not consistently affect the overall amount of PA in the plant. Nevertheless, the variation

among wild type and transgenic plants is noticeable. In wild type, young leaf has the highest amount of PAs across all leaf tissues (Figure 3-6), while in transgenic poplar medium leaf has the highest level of PAs (Figure 3-11).

3.8 PA composition in transgenic poplar analyzed by LC-MS

LC-MS analysis was carried out by Dr. Juha-Pekka Salminen at the University of Turku to investigate if overexpression of PtF3’5’H1 has any effect on the B-ring hydroxylation pattern of PA in poplar. This method is based on fragmenting both the smaller oligomers and larger polymers into the precursors of PAs, and can be used to identify the specific flavan-3-ol subunits (Engström et al., 2014). Both catechin, epicatechin, gallocatechin, and epigallocatechin type subunits were identified in wild-type and transgenic poplar tissues by this method. However, due to relatively low concentration of PAs overall, the subunits could be identified but not quantified with accuracy. A very preliminary survey of the data suggests that PA subunit composition has no significant difference across all the transgenic and wild-type lines, suggesting that the B-ring hydroxylation pattern of PA was not affected by overexpression of PtF3’5’H1 alone. Thus, the preliminary LC-MS analysis of PtF3’5’H1 overexpressing poplar suggests no evident difference in PA subunit composition between wild-type and transgenic poplar.

3.9 qPCR analysis of key flavonoid biosynthetic genes in PtF3’5’H1 overexpressing plants

In order to determine if PtF3’5’H1 overexpression has any effect on the expression level of other genes in the PA pathway, expression of five genes (PtANR1, PtDFR1, PtDFR2, PtCHS1, PtANS1) was tested by RT-qPCR. This was originally done

as an additional control and baseline characterization of the plants, since there was no expectation of altered expression levels of other flavonoid genes.

PtANR1 is specific to the PA pathway, whereas the other genes are general in the flavonoid pathway (Figure 1-4). Previous studies showed that PtANR1 had comparatively greater expression in poplar young leaves than PtANR2 and can be induced by wounding treatment (Tsai et al., 2006). Surprisingly, qPCR analysis showed a significant reduction in PtANR1 expression in transgenic lines 3, 4 and 5 compared to the wild-type (Figure 3-13). However, transgenic lines 1 and 2 showed no significant difference in expression compared to the wild-type plants (t-test, $p > 0.05$).

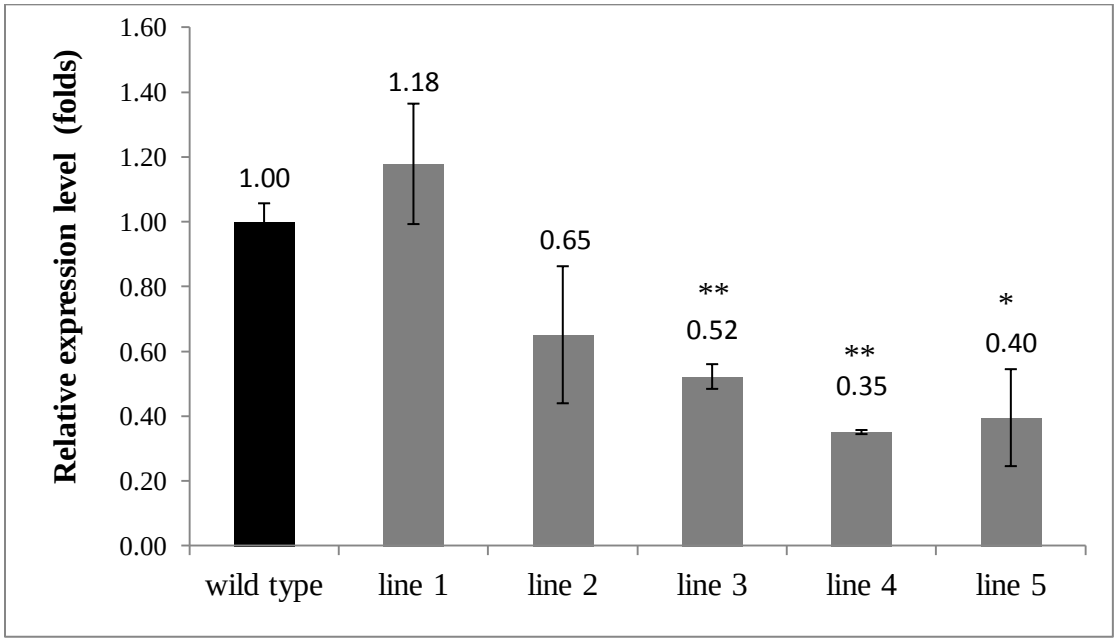

Figure 3-13. The relative expression of PtANR1 in PtF3'5'H1 overexpressing poplar as analyzed by qPCR.
RNA was extracted from medium leaves (LPI 10-12) of wild-type and multiple lines of transgenic 353 poplar (*P. tremula* × *P. tremuloides*) as described. The expression is normalized against the geometric mean of elongation factor 1-β (EF1β) and actin, two housekeeping genes. Black represents wild-type and grey represents transgenic plants. Bars represent the means of expression levels and error bars indicate standard error ($n \geq 5$ plants). A pairwise t-test was done to test for a significant difference between wild-type and each of the transgenic lines. Asterisks indicate the results from t-test of the means ($p \leq 0.05$, *; $p \leq 0.01$, **).

PtDFR1 and PtDFR2 encode enzymes which convert dihydroflavonols into leucoanthocyanidins (Figure 1-4). PtDFR1 showed significant down regulation in transgenic lines 3, 4 and 5 (t-test, $p \leq 0.05$), with a 6.67-, 11.11- and 16.67-fold reduction, respectively (Figure 3-14). Transgenic lines 1 and 2 again showed no significant difference in expression level compared to wild-type (t-test, $p > 0.05$). Similar to PtDFR1, PtDFR2 showed strong down regulation in all the transgenic lines except line 1 (Figure 3-15).

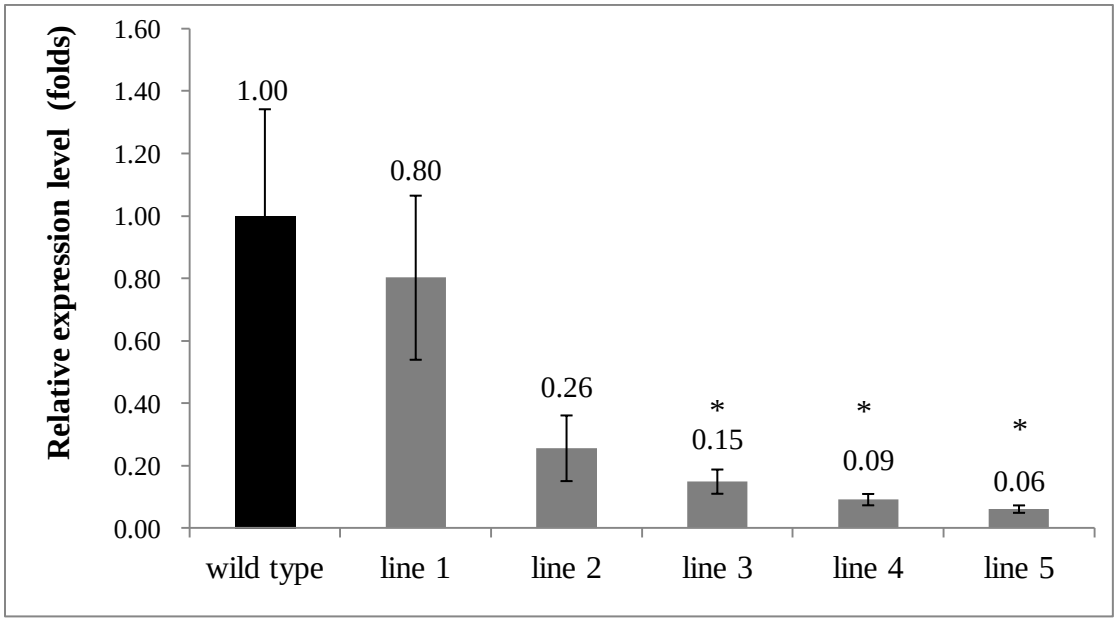

Figure 3-14. The relative expression of PtDFR1 in PtF3'5'H1 overexpression poplar as analyzed by qPCR.
RNA was extracted from medium leaves (LPI 10-12) of wild-type and multiple lines of transgenic 353 poplar (*P. tremula* × *P. tremuloides*) as described. The expression is normalized against the geometric mean of elongation factor 1-β (EF1β) and actin, two housekeeping genes. Black represents wild-type and grey represents transgenic plants. Bars represent means of expression levels and error bars indicate standard error ($n \geq 5$ plants). A pairwise t-test was done to test for a significant difference between wild-type and each of the transgenic lines. Asterisks indicate the results from t-test of the means ($p \leq 0.05$, *).

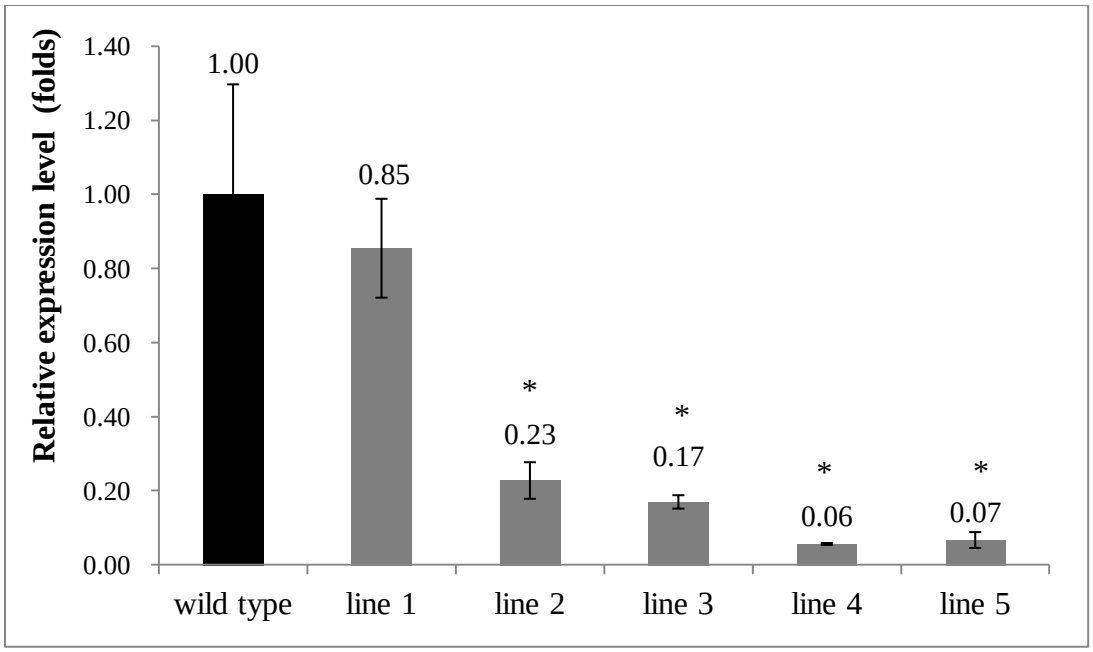

Figure 3-15. The relative expression of PtDFR2 in PtF3'5'H1 overexpression poplar as analyzed by qPCR.
RNA was extracted from medium leaves (LPI 10-12) of wild-type and multiple lines of transgenic 353 poplar (*P. tremula* × *P. tremuloides*) as described. The expression is normalized against the geometric mean of elongation factor 1-β (EF1β) and actin, two housekeeping genes. Black represents wild-type and grey represents transgenic plants. Bars represent means of expression levels and error bars indicate standard error ($n \geq 5$ plants). A pairwise t-test was done to test for a significant difference between wild-type and each of the transgenic lines. Asterisks indicate the results from t-test of the means ($p \leq 0.05$, *).

Chalcone synthase (CHS) catalyzes the first step of general flavonoid production, which is the condensation of three malonyl-CoA molecules with one 4-coumaroyl-CoA molecule to produce a naringenin chalcone (Figure 1-4) (Kreuzaler and Hahlbrock, 1972). According to Tsai et al. (2006), at least six CHS genes are present in the *Populus* genome. Gene expression analysis of CHS in *P. fremontii* × *angustifolia* showed that PtCHS2, PtCHS5 and PtCHS6 do not express in young leaves. Among PtCHS1, PtCHS3 and PtCHS4, PtCHS1 had the highest expression level in young leaves. In addition, PtCHS1 was strongly induced after wounding (Tsai et al., 2006). Thus, PtCHS1 was analyzed

here. In PtF3’5’H1 overexpressing plants, PtCHS1 showed strong down regulation in all the transgenic lines except line 1 (Figure 3-16). All these four transgenic lines showed a significant difference compared to wild-type plants (t-test, $p \leq 0.01$).

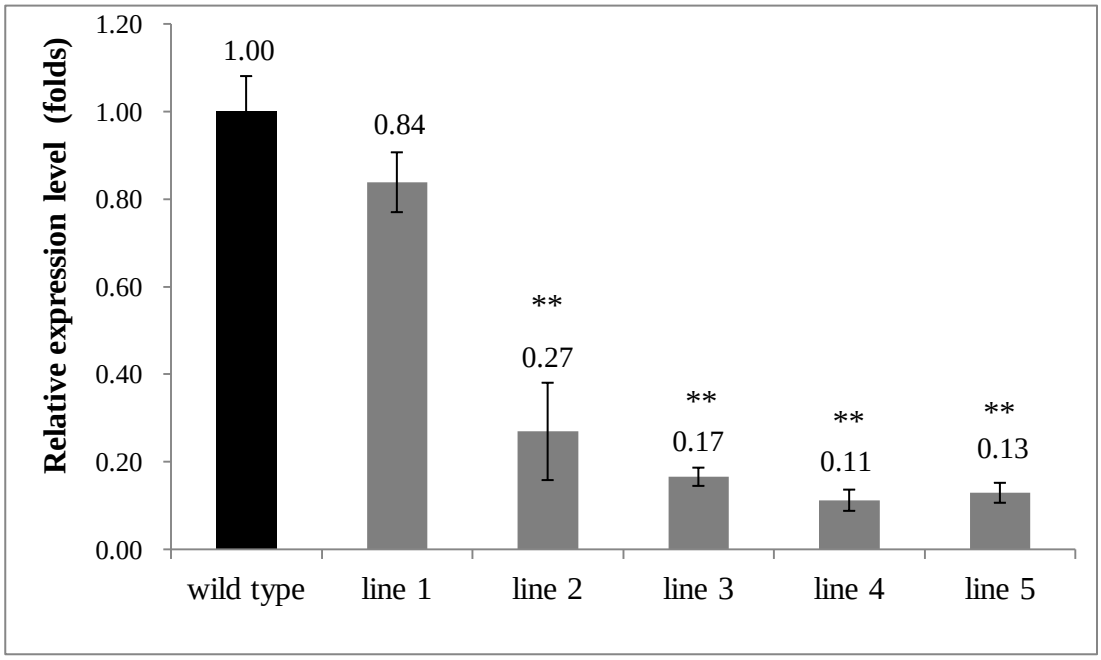

Figure 3-16. The relative expression of PtCHS1 in PtF3’5’H1 overexpression poplar as analyzed by qPCR.
RNA was extracted from medium leaves (LPI 10-12) of wild-type and multiple lines of transgenic 353 poplar (*P. tremula* × *P. tremuloides*) as described. The expression is normalized against the geometric mean of elongation factor 1-β (EF1β) and actin, two housekeeping genes. Black represents wild-type and grey represents transgenic plants. Bars represent means of the expression levels and error bars indicate standard error ($n \geq 5$ plants). A pairwise t-test was done to test for a significant difference between wild-type and each of the transgenic lines. Asterisks indicate the results from t-test of the means ($p \leq 0.01$, **).

The enzyme anthocyanidin synthase (ANS) oxidizes leucoanthocyanidins into anthocyanidins (Figure 1-4) (Saito et al., 1999). ANS is a key enzyme in both anthocyanin and proanthocyanidin synthesis (Liu et al., 2013). In *Populus* genome, there are two copies of PtANS genes. Tsai et al. (2006) found that PtANS1 can be strongly

induced in poplar young leaves by wounding, while the PtANS2 did not change substantially. Therefore, only the expression level of PtANS1 was tested in our PtF3’5’H1 overexpressing plants. qPCR analysis showed that PtANS1 was down regulated in transgenic lines 3, 4 and 5 more than 10-folds (t-test, $p \leq 0.05$) (Figure 3-17). Transgenic lines 1 and 2 showed no significant difference with wild-type.

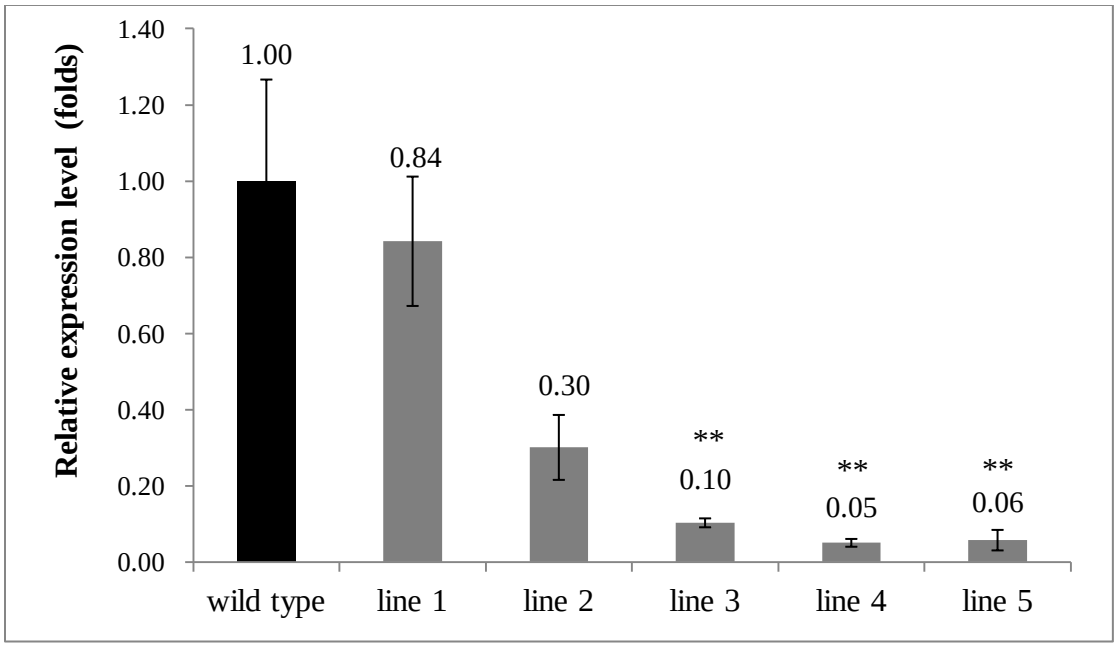

Figure 3-17. The relative expression of PtANS1 in PtF3’5’H1 overexpression poplar as analyzed by qPCR.
RNA was extracted from medium leaves (LPI 10-12) of wild-type and multiple lines of transgenic 353 poplar (*P. tremula* × *P. tremuloides*) as described. The expression is normalized against the geometric mean of elongation factor 1-β (EF1β) and actin, two housekeeping genes. Black represents wild-type and grey represents transgenic plants. Bars represent means of the expression levels and error bars indicate standard error ($n \geq 5$ plants). A pairwise t-test was done to test for a significant difference between wild-type and each of the transgenic lines. Asterisks indicate the results from t-test of the means ($p \leq 0.01$, **).

Overall, the qPCR data for all flavonoid genes tested are consistent and indicate that PtF3’5’H1 overexpression led to a reduction in expression of all flavonoid pathway genes tested. Transgenic plant lines 3, 4 and 5 consistently showed a reduction in all the

five genes (PtANR1, PtDFR1, PtDFR2, PtCHS1, PtANS1), while line 2 plants had down-regulation only in PtDFR2 and PtCHS1. Interestingly, no down-regulation of any of the five genes was found in transgenic line 1, which had the lowest overexpressing level of PtF3’5’H1. Thus, a correlation was evident between the overexpression of PtF3’5’H1 and the reduction of other genes in the flavonoid pathway.

3.10 Overexpressing PtF3’5’H1 in poplar led to enhanced delphinidin accumulation in young leaves

Delphinidin is a tri-hydroxylated anthocyanidin, and thus greater production of delphinidin was predicted by overexpression of the flavonoid 3’, 5’-hydroxylase in transgenic poplars. High-performance liquid chromatography (HPLC) was used to analyze the content and concentration of anthocyanin in both wild-type and PtF3’5’H1 overexpressing plants. Young leaves were chosen as assay material, because under our growth conditions, exposure to natural sunlight led to accumulation of anthocyanin in young leaves (Figure 3-18).

Analysis of anthocyanins by HPLC indicated a change in anthocyanin composition, seen in the appearance of enhanced peaks (Figure 3-19). In my HPLC data, three peaks were tentatively identified as anthocyanins because they had maximum absorption at around 280 and 520 nm (Figure 3-19). The major peak present in all wild type and transgenic poplars showed maximum absorbance at 280 and 517 nm (Figure 3-19). Bunea et al. (2013) compared the absorption spectra of anthocyanins identified by LC-MS from various blueberry extracts (Table A-2). In the blueberry extracts, cyanidin-3-glucoside was the only anthocyanin identified with the same maximum absorbance of

280 and 517 nm compared to the major peak in our data.

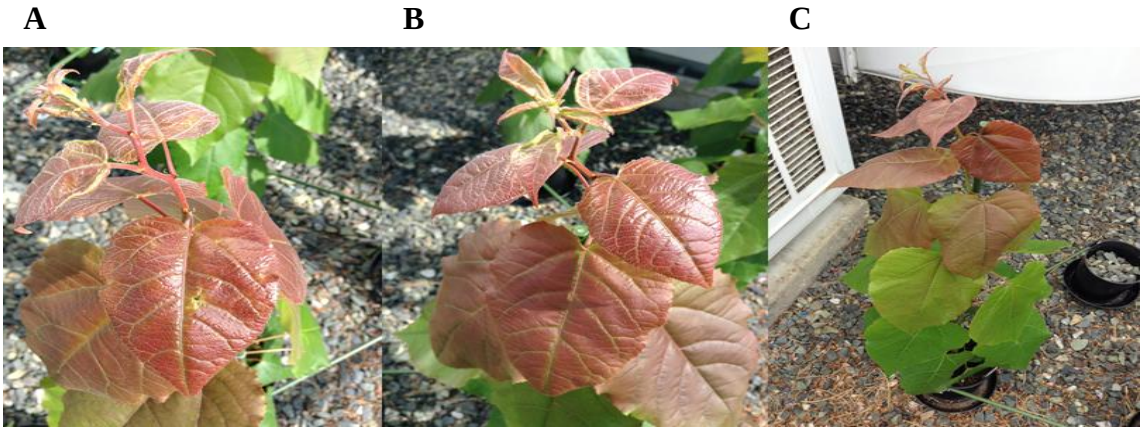

Figure 3-18. The colour of the poplar leaves after receiving one week of natural sunlight.
The plants (wild-type and PtF3'5'H1 overexpressing *P. tremula* × *P. tremuloides*) were moved outside the greenhouse for one week to receive the natural sunlight before harvest. Red colour of the young leaves indicated the accumulation of anthocyanins, but no difference was found between wild type and transgenic plants. A and B show the top leaves while C shows the plant as a whole.

Several reports in poplar and the closely related *Salix* species also found cyanidin-3-glucoside to be the dominant anthocyanin. In *Populus tremula* and *P. alba* × *P. tremula*, anthocyanins isolated from a variety of tissues (leaves from different seasons, catkins, stigmas and stamens) were all found to be cyanidin-derivatives, with cyanidin-3-glucose being the most common one (Bendz and Haglund, 1968). Matsumoto et al. (1970) found that light exposure induced the production of cyanidin-3-glucoside in poplar (*P. nigra* × *P. maximowiczii*) cell suspension culture. A study by Tholakalabavi et al. (1994) showed that poplar (*Populus deltoides*) cell suspensions subjected to osmotic stress with glucose and mannitol induced cyanidin-3-glucoside. In Chinese white poplar (*P. tomentosa Carr.*), cyanidin was found to be the only aglycone of anthocyanin (Wang et al., 2013). Poplar and *Salix* species belong to the same family *Salicaceae*, and have

similar phytochemistry. In Bridle et al. (1973), cyanidin-3-glucoside and delphinidin-3-glucoside were found to be the most common glycosides of anthocyanidins across many cultivars of *Salix* species (*S. purpurea, S. fragilis, S. americana, S. rubra, S. incana, S. aegyptica*, and *S. alba*) with cyanidins as the major component. Thus, combining all the known facts about anthocyanins in poplar and characteristics about anthocyanins, the HPLC peak at 9 min in our data is most likely to be cyanidin-3-glucoside.

In addition, there are two enhanced peaks in the transgenic poplar leaf samples which eluted earlier than the glycosylated cyanidin with peak absorption both at 276/524 nm (Figure 3-19). Although the identity of those two peaks could not be proven directly, the elution and spectral characteristics of anthocyanins are well known and can be used to deduce the most likely structure (Santos-Buelga et al., 2003). The anthocyanidin elution pattern is closely related to their polarity, and more polar compounds will usually elute earlier than less polar ones. Since hydroxyl groups on the B-ring of anthocyanidins can increase their polarity, three anthocyanidins present in poplar should have an elution sequence early to late as delphinidin > cyanidin > pelargonidin. A series of anthocyanins with the same sugar substituents have the same elution pattern as their parent compounds. Since sugar substitution typically increases the polarity, anthocyanins usually elute earlier than their parent anthocyanidin aglycones. The B-ring substitution pattern of anthocyanidin also determines the maximum wavelength of absorption (λ_{max}) in the visible region. A general trend is that the λ_{max} increases when the number of hydroxyl groups increases. For example, tri-hydroxylated anthocyanidins have a λ_{max} 8-12 nm higher than the λ_{max} of di-hydroxylated anthocyanidins. In terms of anthocyanins, sugar substitution on the B-ring has no significant effect on the nature of λ_{max}. As referred to

earlier, a blueberry pigment study identified delphinidins with same λ_{max} as our unknown peaks (Table A-2) (Bunea et al., 2013). Based on the collective information discussed above, the two peaks eluted prior to cyanidin-3-glucoside are most probably glycosylated delphinidins. This hypothesis was corroborated with our analysis of male catkins and studies in the literature.

Male catkins are red in colour, which indicates the presence of anthocyanins. Therefore, they were used as a comparison for the leaf extracts analyzed above. Male catkin collected from native *Populus trichocarpa* (on UVic's campus) showed a similiar anthocyanin profile as the leaves of transgenic plants (Figure 3-20). The three peaks showed same UV spectrum and retention time as those in 353 plants, which suggests that these three peaks in transgenic leaves are native anthocyanins in poplar. In addition, one of the putative delphinidin peaks was quite substantial compared to those in the leaves of wild type. As mentioned before, some species of *Salix* species were found to have delphinidin (Bridle et al., 1973). In poplar, PtF3'5'H1 was found to be highly expressed in male catkins both by *in silico* (Figure 3-2) and RT-qPCR (Figure 3-5) analysis. This suggests that PtF3'5'H1 is very likely to have flavonoid 3', 5'-hydroxylation activity in poplar.

Total anthocyanin concentration was calculated by integrating the peak area of all three anthocyanin peaks from HPLC data in order to test if overexpression of PtF3'5'H1 had an influence on overall anthocyanin concentration. PtF3'5'H1 overexpressing plant lines 2 and 3 showed a slight but significant reduction of total anthocyanins (t-test, $p \leq 0.05$), while other lines showed no difference compared to wild-type (Figure 3-21). As can be seen from HPLC data, all the PtF3'5'H1

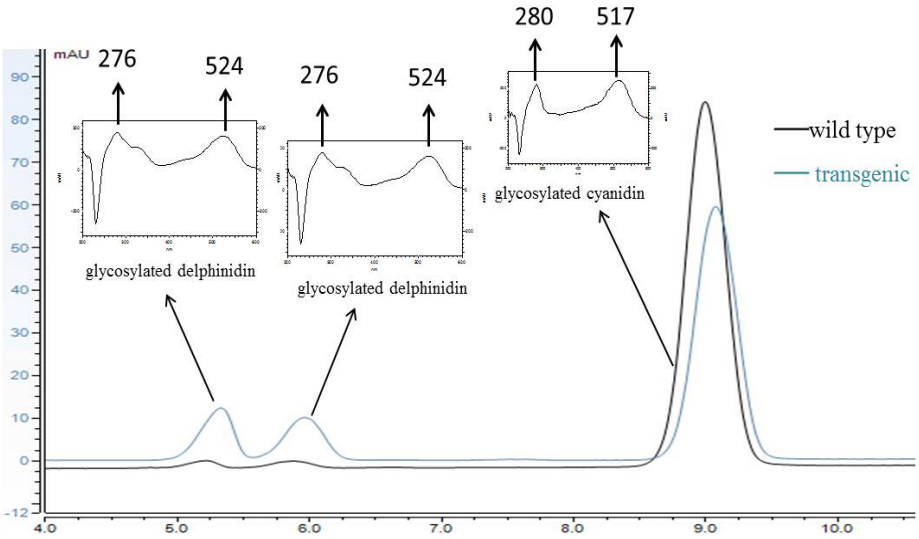

Figure 3-19. Analysis of anthocyanin content in wild-type and PtF3'5'H1 overexpressing plants by HPLC.
Anthocyanins were extracted from the young leaves (LPI 1-6) of wild-type and PtF3'5'H1 overexpressing *P. tremula* × *P. tremuloides*. HPLC traces of wild-type and transgenic anthocyanin extracts were overlaid. UV spectrum was shown for each anthocyanin. Anthocyanins were putatively identified based on elution time and similar UV spectra in the literature as described in text.

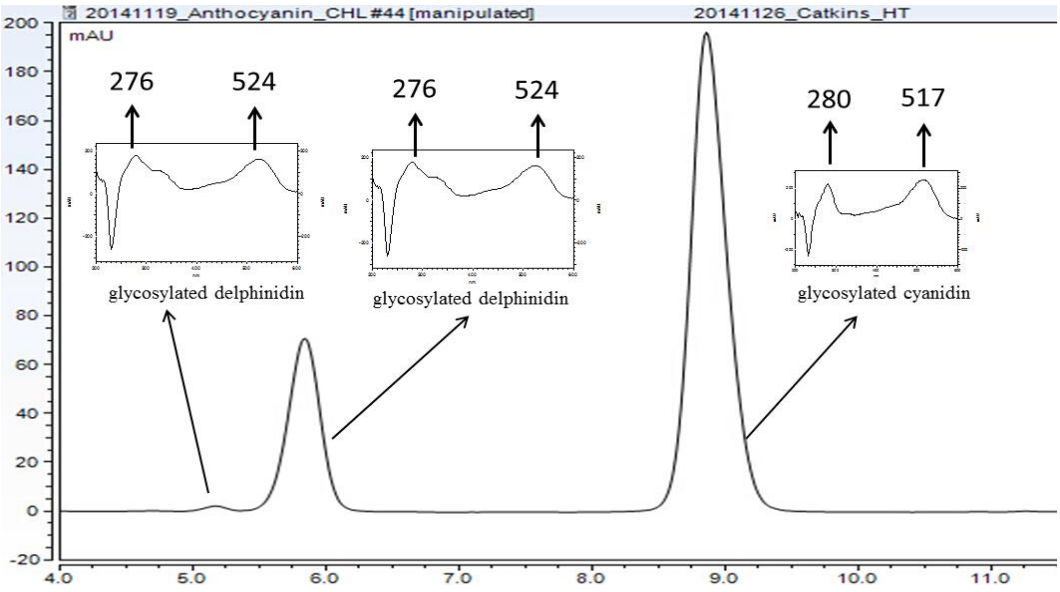

Figure 3-20. HPLC analysis of anthocyanins from *Populus trichocarpa* male catkins (wild-type).
Populus trichocarpa male catkins were collected on campus at the University of Victoria. Anthocyanins were tentatively identified based on elution sequence and similar UV spectra in the literature as described in text.

overexpressing lines showed a significant increase of putative delphinidin content compared to wild-types (t-test, $p \leq 0.001$) (Figure 3-22, 3-23). The ratio of putative delphinidin content in PtF3’5’H1 overexpressing lines ranges from approximately 16% to 23%, while in wild-type is only about 3% (Figure 3-23).

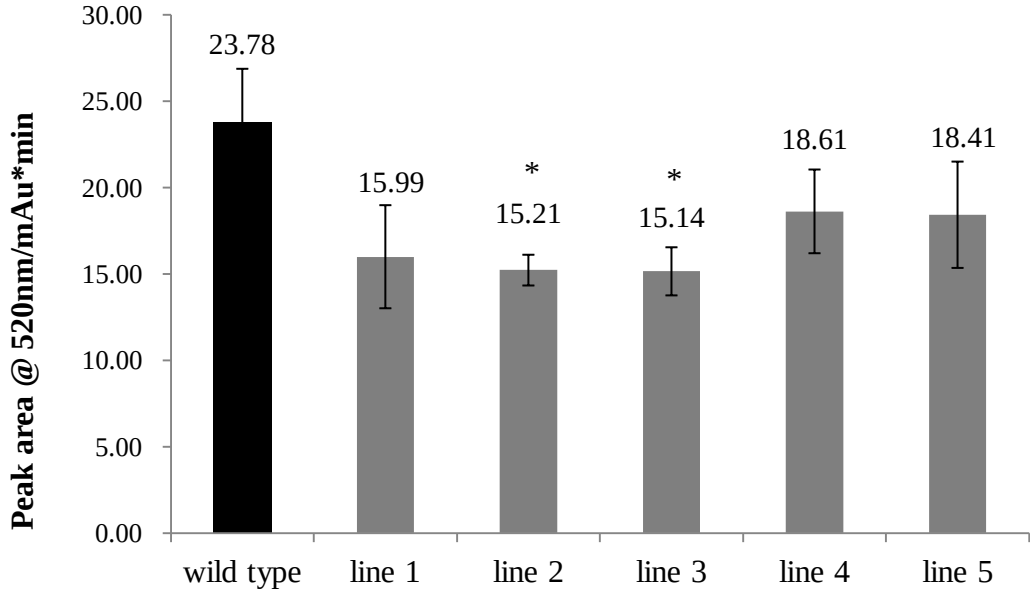

Figure 3-21. Concentration of total anthocyanin in wild-type and PtF3’5’H1 overexpressing plants.
Anthocyanins were extracted from the young leaves (LPI 1-6) of wild-type and PtF3’5’H1 overexpressing *P. tremula* × *P. tremuloides*. Concentration of anthocyanin in leaves was represented by the sum of three peak areas (mAu*min). Bars represent means of peak areas, error bars indicate standard error (n ≥ 5 plants). A pairwise t-test was done to test for a significant difference between wild-type and each of the transgenic lines. Asterisks indicate the results from t-test of the means ($p \leq 0.05$, *).

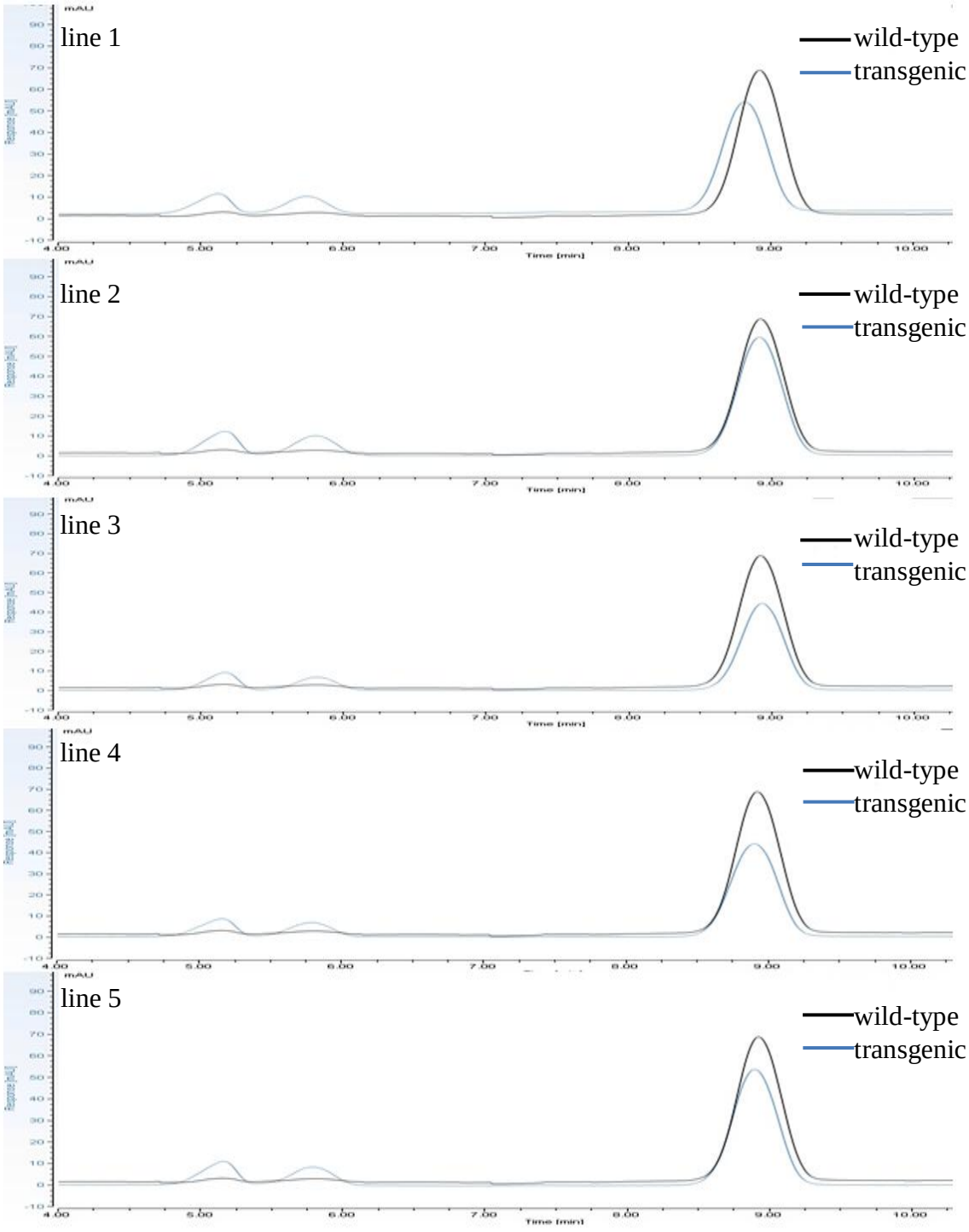

Figure 3-22. Analysis of anthocyanin content in wild-type and all the PtF3’5’H1 overexpressing lines by HPLC.
Anthocyanins were extracted from the young leaves (LPI 1-6) of wild-type and PtF3’5’H1 overexpressing *P. tremula* × *P. tremuloides*. HPLC traces of wild-type and transgenic anthocyanin extracts were overlaid. Five different transgenic lines overexpressing PtF3’5’H1 were included.

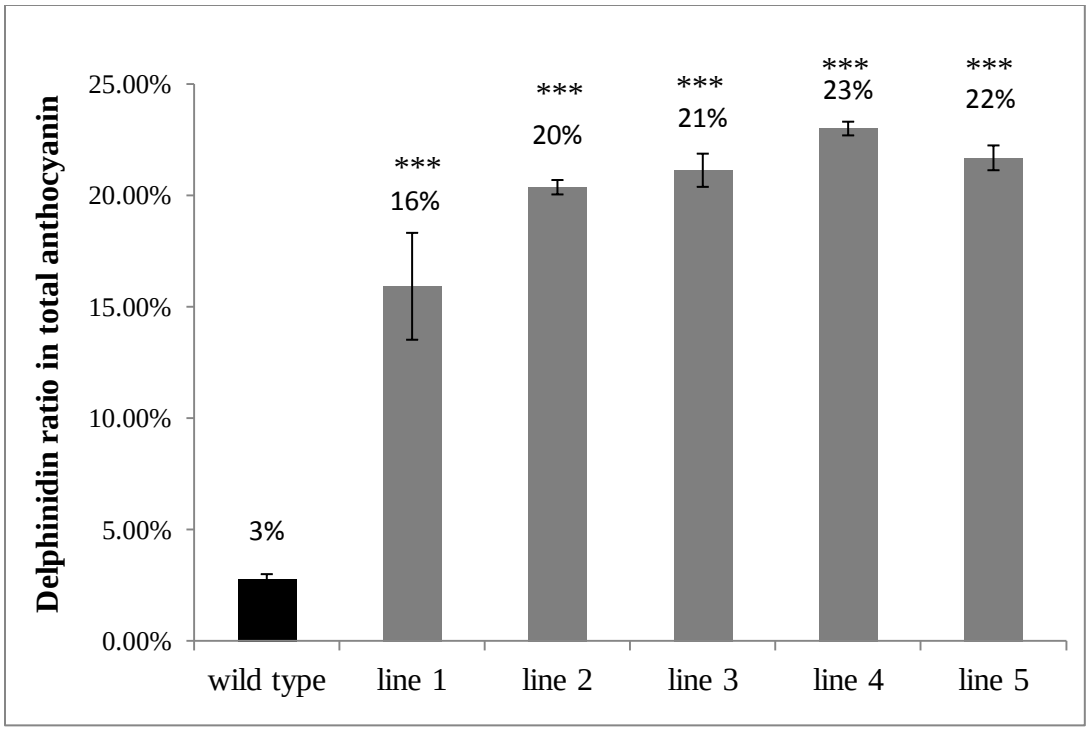

Figure 3-23. Delphinidin ratio of total anthocyanin in wild-type and PtF3'5'H1 overexpressing plants.
Anthocyanins were extracted from the young leaves (LPI 1-6) of wild-type and PtF3'5'H1 overexpressing *P. tremula* × *P. tremuloides*. Delphinidin ratio was calculated according to the peak area (mAu*min). Bars represent means of ratios, error bars indicate standard error ($n \geq 5$ plants). A pairwise t-test was done to test for a significant difference between wild-type and each of the transgenic lines. Asterisks indicate the results from t-test of the means ($p \leq 0.001$, ***).

3.11 Transient overexpression of PtF3'5'H1 in *Nicotiana benthamiana* leaf tissue via agroinfiltration

In order to attempt to confirm the results from poplar transformation and test PtF3'5'H1 in a separate functional assay, the same construct from poplar whole plant transformation was used for transient plant transformation using agroinfiltration of *N. benthamiana*. R2R3 MYB and bHLH transcription factors are two groups of proteins that regulate the synthesis of anthocyanin (Gonzalez et al., 2008). In *Arabidopsis*, MYB-

mediated anthocyanin production requires a bHLH protein (Gonzalez et al., 2008). AtPAP1(Production of Anthocyanin Pigment1, R2R3 MYB) and AtGL3 (Glabra3, bHLH) have been shown in *Arabidopsis* to regulate the anthocyanin synthesis (Borevitz et al., 2000; Payne et al., 2000). Lin-Wang et al. (2010) showed that co-infiltration of *Arabidopsis* AtPAP1 with the *Arabidopsis* bHLH AtGL3 activates anthocyanin biosynthesis in leaf tissue of *N. benthamiana*. Based on this, the goal of the experiments here was to determine if agro-infiltration of PtF3’5’H1 in combination with AtPAP1 and AtGL3 could stimulate delphinidin biosynthesis in *N. benthamiana*, thereby providing confirmation of the function of PtF3’5’H.

Infiltration of AtPAP1 and AtGL3 led to a visible accumulation of anthocyanins after seven days (Figure 3-24). This demonstrated that the agro-infiltration of AtPAP1 and AtGL3 in *N. benthamiana* was successful and led to accumulation of anthocyanins in the leaves. Likewise, anthocyanins were also visible in leaves infiltrated with the PtF3’5’H1 overexpression vector, together with AtPAP1 and AtGL3 (Figure 3-24). By contrast, negative control leaves infiltrated with an empty vector construct showed no accumulation of anthocyanins (Figure 3-24). Anthocyanins were extracted from leaf tissues using the acid-methanol-chloroform method described. Total anthocyanin concentration was measured by spectrophotometer at 530 nm. Total anthocyanin concentration in both positive control and PtF3’5’H1 plus AtPAP1 and AtGL3 had increased more than 20 times, but the difference between them was not significant (Figure 3-24). This demonstrates that overexpression of PtF3’5’H1 in *N. benthamiana* had no effect on anthocyanin concentration.

To further analyze the content of anthocyanins, HPLC was performed. Two peaks were detected (one minor and one major with maximum absorbance at 290/322/527 nm and 283/524 nm, respectively) from all samples with consistent peak size (Figure 3-25). Thus, the addition of PtF3’5’H1 did not cause a change in anthocyanin profile. Recently, Gomez-Roldan et al. (2014) found that introducing Rosea1 and Delila (ROS1, MYB transcription factor; DEL, bHLH transcription factor, both from snapdragon *Antirrhinum majus*) into *N. benthamiana* leaves by agroinfiltration led to specific induction of a single anthocyanin, delphinidin-3-rutinoside. This suggests that delphinidin-3-rutinoside is very likely to be the major native anthocyanin produced by *N. benthamiana*. The characteristics of anthocyanins have been discussed above (Santos-Buelga et al., 2003; Bunea et al., 2013). Here, the major peak has the same λ_{max} at 524 nm as putatively identified delphinidin-derivatives in our transgenic poplar. Therefore, the major peak is likely to be delphinidin derivative. Since acylation can cause a shoulder peak at 305-325 nm with hydroxycinnamic acids and 320-325 nm with caffeic, ferulic and sinapic acids (Santos-Buelga et al., 2003), it is possible that the minor peak is an acylated anthocyanin.

The transient assays in *N. benthamiana* confirmed that AtPAP1 and AtGL3 can induce the production of anthocyanin in *N. benthamiana* leaves. Meanwhile, co-infiltration of PtF3’5’H1 together with AtPAP1 and AtGL3 in *N. benthamiana* leaves showed no difference in the overall amount of anthocyanins compared to co-infiltration of AtPAP1 and AtGL3. Since glycosylated delphinidin was recently found in *N. benthamiana* with the transient expression of MYB and bHLH transcription factor from snapdragon, it can be inferred that *N. benthamiana* has endogenous F3’5’H (Gomez-

Roldan et al., 2014). This could explain why introducing an ectopic F3’5’H from *Populus* had no obvious effect on the pattern of anthocyanin accumulation in *N. benthamiana*.

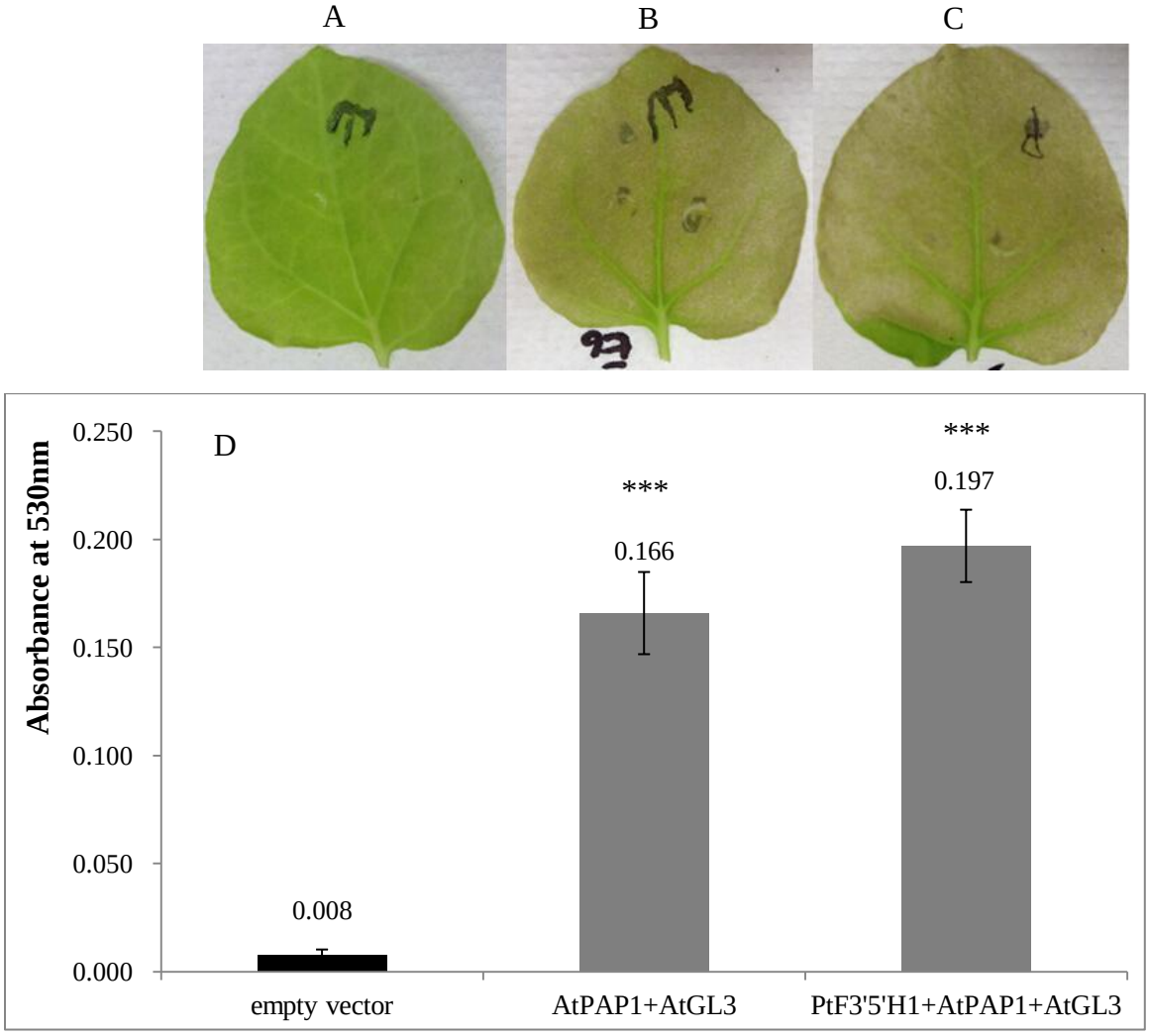

Figure 3-24. Anthocyanin concentration of *Nicotiana benthamiana* infiltrated with different combination of *Agrobacterium*. (A)-(C), Images of leaves infiltrated with empty vector (A), AtPAP1 + AtGL3 (B), PtF3’5’H1+AtPAP1+AtGL3 (C). (D), Activation of anthocyanin synthesis in *N. benthamiana* by agroinfiltration of AtPAP1, AtGL3 and PtF3’5’H1. AtPAP1 and AtGL3 were infiltrated without PtF3’5’H1 as positive controls. The empty vector was infiltrated as negative control. The bars represent the average anthocyanin absorbance readings at 530 nm. Error bars represent standard deviation from the means ($n \geq 7$). A pairwise t-test was done to test for a significant difference between different treatments. Asterisks indicate the results from t-test of the means ($p \leq 0.001$, ***). The photographs show the leaves of *N. benthamiana*, photos were taken one week after the infiltration. Anthocyanin accumulation in leaves changes the colour.

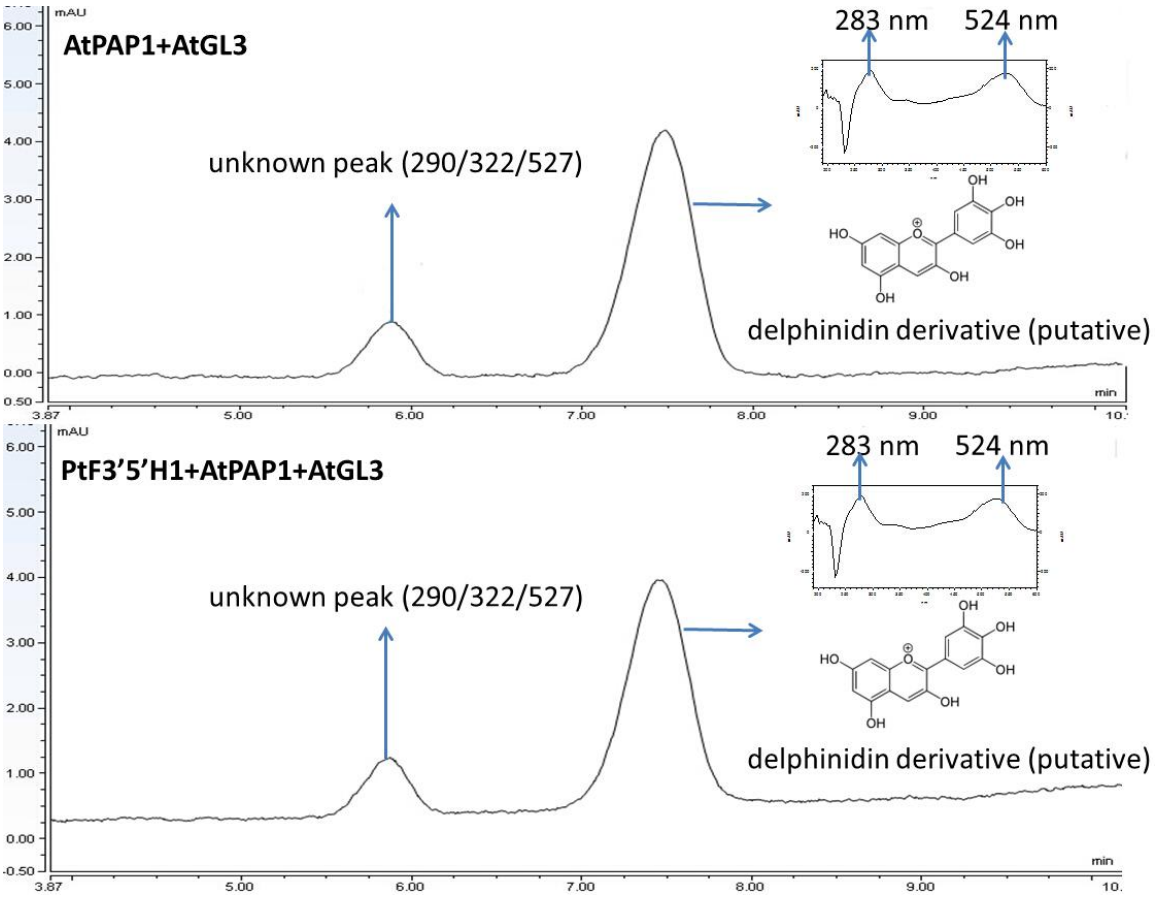

Figure 3-25. HPLC analysis of *Nicotiana benthamiana* leaf infiltrated by AtPAP1, AtGL3 and PtF3'5'H1.

The upper graph is from leaves infiltrated with AtPAP1 and AtGL3 alone, the lower one is from leaves infiltrated with PtF3'5'H1 together with AtPAP1 and AtGL3.Two peaks were detected from all samples, and both show the spectrum of flavonoid. Both combinations of infiltration showed the same results. The unknown compound has a shoulder peak at 322 nm. The peaks were putatively identified as delphinidin by elution sequence and similar UV spectra in previous literature. UV spectrum, structure and label of the compound were provided.

4. Chapter Four: Discussion

4.1 Summary of key results

In transgenic PtF3’5’H1-overexpressing poplar, no significant change in the overall amount and hydroxylation pattern of PA was found. However, the poplars overexpressing PtF3’5’H1 showed a small but significant change in anthocyanin composition. A greater percentage of putative delphinidin derivatives were found (16% to 23% of delphinidin derivatives) in transgenic poplar compared to wild-type (3% of delphinidin derivatives) (Figure 3-19, 3-22 and 3-23). These results indicate that PtF3’5’H1 is functional in the transgenic plants and that it can contribute to the production of tri-hydroxylated anthocyanins in poplar. However, its function in PA synthesis is not yet clear, since PA concentration and expression profile of PtF3’5’H1 do correlate, whereas no effect of PtF3’5’H1 overexpression on PA synthesis was detected. Transient expression of PtF3’5’H1 in *Nicotiana benthamiana* had no effect on the overall amount of anthocyanins or the anthocyanin profile.

4.2 Flavonoid 3’, 5’-hydroxylase and its role in anthocyanin and PA synthesis in different plants

F3’5’H activity was first demonstrated in microsomal preparations of *Verbena hybrida* (Stotz and Forkman, 1982). It was subsequently found in more advanced *Asparagales* subclasses such as *Orchidaceae* (Jeong et al., 2006). Unlike 3’, 4’-hydroxylated flavonoids, 3’, 4’, 5’-hydroxylated flavonoids are not as common in plants (Seitz et al., 2006). In fact, the F3’5’H gene is missing in many species of plants, including common flower species such as roses, carnations, chrysanthemums, lilies, and

gerbera (Tanaka and Ohmiya, 2008). Thus, these species lack violet/blue varieties (Holton and Tanaka, 2014). The important role of F3’5’H in delphinidin based anthocyanin production has been reported in species including *Vitis vinifera*, *Petunia hybrida*, *Pericallis hybrida* and *Camellia sinensis*. Overexpression of F3’5’H from these plants led to delphinidin derivative accumulation (Shimada et al., 2001; Castellarin et al., 2006; Sun et al., 2013; Wang et al., 2014). Since anthocyanin and PA synthesis share intermediates in the flavonoid pathway such as flavanone, dihydroflavonol and leucoanthocyanidin, it is predicted that F3’5’H also has an important role in PA synthesis by determining the hydroxylation pattern of PA precursors (Figure 1-4). Correlation of F3’5’H expression level and tri-hydroxylated flavan-3-ols or prodelphinidin content has been demonstrated in a few cases. In grape (*Vitis vinifera*), higher expression level of F3’5’H is correlated with the accumulation of prodelphinidin in seeds, skins, flower, stem, and tendril (Downey et al., 2003; Bogs et al., 2006; Jeong et al., 2006). PA subunit composition and expression level of PtF3’5’H has been also investigated by Tsai et al. (2006) and Scioneaux et al. (2011). Four poplars with different genetic background were used, including narrowleaf (*P. angustifolia*), Fremont (*P. fremontii*), their F1 hybrids, and back-crosses to narrowleaf. Fremont does not express the F3’5’H and does not accumulate any trihydroxylated prodelphinidin- type flavonoid, while narrowleaf does express F3’5’H and has some prodelphinidin-type proanthocyanidins (Scioneaux et al., 2011). In the F1 hybrid of narrowleaf and Fremont, some prodelphinidin-type subunits were found (Scioneaux et al., 2011). Tsai et al. (2006) confirmed the expression of F3’5’H in the leaves of F1 hybrid. These studies indicate that the expression of F3’5’H may affect the subunit composition of PA in poplar.

Phylogenetic analysis revealed that PtF3’5’H1 is located in the clade of well-characterized F’3’5H (Figure 3-1), which suggests that this gene encodes a functional F3’5’H protein. PtF3’5’H2 is also located in the clade of well-characterized F’3’5H. However, due to low or no expression from previous expression analysis, PtF3’5’H2 was not analyzed further. But it is unlikely to have any effect on the result. In the PtF3’5’H1-overexpressing plants, young leaves accumulated significant amount of anthocyanin with a red color (Figure 3-18), which had a slight but significant enhancement of delphinidin-based anthocyanins (Figure 3-19, 3-22 and 3-23). Therefore, the PtF3’5’H1 gene was active in transgenic plants. By contrast, PA showed no change in concentration, and preliminary LC-MS showed no major changes in hydroxylation pattern (Figure 3-11 and 3-12). Thus, overexpression of PtF3’5’H1 alone in poplar did not affect either the concentration or composition of PA, despite it demonstrated effects in anthocyanins.

4.3 Possible reasons for not accumulating dephinidin-based anthocyanins and prodelphinidin-based proanthoycanidins in transgenic poplar

In my study, overexpression of PtF3’5’H1 in *Populus* had a slight change in anthocyanin content, but not PAs. Possible explanations for the lack of efficient function can be summarized as i) substrate specificity of dihydroflavonol 4-reductase (DFR), ii) the involvement of a cytochrome P450 reductase or cytochrome b5, iii) competition between different enzymes for the same substrate, and iv) correlation of PtF3’5’H1 mRNA levels and protein abundance in the host plant.

Dihydroflavonol 4-reductase (DFR) acts downstream of F3’5’H, converting dihydroflavonols (dihydrokaempferol, dihydroquercetin and dihydromyricetin) to

leucoanthocyanidins (leucopelargonidin, leucocyanidin and leucodelphinidin) (Figure 1-4). DFRs in different species sometimes show different substrate preferences. For example, DFR from petunia and *Cymbidium* does not utilize dihydrokaempferol as a substrate, and no pelargonidin-based anthocyanins can be produced. Thus, these species cannot produce brick red/orange anthocyanins (Forkmann and Heller, 1999; Johnson et al., 1999). In chrysanthemum, introducing a petunia F3'5'H successfully led to accumulation of dihydromyricetin, but the endogenous DFR does not catalyze the reduction of colourless dihydromyricetin efficiently. Thus, delphinidin was not produced (Seo et al., 2007). In petunia, dihydromyricetin is the best substrate for DFR (Gerats et al., 1982). Expression of both petunia F3'5'H and DFR in white carnation cultivars that originally lack DFR led to delphinidin accumulation and showed a significant color shift toward blue (Holton, 1996). Likewise, to obtain blue roses, Katsumoto et al. (2007) down-regulated the endogenous DFR gene and overexpressed the *Iris* × *hollandica* DFR gene together with the viola F3'5'H gene in a rose cultivar. This caused exclusive and dominant production of delphinidin. In poplar, there are two copies of DFR. So far, no detailed studies on the substrate preferences of DFRs in poplar have been performed, but a recombinant protein assay showed that DFR1 can utilize dihydroquercetin as a substrate (Peters and Constabel, 2002). Dihydroquercetin can be further converted into leucocyanidin, and then to cyanidin by ANS. Thus, if DFRs in *Populus* prefer to use dihydroquercetin rather than dihydromyricetin as substrate, it can be the bottleneck for delphinidin and possibly prodelphinidin production.

Another possible explanation for why the transgenic poplars accumulated less delphinidin and prodelphinidin than predicted could be the lack of expression or

deficiency of cytochrome P450 reductase or cytochrome b5. PtF3’5’H1 belongs to the cytochrome P450 (Cyt P45)-dependent monooxygenase family. The activity of P450s is usually dependent on an NADPH: Cyt P450 reductase, which helps the transfer of electrons from NADPH via FAD and FMN to the Cyt P450 protein (Olsen et al., 2010). Cyt b5 may also be an alternative electron donor. As a membrane bound hemoprotein, Cytochrome b5 can function as an electron carrier for several membrane bound oxygenases (Ozols, 1989). Many studies have shown that the activity of Cyt P450s in reconstituted membrane vesicles or in yeast cells can be enhanced by the presence of cytochrome b5 (Yamazaki et al., 1996; Yamazaki et al., 1997; Auchus et al., 1998). For instance, in petunia, full activity of F3’5’H is supported by a specific cytochrome b5 encoded by *DifF*, which can transfer electrons to F3’5’H specifically (Olsen et al., 2010). In poplar, no such cytochrome P450 reductase or cytochrome b5 has been characterized yet, but previous work in the Constabel lab showed a putative cytochrome b5 upregulated in MYB134 and MYB 115 overexpressing plants, together with all other core PA and flavonoid synthesis gene (Mellway, 2009; Franklin, 2013). In MYB 134 overexpressing plants, upregulation of both PtF3’H (27-fold) and cytochrome b5 (48-fold) corresponds to the accumulation of quercetin, a di-hydroxylated flavonol (Mellway, 2009). In MYB115 overexpressing plants, upregulation of both F3’5’H (138-fold) and cytochrome b5 (81-fold) appears to have a correlation with the accumulation of dihydromyricetin, a tri-hydroxylated flavanonol (Franklin, 2013). It is possible that the full activity of PtF3’5’H1 in *Populus* requires a cytochrome P450 reductase or cytochrome b5. Overexpression of PtF3’5’H1 may increase the amount of the enzyme itself. However, the number of electrons that can be transferred by cytochrome P450

reductase or cytochrome b5 may not increase, which could be the bottleneck for this hydroxylation reaction.

In the flavonoid pathway leading to the synthesis of anthocyanins and proanthocyanidins, F3’5’H competes with many other enzymes for the same substrate. It has been discussed that F3’H and F3’5’H competes with flavonol synthase (FLS) and dihydroflavonol 4-reductase (DFR) for the same substrate to determine the branch flow in petunia, potato and tomato (Olsen et al., 2010). In poplar, naringenin and dihydrokaempferol can be potential substrates of PtF3’5’H1. However, these substrates can also be utilized by F3H, F3’H, DFR and FLS (Figure 1-4). The composition of flavonoids is determined by the balance of many enzymes in the pathway, and the synthesis of anthocyanin and PAs may also depend on the competing enzymes (Figure 1-4). This could explain the low delphinidin and prodelphinidin content in transgenic poplar. One strategy for delphinidin and prodelphinidin accumulation can be suppression of those competing enzymes such as the endogenous F3’H by RNAi.

A lack of correlation between PtF3’5’H1 mRNA levels and protein abundance in the host plant can also explain the absence of a strong effect on the production of delphinidin and prodelphinidin. qPCR confirmed the very high expression of PtF3’5’H1 in transgenic poplar at the mRNA level. However, the actual amount of enzyme at protein level may not be as high. Many studies on the correlations of expression of specific mRNAs and corresponding proteins have been done, and a general significant correlation between mRNA levels and corresponding protein has been found (Gry et al., 2009; Vogel and Marcotte, 2012; Ponnala et al., 2014). However, the correlations may also have considerable variability. In a comprehensive survey done by Lan et al. (2012) to test the

changes in protein and transcript profiles in *Arabidopsis* roots in response to phosphate deficiency, down-regulated transcripts were not closely correlated with their corresponding proteins. Likewise, Baerenfaller et al. (2012) conducted a study in *Arabidopsis* and found that despite the decrease in transcript levels, the proteins located in plastids or endomembrane systems still accumulated. In maize, Ponnala et al. (2014) found that the correlation of mRNA levels and protein abundance is much weaker in the leaf transition zone (leaf zone with massive investments of chloroplast biogenesis and photosynthetic capacity). Walley et al. (2013) found that many of the most abundant proteins are not correlated with their mRNA levels in maize seeds, and many of the most abundant mRNAs are not correlated with their proteins abundance. Therefore, in my study, the overexpression of PtF3'5'H1 did succeed in dramatic accumulation of mRNAs, but the abundance of PtF3'5'H1 at protein level may not be that high. Quite a few factors have been proposed to have effects on mRNA-protein correlation, including degradation of mRNA/protein, UTRs (untranslated region), size of mRNA, recruitment of ribosomes to mRNA, mRNA export, impact of microRNAs on translation as well as the protein functions (Vogel et al., 2010; Olivares-Hernández et al., 2011; Vélez-Bermúdez and Schmidt, 2014).

4.4 Agro-infiltration of *Nicotiana benthamiana*

PtF3'5'H1 was expected to participate in anthocyanin synthesis in poplar by both phylogenetic and gene expression analysis. To confirm this role in an independent experimental system, transient expression of PtF3'5'H1 together with AtPAP1 and AtGL3 in *N. benthamiana* was used as an assay to test enzyme function. *N. benthamiana*

is fast growing, and usually only takes around 6 weeks to become mature. This species has been used extensively for agro-infiltration experiments. Importantly, transient co-expression of AtPAP1and AtGL3 has been proven to succeed in induction of anthocyanin synthesis in leaf of *N. benthamiana* (Lin-Wang et al., 2010). In my study, transient expression of AtPAP1 and AtGL3 in *N. benthamiana* yielded approximately the same amount of anthocyanins as transient expression of PtF3’5’H1 with AtPAP1 and AtGL3 (Figure 3-24). Meanwhile, HPLC analysis revealed that the same two HPLC peaks were present in both treatments, and one of them was putatively identified as a delphinidin (Figure 3-25). In recently published work, agroinfiltration of snapdragon MYB and bHLH transcription factors in *N. benthamiana* leaves led to accumulation of delphinidin-3-rutinoside (Gomez-Roldan et al., 2014). This indicates the presence of endogenous F3’5’H in the genome of *N. benthamiana*. Thus, the influence of the endogenous F3’5’H has to be considered when transiently expressing PtF3’5’H1 in *N. benthamiana*. Since no change in overall amount and content of anthocyanins due to poplar F3’5’H expression in *N. benthamiana* was detected, the function of PtF3’5’H1 in this species is difficult to evaluate. A possible explanation of the lack of an effect can be that the PtF3’5’H1 was active in *N. benthamiana*, and it competes with the endogenous F3’5’H for the same substrates in the anthocyanin synthesis (Figure 1-4), and thus no change was found. Another possible explanation is that PtF3’5’H1 cannot perform its normal function because of the lack of specific cytochrome P450 reductase or cytochrome b5 in *N. benthamiana*.

4.5 Down-regulation of general flavonoid and PA synthesis genes in PtF3’5’H1 overexpressing poplar

In transgenic poplar plants overexpressing PtF3’5’H1, downregulation of many key enzymes in the flavonoid pathway (PtANR1, PtDFR1, PtDFR2, PtCHS1, PtANS1) was observed, which was not expected. One speculative explanation is that overexpression of PtF3’5’H1 leads to accumulation of novel tri-hydroxylated flavonoids, which may function as signal compounds to feed back to down-regulate the pathway. For instance, they may trigger the expression of some transcription factors that down-regulate the genes of the flavonoid pathway.

One anomaly in my data is that the PA levels in leaves were not affected even though many genes that encode key enzymes were down-regulated. Plants were moved outside the greenhouse for one week before harvest. During that period, plants were exposed to lower average temperatures and much higher light intensity than inside the greenhouse. If the down-regulation of those genes happened after plants being moved outside, then it is possible that one week is not enough for observation of PA concentration change. Since both the synthesis and transportation of PA take time. It is also possible that the amount of enzymes in the pathway was already excessive in the wild-type plants. Another explanation could be the low concentration of PAs in the leaf tissues. This could nullify the difference between transgenic and wild-type plants.

5. Chapter Five: Overall conclusions and future directions

The objective of this study was to characterize the function of PtF3’5’H1 in poplar PA and anthocyanin synthesis by generating transgenic poplar plants and transient expression of PtF3’5’ H1 in *Nicotiana benthamiana* leaves. In transgenic poplar, accumulation of tri-hydroxylated anthocyanin (delphinidin derivatives) was found, making this the first study overexpressed the endogenous F3’5’H and successfully changed the anthocyanin composition. Preliminary data from LC-MS showed no clear change in the hydroxylation pattern of PAs. Neither the overall amounts of PA or anthocyanin were changed. Transient expression of PtF3’5’H1 together with AtPAP1 and AtGL3 showed the same result as transient expression of AtPAP1 and AtGL3 in *N. benthamiana* leaves, indicating no effect of the PtF3’5’H1 gene. Therefore, PtF3’5’H1 has a potential role in controlling the B-ring hydroxylation pattern of anthocyanins in poplar. Overexpression of PtF3’5’H1 alone in poplar was not sufficient to accumulate prodelphinidin, and therefore it remains unclear if this gene contributes to PA synthesis.

The possible reasons for less or no accumulation of delphinidin, prodelphinidin have been discussed above. In addition, F3’5’H may also exhibit the F3’H activity (Seitz et al., 2006; Sun et al., 2013). Several experiments can be proposed to investigate further mechanisms why the effects of PtF3’5’H1 are limited in my experiments. First of all, to verify the function of PtF3’5’H in anthocyanin and PA synthesis in poplar, PtF3’5’H1 knock down plants can be generated. In addition, recombinant protein assays can be conducted to test the substrate specificity of PtDFR1 and PtDFR2. Furthermore, characterizing the cytochrome b5 in *Populus* can help us to understand the function of PtF3’5’H better. By inactivating the gene using targeted transposon mutagenesis and

analyzing the composition of anthocyanin and PAs, the function of cytochrome b5 in *Populus* can be determined. RNAi technique can also be used to knock down some PtF3’5’H competing enzymes, including F3’H, FLS. Since the correlation between mRNA level and protein abundance of PtF3’5’H1 is unknown, it will be worthwhile to test their correlation in transgenic poplar. Overexpression of PtF3’5’H1 in poplar also led to some changes in the phenolic profile. Two new peaks were found in all transgenic plants while not in wild-type (Figure A-2). LC-MS could be used to further characterize those peaks as well as to identify the putative delphinidin derivatives from poplar and *N. benthamiana* leaf samples.

Here, PtF3’5’H1 was characterized as an enzyme that can contribute to determining the B-ring hydroxylation pattern of anthocyanins in poplar. Overexpression of PtF3’5’H1 alone was not able to change the composition of PAs, however. In future work, if it becomes possible to manipulate the B-ring hydroxylation of PA, the biological activities may change, including anti-herbivore activity (Ayres et al., 1997), reactive activity (Kraus et al., 2003), the rate of leaf decomposition (Scioneaux et al., 2011), and N mineralization rates (Nierop et al., 2006). Our work thus provides additional future directions for PA and anthocyanin research in poplar. If the hydroxylation pattern of PAs can be successfully manipulated by PtF3’5’H1 in the future, it may become possible to test the functional importance of the hydroxylation pattern in PA.

Bibliography

Abrahams S, Tanner GJ, Larkin PJ, Ashton AR (2002) Identification and biochemical characterization of mutants in the proanthocyanidin pathway in *Arabidopsis*. Plant Physiol **130**: 561–576

Acamovic T, Brooker JD (2005) Biochemistry of plant secondary metabolites and their effects in animals. Proc Nutr Soc **64**: 403–412

Akada S, Dube SK (1995) Organization of soybean chalcone synthase gene clusters and characterization of a new member of the family. Plant Mol Biol **29**: 189–199

Aoki T, Akashi T, Ayabe S (2000) Flavonoids of leguminous plants: structure, biological activity, and biosynthesis. J Plant Res **113**: 475–488

Arcas MC, Botía JM, Ortuño AM, Del Río JA (2000) UV irradiation alters the levels of flavonoids involved in the defence mechanism of *Citrus aurantium* fruits against *Penicillium digitatum*. Eur J Plant Pathol **106**: 617–622

Auchus RJ, Lee TC, Miller WL (1998) Cytochrome b5 augments the 17, 20-lyase activity of human P450c17 without direct electron transfer. J Biol Chem **273**: 3158–3165

Ayres MP, Clausen TP, Maclean SF, Redman AM, Reichardt PB (1997) Diversity of structure and antiherbivore activity in condensed tannins. Ecology **78**: 1696–1712

Baerenfaller K, Massonnet C, Walsh S, Baginsky S, Bühlmann P, Hennig L, Hirsch-Hoffmann M, Howell KA, Kahlau S, Radziejwoski A (2012) Systems-based analysis of *Arabidopsis* leaf growth reveals adaptation to water deficit. Mol Syst Biol. doi: 10.1038/msb.2012.39

Barbehenn RV, Constabel CP (2011) Tannins in plant-herbivore interactions. Phytochemistry **72**: 1551–1565

Barceló J, Poschenrieder C (2002) Fast root growth responses, root exudates, and internal detoxification as clues to the mechanisms of aluminium toxicity and resistance: a review. Environ Exp Bot **48**: 75–92

Baudry A, Heim MA, Dubreucq B, Caboche M, Weisshaar B, Lepiniec L (2004) TT2, TT8, and TTG1 synergistically specify the expression of BANYULS and proanthocyanidin biosynthesis in *Arabidopsis thaliana*. Plant J **39**: 366–380

Beckman CH (2000) Phenolic-storing cells: keys to programmed cell death and periderm formation in wilt disease resistance and in general defence responses in plants? Physiol Mol Plant Pathol **57**: 101–110

B**ehrens A, Maie N, Knicker H, K ögel-Knabner I** (2003) MALDI-TOF mass spectrometry and PSD fragmentation as means for the analysis of condensed tannins in plant leaves and needles. Phytochemistry **62**: 1159–1170

Bendz G, Haglund Å (1968) *Populus tremula*. The anthocyanins of leaves and catkins. Acta Chem Scand **22**: 1365–1365

Benoit LF, Berry AM (1997) Flavonoid-like compounds from seeds of red alder (*Alnus rubra*) influence host nodulation by *Frankia* (Actinomycetales). Physiol Plant **99**: 588–593

Bernays EA, Chamberlain DJ, Leather EM (1981) Tolerance of acridids to ingested condensed tannin. J Chem Ecol **7**: 247–256

Bieza K, Lois R (2001) An *Arabidopsis* mutant tolerant to lethal ultraviolet-B levels shows constitutively elevated accumulation of flavonoids and other phenolics. Plant Physiol **126**: 1105–1115

Boase MR, Lewis DH, Davies KM, Marshall GB, Patel D, Schwinn KE, Deroles SC (2010) Isolation and antisense suppression of flavonoid 3', 5'-hydroxylase modifies flower pigments and colour in cyclamen. BMC Plant Biol **10**: 107

Bogs J, Downey MO, Harvey JS, Ashton AR, Tanner GJ, Robinson SP (2005) Proanthocyanidin synthesis and expression of genes encoding leucoanthocyanidin reductase and anthocyanidin reductase in developing grape berries and grapevine leaves. Plant Physiol **139**: 652–663

Bogs J, Ebadi A, Mcdavid D, Robinson SP (2006) Identification of the flavonoid hydroxylases from grapevine and their regulation during fruit development. Plant Physiol **140**: 279–291

Borevitz JO, Xia Y, Blount J, Dixon RA, Lamb C (2000) Activation tagging identifies a conserved MYB regulator of phenylpropanoid biosynthesis. Plant Cell Online **12**: 2383–2393

Bridle P, Stott KG, Timberlake CF (1973) Anthocyanins in *Salix* species: A new anthocyanin in *Salix purpurea* bark. Phytochemistry **12**: 1103–1106

Brugliera F, Barri-Rewell G, Holton TA, Mason JG (1999) Isolation and characterization of a flavonoid 3'-hydroxylase cDNA clone corresponding to the Ht1 locus of *Petunia hybrida*. Plant J **19**: 441–451

Brunner AM, Busov VB, Strauss SH (2004) Poplar genome sequence: functional genomics in an ecologically dominant plant species. Trends Plant Sci **9**: 49–56

Bryant JP, Reichardt PB, Clausen TP, Werner RA (1993) Effects of mineral nutrition on delayed inducible resistance in Alaska paper birch. Ecology **74**: 2072–2084

Bunea A, Rugină D, Sconţa Z, Pop RM, Pintea A, Socaciu C, Tăbăran F, Grootaert C, Struijs K, VanCamp J (2013) Anthocyanin determination in blueberry extracts from various cultivars and their anti-proliferative and apoptotic properties in B16-F10 metastatic murine melanoma cells. Phytochemistry **95**: 436–444

Cain C, Saslowsky D, Walker R, Shirley B (1997) Expression of chalcone synthase and chalcone isomerase proteins in *Arabidopsis* seedlings. Plant Mol Biol **35**: 377–381

Castellarin SD, Di Gaspero G, Marconi R, Nonis A, Peterlunger E, Paillard S, Adam-Blondon AF, Testolin R (2006) Colour variation in red grapevines (*Vitis vinifera* L.): genomic organisation, expression of flavonoid 3'-hydroxylase, flavonoid 3', 5'-hydroxylase genes and related metabolite profiling of red cyanidin-/blue delphinidin-based anthocyanins in berry skin. BMC Genomics **7**: 12

Chen F, Liu CJ, Tschaplinski TJ, Zhao N (2009) Genomics of secondary metabolism in *Populus*: interactions with biotic and abiotic environments. Crit Rev Plant Sci **28**: 375–392

Chen K, Ohmura W, Doi S, Aoyama M (2004) Termite feeding deterrent from Japanese larch wood. Bioresour Technol **95**: 129–134

Cone K (2007) Anthocyanin synthesis in maize aleurone tissue. *In* O-A Olsen, ed, Endosperm SE- 117. Springer Berlin Heidelberg, pp 121–139

Constabel CP, Lindroth RL (2010) The impact of genomics on advances in herbivore defense and secondary metabolism in *Populus*. *In* S Jansson, R Bhalerao, A Groover, eds, Genetics and Genomics of *Populus*. SE- 13. Springer New York, pp 279–305

Cooper JE (2004) Incorporating advances in plant pathology. Adv Bot Res **41**: 1–62

Cushnie TPT, Lamb AJ (2005) Antimicrobial activity of flavonoids. Int J Antimicrob Agents **26**: 343–356

Dixon RA (2005) Engineering of plant natural product pathways. Curr Opin Plant Biol **8**: 329–336

Downey MO, Harvey JS, Robinsin SP (2003) Analysis of tannins in seeds and skins of Shiraz grapes throughout berry development. Aust J Grape Wine Res **9**: 15–27

Engström MT, Pälijärvi M, Fryganas C, Grabber JH, Mueller-Harvey I, Salminen JP (2014) Rapid qualitative and quantitative analyses of proanthocyanidin oligomers and polymers by UPLC-MS/MS. J Agric Food Chem **62**: 3390–3399

Eyles A, Davies NW, Yuan ZQ, Mohammed C (2003) Host responses to natural infection by *Cytonaema* sp. in the aerial bark of *Eucalyptus globulus*. For Pathol **33**: 317–331

Feeny P (1970) Seasonal changes in oak leaf tannins and nutrients as a cause of spring feeding by winter moth caterpillars. Ecology **51**: 565–581

Fillatti J, Sellmer J, McCown B, Haissig B, Comai L (1987) *Agrobacterium* mediated transformation and regeneration of *Populus*. Mol Gen Genet **206**: 192–199

Ford CM, Boss PK, Høj PB (1998) Cloning and characterization of *Vitis vinifera* UDP-glucose:flavonoid 3-*O*-glucosyltransferase, a homologue of the enzyme encoded by the maize bronze-1locus that may primarily serve to glucosylate anthocyanidins *in vivo*. J Biol Chem **273**: 9224–9233

Forkmann G, Heller W (1999) Comprehensive natural products chemistry. Compr Nat Prod Chem **1**: 713–748

Forkmann G, Martens S (2001) Metabolic engineering and applications of flavonoids. Curr Opin Biotechnol **12**: 155–160

Franklin AM (2013) Functional characterization of PtMYB115, a regulator of condensed tannin synthesis in poplar. MSc Thesis. University of Victoria, Victoria, BC, Canada

Fukui Y, Tanaka Y, Kusumi T, Iwashita T, Nomoto K (2003) A rationale for the shift in colour towards blue in transgenic carnation flowers expressing the flavonoid 3', 5'-hydroxylase gene. Phytochemistry **63**: 15–23

Gerats AGM, Vlaming P, Doodeman M, Al B, Schram AW (1982) Genetic control of the conversion of dihydroflavonols into flavonols and anthocyanins in flowers of *Petunia hybrida*. Planta **155**: 364–368

Giusti MM, Rodr ́guez-Saona LE, Wrolstad RE (1999) Molar absorptivity and color characteristics of acylated and non-acylated pelargonidin-based anthocyanins. J Agric Food Chem **47**: 4631–4637

Gomez-Roldan V, de Vos RCH, Bosch D, Beekwilder J, Outchkourov NS, Hall RD, Carollo CA (2014) Control of anthocyanin and non-flavonoid compounds by anthocyanin-regulating MYB and bHLH transcription factors in *Nicotiana benthamiana* leaves. Front Plant Sci **5**: 1–9

Gonzalez A, Zhao M, Leavitt JM, Lloyd AM (2008) Regulation of the anthocyanin biosynthetic pathway by the TTG1/bHLH/Myb transcriptional complex in *Arabidopsis* seedlings. Plant J **53**: 814–827

Graham SE, Peterson JA (1999) How similar are P450s and what can their differences teach us ? Arch Biochem Biophys **369**: 24–29

Gry M, Rimini R, Strömberg S, Asplund A, Pontén F, Uhlén M, Nilsson P (2009) Correlations between RNA and protein expression profiles in 23 human cell lines. BMC Genomics **10**: 365

Hagerman AE, Rice ME, Ritchard NT (1998) Mechanisms of protein precipitation for two tannins, pentagalloyl glucose and epicatechin16 (4→8) catechin (procyanidin). J Agric Food Chem **46**: 2590–2595

Han Y, Vimolmangkang S, Soria-Guerra RE, Rosales-Mendoza S, Zheng D, Lygin AV, Korban SS (2010) Ectopic expression of apple F3'H genes contributes to anthocyanin accumulation in the *Arabidopsis* tt7 mutant grown under nitrogen stress. Plant Physiol **153**: 806–820

Harbertson JF, Kilmister RL, Kelm MA, Downey MO (2014) Impact of condensed tannin size as individual and mixed polymers on bovine serum albumin precipitation. Food Chem **160**: 16–21

Haribal M, Feeny P (2003) Combined roles of contact stimulant and deterrents in assessment of host-plant quality by ovipositing zebra swallowtail butterflies. J Chem Ecol **29**: 653–670

Hasemann CA, Kurumbail RG, Boddupalli SS, Peterson JA, Deisenhofer J (1995) Structure and function of cytochromes P450: a comparative analysis of three crystal structures. Structure **3**: 41–62

He F, Pan QH, Shi Y, Duan CQ (2008) Biosynthesis and genetic regulation of proanthocyanidins in plants. Molecules **13**: 2674–2703

He H, Ke H, Keting H, Qiaoyan X, Silan D (2013) Flower colour modification of chrysanthemum by suppression of F3'H and overexpression of the exogenous *Senecio cruentus* F3'5'H Gene. PLoS One **8**: e74395

Helsper JPFG, Hoogendijk JM, van Norel A, Kolodziej H (1993) Characterization and trypsin inhibitor activity of proanthocyanidins from *Vicia faba*. Phytochemistry **34**: 1255–1260

Holton, TA (1996) Transgenic plants exhibiting altered flower colour and methods for producing same. WO/1996/036716

Holton TA, Brugliera F, Lester DR, Tanaka Y, Hyland CD, Menting JGT, Lu CY, Farcy E, Stevenson TW, Cornish EC (1993) Cloning and expression of cytochrome P450 genes controlling flower colour. Nature **366**: 276–279

Holton TA, Tanaka Y (2014) Blue roses — a pigment of our imagination? Trends Biotechnol **12**: 40–42

Huang W, Sun W, Wang Y (2012) Isolation and molecular characterisation of flavonoid 3’-hydroxylase and flavonoid 3’, 5’-hydroxylase genes from a traditional Chinese medicinal plant, *Epimedium sagittatum*. Gene **497**: 125–130

Iwashina T (2000) The structure and distribution of the flavonoids in plants. J Plant Res **113**: 287–299

Jende-Strid B (1993) Genetic control of flavonoid biosynthesis in barley. Hereditas **119**: 187–204

Jeong ST, Goto-Yamamoto N, Hashizume K, Esaka M (2006) Expression of the flavonoid 3’-hydroxylase and flavonoid 3’, 5’-hydroxylase genes and flavonoid composition in grape (*Vitis vinifera*). Plant Sci **170**: 61–69

Johnson ET, Ryu S, Yi H, Shin B, Cheong H, Choi G (2001) Alteration of a single amino acid changes the substrate specificity of dihydroflavonol 4-reductase. Plant J **25**: 325–333

Johnson ET, Yi H, Shin B, Oh BJ, Cheong H, Choi G (1999) *Cymbidium hybrida* dihydroflavonol 4-reductase does not efficiently reduce dihydrokaempferol to produce orange pelargonidin-type anthocyanins. Plant J **19**: 81–85

Kaltenbach M, Schröder G, Schmelzer E, Lutz V, Schröder J (1999) Flavonoid hydroxylase from *Catharanthus roseus*: cDNA, heterologous expression, enzyme properties and cell-type specific expression in plants. Plant J **19**: 183–193

Kang JH, McRoberts J, Shi F, Moreno J, Jones D, Howe GA (2014) The flavonoid biosynthetic enzyme chalcone isomerase modulates terpenoid production in glandular trichomes of tomato. Plant Physiol **164**: 1161–1174

Katsumoto Y, Fukuchi-Mizutani M, Fukui Y, Brugliera F, Holton TA, Karan M, Nakamura N, Yonekura-Sakakibara K, Togami J, Pigeaire A (2007) Engineering of the rose flavonoid biosynthetic pathway successfully generated blue-hued flowers accumulating delphinidin. Plant Cell Physiol **48**: 1589–1600

Kobayashi H, Graven YN, Broughton WJ, Perret X (2004) Flavonoids induce temporal shifts in gene-expression of nod-box controlled loci in *Rhizobium* sp. NGR234. Mol Microbiol **51**: 335–347

Kraus TEC, Yu Z, Preston CM, Dahlgren RA, Zasoski RJ (2003) Linking chemical reactivity and protein precipitation to structural characteristics of foliar tannins. J Chem Ecol **29**: 703–730

Kreuzaler F, Hahlbrock K (1972) Enzymatic synthesis of aromatic compounds in higher plants: Formation of naringenin (5,7,4'-trihydroxyflavanone) from *p*-coumaroyl coenzyme A and malonyl coenzyme A. FEBS Lett **28**: 69–72

Lan P, Li W, Schmidt W (2012) Complementary proteome and transcriptome profiling in phosphate-deficient *Arabidopsis* roots reveals multiple levels of gene regulation. Mol Cell Proteomics **11**: 1156–1166

Lattanzio V (2003) Bioactive polyphenols: Their role in quality and storability of fruit and vegetables. J Appl Bot **77**: 128–146

Lea U, Slimestad R, Smedvig P, Lillo C (2007) Nitrogen deficiency enhances expression of specific MYB and bHLH transcription factors and accumulation of end products in the flavonoid pathway. Planta **225**: 1245–1253

Lepiniec L, Debeaujon I, Routaboul JM, Baudry A, Pourcel L, Nesi N, Caboche M (2006) Genetics and biochemistry of seed flavonoids. Annu Rev Plant Biol **57**: 405–430

Li J, Ou-Lee TM, Raba R, Amundson RG, Last RL (1993) *Arabidopsis* flavonoid mutants are hypersensitive to UV-B irradiation. Plant Cell Online **5**: 171–179

Lindroth RL, Hwang SY (1996) Diversity, redundancy, and multiplicity in chemical defense systems of aspen. *In* J Romeo, J Saunders, P Barbosa, eds, Phytochem. Divers. Redundancy Ecol. Interact. SE- 2. Springer US, pp 25–56

Lindroth RL, Roth S, Nordheim EV (2001) Genotypic variation in response of quaking aspen (*Populus tremuloides*) to atmospheric CO_2 enrichment. Oecologia 126: 371–379

Lin-Wang K, Bolitho K, Grafton K, Kortstee A, Karunairetnam S, McGhie TK, Espley RV, Hellens RP, Allan AC (2010) An R2R3 MYB transcription factor associated with regulation of the anthocyanin biosynthetic pathway in Rosaceae. BMC Plant Biol **10**: 50

Liu Y, Shi Z, Maximova S, Payne MJ, Guiltinan MJ (2013) Proanthocyanidin synthesis in *Theobroma cacao*: genes encoding anthocyanidin synthase, anthocyanidin reductase, and leucoanthocyanidin reductase. BMC Plant Biol **13**: 202

Livak KJ, Schmittgen TD (2001) Analysis of relative gene expression data using real-time quantitative PCR and the $2^{-\Delta\Delta CT}$ method. Methods **25**: 402–408

Major IT, Constabel CP (2006) Molecular analysis of poplar defense against herbivory: comparison of wound- and insect elicitor-induced gene expression. New Phytol **172**: 617–635

Mallikarjuna N, Kranthi KR, Jadhav DR, Kranthi S, Chandra S (2004) Influence of foliar chemical compounds on the development of *Spodoptera litura* (Fab.) in interspecific derivatives of groundnut. J Appl Entomol **128**: 321–328

Marinova K, Pourcel L, Weder B, Schwarz M, Barron D, Routaboul JM, Debeaujon I, Klein M (2007) The *Arabidopsis* MATE transporter TT12 acts as a vacuolar flavonoid/H+-antiporter active in proanthocyanidin-accumulating cells of the seed coat. Plant Cell Online **19**: 2023–2038

Marles MAS, Ray H, Gruber MY (2003) New perspectives on proanthocyanidin biochemistry and molecular regulation. Phytochemistry **64**: 367–383

Martin M, Rockholm D, Martin J (1985) Effects of surfactants, pH, and certain cations on precipitation of proteins by tannins. J Chem Ecol **11**: 485–494

Mathesius U (2003) Conservation and divergence of signalling pathways between roots and soil microbes – the *Rhizobium*-legume symbiosis compared to the development of lateral roots, mycorrhizal interactions and nematode-induced galls. Plant Soil **255**: 105–119

Matsumoto T, Nishida K, Noguchi M, Tamaki E (1970) Isolation and identification of an anthocyanin from the cell suspension culture of poplar. Agric Biol Chem **34**: 1110–1114

McArt SH, Spalinger DE, Collins WB, Schoen ER, Stevenson T, Bucho M (2009) Summer dietary nitrogen availability as a potential bottom-up constraint on moose in south-central Alaska. Ecology **90**: 1400–1411

McCullough ML, Peterson JJ, Patel R, Jacques PF, Shah R, Dwyer JT (2012) Flavonoid intake and cardiovascular disease mortality in a prospective cohort of US adults. Am J Clin Nutr. doi: 10.3945/ajcn.111.016634

Mellway RD (2009) The regulation of stress-induced proanthocyanidin metabolism in poplar. PhD Thesis. University of Victoria, Victoria, BC, Canada

Mellway RD, Tran LT, Prouse MB, Campbell MM, Constabel CP (2009) The wound-, pathogen-, and ultraviolet B-responsive MYB134 gene encodes an R2R3 MYB transcription factor that regulates proanthocyanidin synthesis in poplar. Plant Physiol **150**: 924–941

Miranda M, Ralph SG, Mellway R, White R, Heath MC, Bohlmann J, Constabel CP (2007) The transcriptional response of hybrid poplar (*Populus trichocarpa x P. deltoids*) to infection by *Melampsora medusae* leaf rust involves induction of flavonoid pathway genes leading to the accumulation of proanthocyanidins. Mol Plant-Microbe Interact **20**: 816–831

Mol J, Grotewold E, Koes R (1998) How genes paint flowers and seeds. Trends Plant Sci **3**: 212–217

Moore JP, Westall KL, Ravenscroft N, Farrant JM, Lindsey GG, Brandt WF (2005) The predominant polyphenol in the leaves of the resurrection plant *Myrothamnus flabellifolius*, 3,4,5 tri-*O*-galloylquinic acid, protects membranes against desiccation and free radical-induced oxidation. Biochem J **385**: 301–308

Muoki R, Paul A, Kumari A, Singh K, Kumar S (2012) An improved protocol for the isolation of RNA from roots of tea (*Camellia sinensis* (L.) O. Kuntze). Mol Biotechnol **52**: 82–88

Nebert DW, Nelson DR (1991) Cytochrome P450. Methods Enzymol **206**: 3–11

Nelson DR, Schuler MA, Paquette SM, Werck-Reichhart D, Bak S (2004) Comparative genomics of rice and *Arabidopsis*. Analysis of 727 cytochrome P450 genes and pseudogenes from a monocot and a dicot. Plant Physiol **135**: 756–772

Nemie-Feyissa D, Olafsdottir SM, Heidari B, Lillo C (2014) Nitrogen depletion and small R3-MYB transcription factors affecting anthocyanin accumulation in *Arabidopsis* leaves. Phytochemistry **98**: 34–40

Nesi N, Jond C, Debeaujon I, Caboche M, Lepiniec L (2001) The *Arabidopsis* TT2 gene encodes an R2R3 MYB domain protein that acts as a key determinant for proanthocyanidin accumulation in developing seed. Plant Cell **13**: 2099–2114

Nierop K, Preston C, Verstraten J (2006) Linking the B ring hydroxylation pattern of condensed tannins to C, N and P mineralization. A case study using four tannins. Soil Biol Biochem **38**: 2794–2802

Nimal Punyasiri PA, Tanner GJ, Abeysinghe ISB, Kumar V, Campbell PM, Pradeepa NHL (2004) *Exobasidium vexans* infection of *Camellia sinensis* increased 2, 3-cis isomerisation and gallate esterification of proanthocyanidins. Phytochemistry **65**: 2987–2994

Nishihara M, Nakatsuka T, Yamamura S (2005) Flavonoid components and flower color change in transgenic tobacco plants by suppression of chalcone isomerase gene. FEBS Lett **579**: 6074–6078

Olivares-Hernández R, Bordel S, Nielsen J (2011) Codon usage variability determines the correlation between proteome and transcriptome fold changes. BMC Syst Biol **5**: 33

Olsen KM, Hehn A, Jugdé H, Slimestad R, Larbat R, Bourgaud F, Lillo C (2010) Identification and characterisation of CYP75A31, a new flavonoid 3'5'-hydroxylase, isolated from *Solanum lycopersicum*. BMC Plant Biol **10**: 21

Orsolić N, Knezević AH, Sver L, Terzić S, Basić I (2004) Immunomodulatory and antimetastatic action of propolis and related polyphenolic compounds. J Ethnopharmaco**l 94**: 307–315

Osier T, Lindroth RL (2006) Genotype and environment determine allocation to and costs of resistance in quaking aspen. Oecologia **148**: 293–303

Osier TL, Hwang SY, Lindroth RL (2000) Effects of phytochemical variation in quaking aspen *Populus tremuloides* clones on gypsy moth *Lymantria dispar* performance in the field and laboratory. Ecol Entomol **25**: 197–207

Ozols J (1989) Structure of cytochrome b5 and its topology in the microsomal membrane. Biochim Biophys Acta - Protein Struct Mol Enzymol **997**: 121–130

Padmavati M, Sakthivel N, Thara KV, Reddy AR (1997) Differential sensitivity of rice pathogens to growth inhibition by flavonoids. Phytochemistry **46**: 499–502

Pang Y, Peel GJ, Wright E, Wang Z, Dixon RA (2007) Early steps in proanthocyanidin biosynthesis in the model legume *Medicago truncatula*. Plant Physiol **145**: 601–615

Patra B, Schluttenhofer C, Wu Y, Pattanaik S, Yuan L (2013) Transcriptional regulation of secondary metabolite biosynthesis in plants. Biochim Biophys Acta **1829**: 1236–1247

Payne CT, Zhang F, Lloyd AM (2000) GL3 encodes a bHLH protein that regulates trichome development in *Arabidopsis* through interaction with GL1 and TTG1. Genet **156**: 1349–1362

Peer WA, Murphy AS (2007) Flavonoids and auxin transport: modulators or regulators? Trends Plant Sci **12**: 556–563

Peltonen PA, Vapaavuori E, Julkunen-tiitto R (2005) Accumulation of phenolic compounds in birch leaves is changed by elevated carbon dioxide and ozone. Glob Chang Biol **11**: 1305–1324

Peters DJ, Constabel CP (2002) Molecular analysis of herbivore-induced condensed tannin synthesis: cloning and expression of dihydroflavonol reductase from trembling aspen (*Populus tremuloides*). Plant J **32**: 701–712

Pichersky E, Sharkey TD, Gershenzon J (2006) Plant volatiles: a lack of function or a lack of knowledge? Trends Plant Sci **11**: 421

Pizzi A, Cameron FA (1986) Flavonoid tannins — structural wood components for drought-resistance mechanisms of plants. Wood Sci Technol **20**: 119–124

Ponnala L, Wang Y, Sun Q, van Wijk KJ (2014) Correlation of mRNA and protein abundance in the developing maize leaf. Plant J **78**: 424–440

Porter LJ, Hrstich LN, Chan BG (1985) The conversion of procyanidins and prodelphinidins to cyanidin and delphinidin. Phytochemistry **25**: 223–230

Price MN, Dehal PS, Arkin AP (2009) FastTree: Computing large minimum evolution trees with profiles instead of a distance matrix. Mol Biol Evol **26**: 1641–1650

Qi Y, Lou Q, Quan Y, Liu Y, Wang Y (2013) Flower-specific expression of the *Phalaenopsis* flavonoid 3', 5'-hydoxylase modifies flower color pigmentation in *Petunia* and *Lilium*. Plant Cell Tissue Organ Cult **115**: 263–273

Rehill B, Whitham T, Martinsen G, Schweitzer J, Bailey J, Lindroth R (2006) Developmental trajectories in cottonwood phytochemistry. J Chem Ecol **32**: 2269–2285

Robbins MP, Bavage AD, Allison G, Davies T, Hauck B, Morris P (2005) A comparison of two strategies to modify the hydroxylation of condensed tannin polymers in *Lotus corniculatus* L. Phytochemistry **66**: 991–999

Rupasinghe S, Baudry J, Schuler MA (2003) Common active site architecture and binding strategy of four phenylpropanoid P450s from *Arabidopsis thaliana* as revealed by molecular modeling. Protein Eng **16**: 721–731

Saito K, Kobayashi M, Gong Z, Tanaka Y, Yamazaki M (1999) Direct evidence for anthocyanidin synthase as a 2-oxoglutarate-dependent oxygenase: molecular cloning and functional expression of cDNA from a red forma of *Perilla frutescens*. Plant J **17**: 181–189

Samieri C, Sun Q, Townsend MK, Rimm EB, Grodstein F (2014) Dietary flavonoid intake at midlife and healthy aging in women. Am J Clin Nutr. doi: 10.3945/ajcn.114.085605

Santos-Buelga C, García-Viguera C, Tomás-Barberán FA (2003) On-line identification of flavonoids by HPLC coupled to diode array detection. *In* C Santos-Buelga, G Williamson., eds, Methods polyphen. Anal. Chapter 5. The Royal Society of Chemistry, Cambridge, pp 92–124

Santos-Buelga C, Scalbert A (2000) Proanthocyanidins and tannin-like compounds – nature, occurrence, dietary intake and effects on nutrition and health. J Sci Food Agric **80**: 1094–1117

Sarni-Manchado P, Cheynier V, Moutounet M (1998) Interactions of grape seed tannins with salivary proteins. J Agric Food Chem **47**: 42–47

Saslowsky D, Winkel-Shirley B (2001) Localization of flavonoid enzymes in *Arabidopsis* roots. Plant J **27**: 37–48

Scalbert A (1991) Antomicrobial properties of tannins. Phytochemistry **30**: 3875–3883

Schaart JG, Dubos C, Romero De La Fuente I, van Houwelingen AMML, de Vos RCH, Jonker HH, Xu W, Routaboul JM, Lepiniec L, Bovy AG (2013) Identification and characterization of MYB-bHLH-WD40 regulatory complexes controlling proanthocyanidin biosynthesis in strawberry (*Fragaria* × *ananassa*) fruits. New Phytol **197**: 454–467

Schoenbohm C, Martens S, Eder C, Forkmann G, Weisshaar B (2000) Identification of the *Arabidopsis thaliana* flavonoid 3'-hydroxylase gene and functional expression of the encoded P450 enzyme. Biol Chem **381**: 749–753

Schuler MA, Werck-Reichhart D (2003) Functional genomics of P450s. Annu Rev Plant Biol **54**: 629–667

Scioneaux A, Schmidt M, Moore M, Lindroth R, Wooley S, Hagerman A (2011) Qualitative variation in proanthocyanidin composition of *Populus* species and hybrids: Genetics is the key. J Chem Ecol **37**: 57–70

Seitz C, Eder C, Deiml B, Kellner S, Martens S, Forkmann G (2006) Cloning, functional identification and sequence analysis of flavonoid 3'-hydroxylase and flavonoid 3', 5'-hydroxylase cDNAs reveals independent evolution of flavonoid 3', 5'-hydroxylase in the *Asteraceae* family. Plant Mol Biol **61**: 365–381

Seitz C, Vitten M, Steinbach P, Hartl S, Hirsche J, Rathje W, Treutter D, Forkmann G (2007) Redirection of anthocyanin synthesis in *Osteospermum hybrida* by a two-enzyme manipulation strategy. Phytochemistry **68**: 824–833

Seo J, Kim S, Kim J, Cha H, Liu J (2007) Co-expression of flavonoid 3' 5'-hydroxylase and flavonoid 3'-hydroxylase accelerates decolorization in transgenic chrysanthemum petals. J Plant Biol **50**: 626–631

Sharma SB, Dixon RA (2005) Metabolic engineering of proanthocyanidins by ectopic expression of transcription factors in *Arabidopsis thaliana*. Plant J **44**: 62–75

Shimada T (2006) Salivary proteins as a defense against dietary tannins. J Chem Ecol **32**: 1149–1163

Shimada Y, Ohbayashi M, Nakano-Shimada R, Okinaka Y, Kiyokawa S, Kikuchi Y (2001) Genetic engineering of the anthocyanin biosynthetic pathway with flavonoid-3', 5'-hydroxylase: specific switching of the pathway in petunia. Plant Cell Rep **20**: 456–462

Sievers F, Wilm A, Dineen D, Gibson TJ, Karplus K, Li W, Lopez R, McWilliam H, Remmert M, Söding J (2011) Fast, scalable generation of high-quality protein multiple sequence alignments using Clustal Omega. Mol Syst Biol **7**: 539

Skadhauge B, Thomsen KK, Von Wettstein D (1997) The role of the barley testa layer and its flavonoid content in resistance to *Fusarium* infections. Hereditas **126**: 147–160

Sparvoli F, Martin C, Scienza A, Gavazzi G, Tonelli C, Celoria V (1994) Cloning and molecular analysis of structural genes involved in flavonoid and stilbene biosynthesis in grape (*Vitis vinifera* L.). Plant Mol Biol **24**: 743–755

Stapleton AE, Walbot V (1994) Flavonoids can protect maize DNA from the induction of ultraviolet radiation damage. Plant Physiol **105**: 881–889

Stotz G, Forkman G (1982) Hydroxylation of the B-ring of flavonoids in the 3'- and 5'-position with enzyme extracts from flowers of *Verbena hybrida*. Zeitschrift für Naturforsch C **37 c**: 19–23

Sun Y, Huang H, Meng L, Hu K, Dai SL (2013) Isolation and functional analysis of a homolog of flavonoid 3', 5'-hydroxylase gene from *Pericallis* × *hybrida*. Physiol Plant **149**: 151–159

Sun Y, Tian Q, Yuan L, Jiang Y, Huang Y, Sun M, Tang S, Luo K (2011) Isolation and promoter analysis of a chalcone synthase gene PtrCHS4 from *Populus trichocarpa*. Plant Cell Rep **30**: 1661–1671

Tanaka Y (2006) Flower colour and cytochromes P450. Phytochem Rev **5**: 283–291

Tanaka Y, Brugliera F (2013) Flower colour and cytochromes P450. Philos. Trans. R. Soc. London B Biol. Sci. **368**: 20120432.

Tanaka Y, Katsumoto Y, Brugliera F, Mason J (2005) Genetic engineering in floriculture. Plant Cell Tissue Organ Cult **80**: 1–24

Tanaka Y, Ohmiya A (2008) Seeing is believing: engineering anthocyanin and carotenoid biosynthetic pathways. Curr Opin Biotechnol **19**: 190–197

Tanaka Y, Sasaki N, Ohmiya A (2008) Biosynthesis of plant pigments: anthocyanins, betalains and carotenoids. Plant J **54**: 733–749

Tanaka Y, Tsuda S, Kusumi T (1998) Metabolic engineering to modify flower color. Plant Cell Physiol **39**: 1119–1126

Tanaka Y, Yonekura K, Fukuchi-Mizutani M, Fukui Y, Fujiwara H, Ashikari T, Kusumi T (1996) Molecular and biochemical characterization of three anthocyanin synthetic enzymes from *Gentiana triflora*. Plant Cell Physiol **37**: 711–716

Tanner GJ, Francki KT, Abrahams S, Watson JM, Larkin PJ, Ashton AR (2003) Proanthocyanidin biosynthesis in plants. Purification of legume leucoanthocyanidin reductase and molecular cloning of its cDNA. J Biol Chem **278**: 31647–31656

Tattini M, Galardi C, Pinelli P, Massai R, Remorini D, Agati G (2004) Differential accumulation of flavonoids and hydroxycinnamates in leaves of *Ligustrum vulgare* under excess light and drought stress. New Phytol **163**: 547–561

Theis N, Lerdau M (2003) The evolution of function in plant secondary metabolites. Int J Plant Sci **164**: S93–S102

Thoison O, Sévenet T, Niemeyer HM, Russell GB (2004) Insect antifeedant compounds from *Nothofagus dombeyi* and *N. pumilio*. Phytochemistry **65**: 2173–2176

Tholakalabavi A, Zwiazek J, Thorpe T (1994) Effect of mannitol and glucose-induced osmotic stress on growth, water relations, and solute composition of cell suspension cultures of poplar (*Populus deltoides* var.*Occidentalis*) in relation to anthocyanin accumulation. Vitr Cell Dev Biol - Plant **30**: 164–170

Tsai CJ, Harding SA, Tschaplinski TJ, Lindroth RL, Yuan Y (2006) Genome-wide analysis of the structural genes regulating defense phenylpropanoid metabolism in *Populus*. New Phytol **172**: 47–62

Tuskan GA, DiFazio S, Jansson S, Bohlmann J, Grigoriev I, Hellsten U, Putnam N, Ralph S, Rombauts S, Salamov A (2006) The genome of black cottonwood, *Populus trichocarpa* (Torr. & Gray). Science **313**: 1596–1604

Vélez-Bermúdez IC, Schmidt W (2014) The conundrum of discordant protein and mRNA expression. Are plants special? Front Plant Sci **5**: 619

Vetten ND, ter Horst J, van Schaik HP, de Boer A, Mol J, Koes R (1999) A cytochrome b5 is required for full activity of flavonoid 3', 5'-hydroxylase, a cytochrome P450 involved in the formation of blue flower colors. Proc Natl Acad Sci **96**: 778–783

Vogel C, Marcotte EM (2012) Insights into the regulation of protein abundance from proteomic and transcriptomic analyses. Nat Rev Genet **13**: 227–232

Vogel C, de Sousa Abreu R, Ko D, Le S, Shapiro BA, Burns SC, Sandhu D, Boutz DR, Marcotte EM, Penalva LO (2010) Sequence signatures and mRNA concentration can explain two - thirds of protein abundance variation in a human cell line. Mol. Syst. Biol. **6**: 400. Doi:10.1038/msb.2010.59

Walley JW, Shen Z, Sartor R, Wu KJ, Osborn J, Smith LG, Briggs SP (2013) Reconstruction of protein networks from an atlas of maize seed proteotypes. Proc Natl Acad Sc **110** : E4808–E4817

Wang L, Jiang Y, Yuan L, Lu W, Yang L, Karim A, Luo K (2013) Isolation and characterization of cDNAs encoding leucoanthocyanidin reductase and anthocyanidin reductase from *Populus trichocarpa*. PLoS One **8**: e64664

Wang YS, Xu YJ, Gao LP, Yu O, Wang XZ, He XJ, Jiang XL, Liu YJ, Xia T (2014) Functional analysis of flavonoid 3', 5'-hydroxylase from tea plant (*Camellia sinensis*): critical role in the accumulation of catechins. BMC Plant Biol **14**: 1–14

Warren JM, Bassman JH, Fellman JK, Mattinson DS, Eigenbrode S (2003) Ultraviolet-B radiation alters phenolic salicylate and flavonoid composition of *Populus trichocarpa* leaves. Tree Physiol **23**: 527–535

Weber HA, Hodges AE, Guthrie JR, O'Brien BM, Robaugh D, Clark AP, Harris RK, Algaier JW, Smith CS (2006) Comparison of proanthocyanidins in commercial antioxidants: Grape seed and pine bark extracts. J Agric Food Chem **55**: 148–156

Webster G, Jain V, Davey MR, Gough C, Vasse J, Dénarié J, Cocking EC (1998) The flavonoid naringenin stimulates the intercellular colonization of wheat roots by *Azorhizobium caulinodans*. Plant Cell Environ **21**: 373–383

Werck-reichhart D, Feyereisen R (2000) Protein family review cytochromes P450 : a success story. Genome Biol **1**: 1–9

Wilkins O, Nahal H, Foong J, Provart NJ, Campbell MM (2009) Expansion and diversification of the *Populus* R2R3-MYB family of transcription factors. Plant Physiol **149**: 981–993

Winkel-Shirley B (2002) Biosynthesis of flavonoids and effects of stress. Curr Opin Plant Biol **5**: 218–223

Winkel-Shirley B (2001) Flavonoid biosynthesis. A colorful model for genetics, biochemistry, cell biology, and biotechnology. Plant Physiol **126**: 485–493

Xie DY, Dixon RA (2005) Proanthocyanidin biosynthesis--still more questions than answers? Phytochemistry **66**: 2127–2144

Xie DY, Sharma SB, Dixon RA (2004) Anthocyanidin reductases from *Medicago truncatula* and *Arabidopsis thaliana*. Arch Biochem Biophys **422**: 91–102

Xie DY, Sharma SB, Paiva NL, Ferreira D, Dixon RA (2003) Role of anthocyanidin reductase, encoded by BANYULS in plant flavonoid biosynthesis. Science **299**: 396–399

Yamazaki H, Gillam EM, Dong MS, Johnson WW, Guengerich FP, Shimada T (1997) Reconstitution of recombinant cytochrome P450 2C10(2C9) and comparison with cytochrome P450 3A4 and other forms: effects of cytochrome P450-P450 and cytochrome P450-b5 interactions. Arch Biochem Biophys **342**: 329–337

Yamazaki H, Johnson WW, Ueng YF, Shimada T, Guengerich FP (1996) Lack of electron transfer from cytochrome b5 in stimulation of catalytic activities of Cytochrome P450 3A4: Characterization of a reconstituted cytochrome p450 3A4/NADPH-cytochrome p450 reductase system and studies with apo-cytochrome b5 . J Biol Chem **271**: 27438–27444

Yan M, Liu X, Guan C, Chen X, Liu Z (2011) Cloning and expression analysis of an anthocyanidin synthase gene homolog from *Brassica juncea*. Mol Breed **28**: 313–322

Yang F, Moss LG, Phillips GN (1996) The molecular structure of green fluorescent protein. Nat Biotech **14**: 1246–1251

Yokozawa T, Cho EJ, Park CH, Kim JH (2012) Protective effect of proanthocyanidin against diabetic oxidative stress. Evid Based Complement Alternat Med **2012**: 623879

Yoshida K, Mori M, Kondo T (2009) Blue flower color development by anthocyanins: from chemical structure to cell physiology. Nat Prod Rep **26**: 884–915

Yuan L, Wang L, Han Z, Jiang Y, Zhao L, Liu H, Yang L, Luo K (2012) Molecular cloning and characterization of PtrLAR3, a gene encoding leucoanthocyanidin reductase from *Populus trichocarpa*, and its constitutive expression enhances fungal resistance in transgenic plants. J Exp Bot **63**: 2513–2524

Zhao J, Dixon RA (2009) MATE transporters facilitate vacuolar uptake of epicatechin 3'-*O*-glucoside for proanthocyanidin biosynthesis in *Medicago truncatula* and *Arabidopsis*. Plant Cell **21**: 2323–2340

Zucker WV, The S, Naturalist A, Mar N (1983) Tannins : Does structure determine function ? An ecological perspective. Am Nat **121**: 335–365

Appendix A: Supplemental Figures and Tables

This appendix contains the following supplemental material:

Figure A-1 Semi-quantitative PCR of PtF3’5’H1 in PtF3’5’H1 overexpressing and wild type lines.

Figure A-2. HPLC analysis of soluble phenolic metabolites from PtF3’5’H1 overexpressing and wild-type poplar leaf tissues.

Table A-1. Medium composition.

Table A-2. Anthocyanins identified from various blueberry extracts by LC-MS (Bunea et al., 2013).

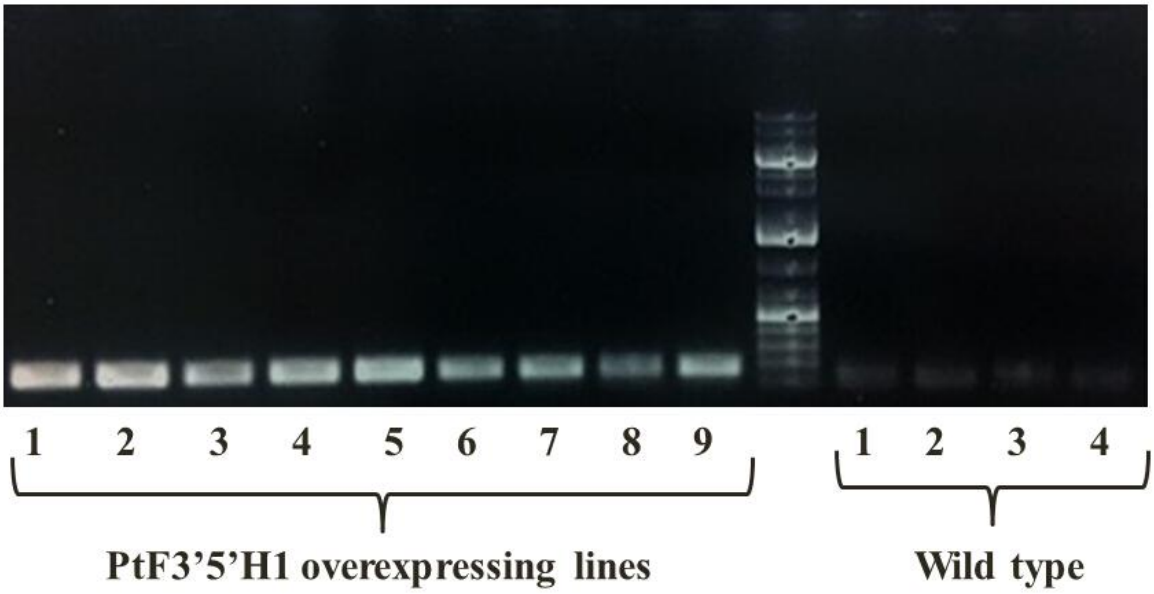

Figure A-1. Semi-quantitative PCR of PtF3'5'H1 in PtF3'5'H1 overexpressing and wild type lines.
RNA was extracted from young leaves of PtF3'5'H1 overexpressing and wild-type plants (2 month old in magenta box). RT-PCR was performed to generate cDNA, expression level of PtF3'5'H1 was normalized against EF1β (a house-keeping gene).

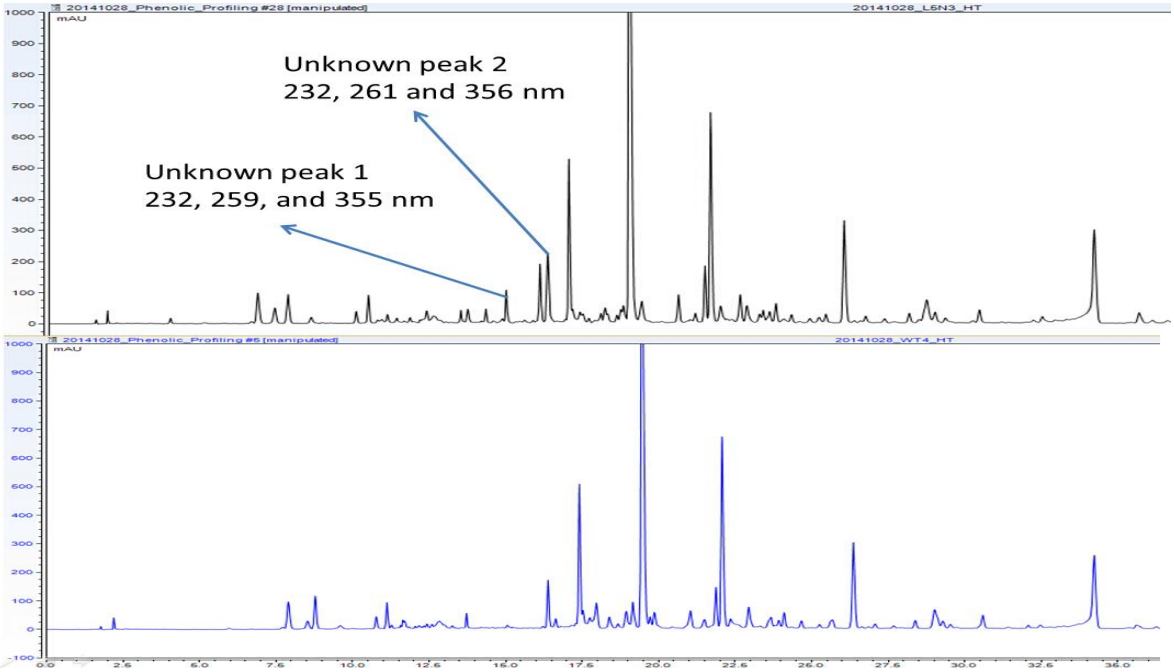

Figure A-2. HPLC analysis of soluble phenolic metabolites from PtF3'5'H1 overexpressing and wild-type poplar leaf tissues.
Transgenic poplar is indicated in black, while wild-type poplar is shown in blue. Two new peaks were found from PtF3'5'H1 overexpressing poplar leaf tissue (LPI 10-12, 353-38 background). These two peaks present in all transgenic poplars while absent in all wild-type poplar plants.

Table A-1. Medium composition.

Name	Volume	Composition	Antibiotics
McCown's woody plant medium	1L	2.3 g Lloyd & McCown's Woody Plant Basal Salts, 10 mL 100×myo-Inositol (10 mg/ml), 20 g sucrose, 7 g phytaagar, 1 mL 1000 × vitamins stock (100 mg nicotinic acid, 100 mg pyroxidine HCl, 100 mg thiamine HCl and 100 mg calcium pantothenate in 100 ml H_2O), 9 mL IBA (50 mg/L), pH to 5.5-5.6	
LB liquid medium	500 mL	5 g tryptone powder, 2.5 g yeast extract, 2.5 g NaCl	
LB solid medium with antibiotics	500 mL	5 g tryptone powder, 2.5 g yeast extract, 2.5 g NaCl, 7.5 g agar	7 μg/mL gentamicin, 50 μg/mL kanamycin, 50 μg/mL rifampicin
LB liquid medium with antibiotics	500 mL	5 g tryptone powder, 2.5 g yeast extract, 2.5 g NaCl	7 μg/mL gentamicin, 50 μg/mL kanamycin, 50 μg/mL rifampicin
Induction medium	500 mL	2.2 g Murashige & Skoog Basal Salts, 0.93 g galactose, 12.5 mg MES, 0.5 mL 1000 × vitamins stock, 2.5 mL acetosyringone stock (10 mM), pH to 5.7-5.8	
Callus induction medium 1	500 mL	2.2 g Murashige & Skoog Basal Salts, 15 g sucrose, 100 mg L-glutamine, 1.5 g phytoagar, 1g phytoblend, 0.5 mL 1000 × vitamins stock, 2.5 mL 1mM 2-isopentnyl adenine, 5 mL 1 mM 1-naphthaleneacetic acid, pH to 5.7-5.8	
Callus induction medium 2	500 mL	2.2 g Murashige & Skoog Basal Salts, 15 g sucrose, 100 mg L-glutamine, 1.5 g phytoagar, 1g phytoblend, 0.5 mL 1000 × vitamins stock, 2.5 mL 1mM 2-isopentnyl adenine, 5 mL 1 mM 1-naphthaleneacetic acid, pH to 5.7-5.8	250 mg/L cefotaxime, 500 mg/L carbenicillin, 10 mg/L hygromycin
Shoot induction medium	500 mL	2.2 g Murashige & Skoog Basal Salts, 15 g sucrose, 100 mg L-glutamine, 1.5 g phytoagar, 1g phytoblend, 0.5 mL 1000 × vitamins stock, 0.2 μM thidiazuron	250 mg/L cefotaxime, 500 mg/L carbenicillin, 10 mg/L hygromycin
Root induction medium	500 mL	1.1 g Murashige & Skoog Basal Salts, 7.5 g sucrose, 50 mg L-glutamine, 0.5 mL 1000 × vitamins stock, 0.5 μM IBA	10 mg/L hygromycin
MG/L medium	500 mL	10 g mannitol, 6.85 mL 1 M L-glutamic acid, 0.25 g KH_2PO_4, 5.2 g NaCl, 0.2 g $MgSO_4 \cdot 7H_2O$, 5 g tryptone powder, 2.5 g yeast extract, 0.8 μg/L biotin，pH to 7.0	50 mg/L kanamycin
Induction broth	500 mL	0.125 g MES, 5 mL 100 × myo-Inositol (10 mg/mL), 15 g sucrose, 2.165 g Murashige & Skoog Basal Salts, 1 mg nicotinic acid, 1 mg pyroxidine HCl, 1 mg thiamine HCl, 1 mg calcium pantothenate and 250 μL of 200 μM acetosyringone，pH to 5.7-5.9	
Co-cultivation medium	500 mL	0.125 g MES, 5 mL 100 × myo-Inositol (10 mg/mL), 15 g sucrose, 2.165 g Murashige & Skoog Basal Salts, 1.5 g phytagar, 1 g phytagel, 1 mg nicotinic acid, 1 mg pyroxidine HCl, 1 mg thiamine HCl, 1 mg calcium pantothenate, 250 uL of 200 mM acetosyringone, pH to 5.7-5.9	
Antibiotic-containing solid medium	500 mL	0.125 g MES, 5 mL 100 × myo-Inositol (10 mg/mL), 15 g sucrose, 2.165 g Murashige & Skoog Basal Salts, 1.5 g phytagar, 1 g phytagel, 1 mg nicotinic acid, 1 mg pyroxidine HCl, 1 mg thiamine HCl, 1 mg calcium pantothenate, , pH to 5.7-5.9	300 mg/L timentin, 500 mg/mL cefotaxime
Selection medium	500 mL	0.125 g MES, 5 mL 100 × myo-Inositol (10 mg/mL), 15 g sucrose, 2.165 g Murashige & Skoog Basal Salts, 1.5 g phytagar, 1 g phytagel, 1 mg nicotinic acid, 1 mg pyroxidine HCl, 1 mg thiamine HCl, 1 mg calcium pantothenate, pH to 5.7-5.9	300 mg/L timentin, 500 mg/mL cefotaxime, 25 mg/L kanamycin, 10 mg/L hygromycin
Murashige & Skoog medium	500 mL	2.2 g Murashige & Skoog Basal Salts	

Table A-2. Anthocyanins identified from various blueberry extracts by LC-MS (Bunea et al., 2013).

Peak	Time (min)	Maximum absorptions (nm)	Substance
An 1	8.1	276; 526	Delphinidin-3-O-galactoside
An 2	9.3	276; 524	Delphinidin-3-O-glucoside
An 3	11.2	279; 517	Cyanidin-3-O-galactoside
An 4	11.5	276; 524	Delphinidin-3-O-arabinoside
An 5	12.9	280; 517	Cyanidin-3-O-glucoside
An 6	13.6	276; 526	Petunidin-3-O-galactoside
An 7	15.2	279; 517	Cyanidin-3-O-arabinoside
An 8	18	276; 526	Paeonidin-3-O-galactoside
An 9	18.2	276; 526	Petunidin-3-O-arabinoside
An 10	20.5	276; 527	Malvidin-3-O-galactoside
An 11	23.4	276; 526	Malvidin-3-O-glucoside
An 12	26.3	276; 528	Malvidin-3-O-arabinoside